

**FORMATION EVALUATION OF UPPER
QAMCHUQA RESERVOIR, KHABBAZ OIL
FIELD, KIRKUK AREA, NORTHEASTERN IRAQ**

A THESIS

**SUBMITTED TO THE COLLEGE OF SCIENCE, UNIVERSITY OF
SULAIMANI, IN PARTIAL FULFILLMENT OF THE REQUIRMENTS
FOR THE DEGREE OF DOCTORATE OF PHILOSOPHY
*IN GEOLOGY***

By

Fuad Mohammad Qadir

M Sc. in Geology, Baghdad University, 1999

Supervised by

Dr. Basim Al-Qayim

(Professor)

Dr. Fawzi Al Beyati

(Assistant Professor)

June 2008 A.D

Poshpar 2708 Kurdish

بِسْمِ اللَّهِ الرَّحْمَنِ الرَّحِيمِ
وَالْأَرْضَ مَدَدْنَا هَا وَالْقِيَامَةَ فِيهَا رَوَّاسِي وَأَنْبَتْنَا فِيهَا مِنْ كُلِّ شَيْءٍ
مَّوْزُونٍ ﴿١٩﴾ وَجَعَلْنَا لَكُمْ فِيهَا مَعَايِشَ وَمَنْ لَسْتُمْ لَهُ بِرَازِقِينَ ﴿٢٠﴾
وَإِنْ مِنْ شَيْءٍ إِلَّا عِنْدَنَا خَزَائِنُهُ وَمَا نُنزِّلُهُ إِلَّا بِقَدَرٍ مَّعْلُومٍ ﴿٢١﴾
صَدَقَ اللَّهُ الْعَظِيمَ

سورة الحجر / آيات 19-21

And the earth we have spread out (like a carpet); set thereon mountains firm and immovable; and produced therein all kinds of things in due balance (19) And we have provided therein means of subsistence, for you and for those for whose sustenance ye are not responsible (20) And there is not a thing but its (sources and) treasures (inexhaustible) are with us; but we only send down thereof in due and ascertainable measures (21).

Surah Al Hujrat/ Āyat 19-21

Supervisors Certification

We certify that this thesis (**Formation Evaluation of Upper Qamchuqa Reservoir, Khabbaz Oil Field, Kirkuk Area, Northeastern Iraq**) has been prepared under our supervision in the Department of Geology of the University of Sulaimani, in partial fulfillment of the requirement for the degree of Doctorate of philosophy in Geology.

Signature:



Name: Dr. Basim Al Qayim

Title: Professor

Address: University of Sulaimani
College of Science
Department of Geology

Date:

Signature:



Name: Dr. Fawzi Al Beyati

Title: Assistant professor

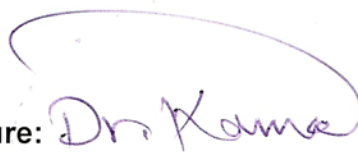
Address: Kirkuk Technical College
Department of Survey

Date:

The Certification of the Chairman of the Committee of Higher Studies:

According to the recommendation submitted by the supervisors, I nominate this thesis for discussion.

Signature:



Name: Dr. Kamal Haji Karim

Title: Assistant professor

Address: University of Sulaimani
College of Science
Department of Geology

Date:

26-8-2008

We, The Examining committee, hereby certify that we have read this thesis
(Formation Evaluation of Upper Qamchuqa Reservoir, Khabbaz Oil Field, Kirkuk Area, Northeastern Iraq) and examined the student in its contents and whatever relevant to it and, in our opinion; it is adequate to be acceptance for the Degree of Doctorate of Philosophy in Geology/ **Reservoir Geology and Well Logging**

Signature:



Name: Dr. Mazin Y. Tamar-Agha

Title: Professor

Address: University of Salahaddin

Date:

(Chairman)

Signature:



Name: Dr. Nawzad O. Abdulrahim

Title: Assistant professor

Address: University of Sulaimani

Date:

Signature:



Name: Dr. Madhat E. Nasser

Title: Assistant professor

Address: University of Baghdad

Date:

(Member)

Signature:



Name: Dr. Ali M. Surdashi

Title: Assistant professor

Address: University of Koya

Date:

(Member)

Signature:



Name: Dr. Khalid M. I. Sharbazheri

Title: Assistant professor

Address: University of Sulaimani

Date: 27-8-2008

(Member)

(Member)

Signature:



Name: Dr. Basim A. Al Qayim

Title: professor

Address: University of Sulaimani

Date:

Signature:



Name: Dr. Fawzi M. AL Beyati

Title: Assistant professor

Address: Kirkuk Technical College

Date:

(Supervisor and Member)

(Supervisor and Member)

Approved by the Council of the College of Science

Signature:

Name: Dr. Parekhan M. Abdul-Rahman

Title: Assistant professor

Address: University of Sulaimani

Date:

Dedicated
to
Memorable Soul of My
Late Elder Brother
(Mamosta As'ad)
Who Always Wished
to See Me
as a
Ph.D Holder

Dedication

Dedicated

to

Memorable Soul of My

Late Elder Brother

Mamosta As'ad

Who Always Wish

to See Me

as

Ph.D Holder

ACKNOWLEDGEMENTS

Support for this study was provided by University of Sulaimani, the author is grateful to this institution, represented by College of Science and Geology department.

I express my appreciation to the both of my supervisors: Professor Dr. Basim Al-Qaym, and Assistant Professor Dr. Fawzi AL Beyati, for their valuable discussions, and for unlimited support for all the plans and suggestions.

It was my pleasure of work closely with Mr. Husain Sultan, Geology Department manager of North Oil Company (N. O. C.), also his assistant Mr. Nasrat and their staff. There is no doubt that their help in preparing the final well reports, the well log data and the core samples have been important for this dissertation

Thanks for Petroleum Engineering Department of N.O.C for providing the available data of core analyses, reservoir condition and formation water analyses.

Thanks for Mr. Sabah, the head of Research and Quality Control Department of N. O. C. for additional core measurements and crude oil analyses

Additional thanks go to TOTAL Oil Company represented by Jean Mouillac from TPA and Gilles Sermondadaz, the Head of Fluid and Organic Geochemistry Department, for providing access to laboratory facilities of crude oil geochemical analyses.

Everyone who has helped me (in one way or another) in completing this thesis deserves a personal greeting. This is unfortunately not possible in this context as I have enjoyed helpful comments, a helping hand in the laboratory and fruitful discussions with many brilliant persons.

There are also a lot of people from the other world {outside the academic circles} who deserve acknowledgment. My friends, who always make me go ahead, are thanked. My family have always supported me and made my lasting studies possible and they deserve my everlasting gratitude.

Fuad

Abstract

Khabbaz oil field located in *Konarewi valley*, 23 km to the west to northwestern of Kirkuk city in north Iraq. Tectonically, the field located in the Foothill zone (Hamrin - Makhul sub zone). The field represents asymmetrical subsurface anticline, with around 20 Km length and 4 Km width. Despite of its comparatively small size; it is one of the giant Iraqi oil fields. This field is characterized by multiple pay zones similar to most of the northern Iraq oil fields, which produces from Tertiary (Jeribe reservoir) and Cretaceous (Upper and Lower Qamchuqa Reservoirs). The Upper Qamchuqa shallow-water carbonate is one of the most prolific Khabbaz reservoirs with 156 to 180 m thickness. It is subdivided into three lithological units, named from the top to bottom: Unit (A) with an average of 66m, Unit (B) with an average of 73m, and Unit (C) with an average of 34m.

The dolomitization is pervasive and affects most of the formation section especially the middle and lower part of Unit (A), the upper part of Unit (B), and some intervals of Unit (C). The rest of the formation consists of inter-bedded limestone with dolomitic limestone, and the dominance of marly limestone, marl and shale over Unit (C) is due to gradational change to the underlain Upper Sarmord Formation.

Petrophysical characteristics are studied from a group of data and tools selected from ten wells (Kz-1, Kz-2, Kz-3, Kz-4, Kz-5, Kz-7, Kz-11, Kz-13, Kz-14 and Kz-16), including the following types:

(a)- Wireline log data deriving from: Resistivity logs (LLD, LLs, ILD, ILm, and μ SFL), Porosity logs (CNT, FDC, and BHC) type, and Gamma Ray (GR). (b)- Lithologic description of core interval and thin sections using polarizing microscope. (c)- Core plugs laboratory measurements (porosity, permeability, and resistivity) were used in petrophysical evaluation and log measurements calibration.

From the analyses of the above data, this study concludes that the best reservoir characters are associated with Unit (A). It is classified into six continuous reservoir subunits, from the top named (A1, A2, A3, A4, A5, and A6).

These reservoir subunits have good correlation, laterally and vertically, which make them easily followed by mean of well logs, especially porosity logs.

The other porous subunits are associated with lithologic unit (B), they are named B1, B2, and B3, and lithologic Unit (C) including subunit C1. These subunits are less uniform, poorly lateral correlated and with poorer reservoir characters.

Also according to the results of geochemical analysis of the formation water, the study concludes that the Upper Qamchuqa Formation water belongs to the Chloride calcium type. This type of water is associated with a closed system reservoir. It is isolated from influence of infiltration waters, and considered as a good zone for preservation of hydrocarbon accumulations.

In addition to utilization of the enormous geochemical data of crude oil which were made during the drilling operation of the wells and development of the field, new samples of crude oil were selected from the five present day producing wells within the Upper Qamchuqa reservoir interval, and a sample from Lower Qamchuqa reservoir. The samples were used for further detailed geochemical analyses and gas chromatography-mass spectrometry (GC-MS) measurements.

The geochemical analyses of the crude oils indicate marine to mix origin environments of the source rock. Also the correlation between the oil chemistry of the Upper Qamchuqa reservoir and the Lower Qamchuqa reservoir suggest that the two reservoirs have the same origin source rock, both belonging to the same oil family and reservoir condition system.

This study suggests that the heavy oil problem of the well Kz-4 belongs to some misconduct and unusual production technique. It is related to the extreme production or gas injection to the well, which both lead to the precipitation of the residual fraction of the oil (deasphalting) around the well section and isolate the well from the lighter oil in the rest of the reservoir. The problem can be treated by washing the well and stabilizing it, later it could be produce from it with steady state until comes back to its natural condition.

LIST OF CONTENT

Subject	Page
Chapter One: Introduction	
1.1 Preface	1
1.2 Previous Works	2
1.3 Aim of the study	6
1.4 Methods of research	7
1.5 Khabbaz Field	9
Chapter Two: Stratigraphy and Sedimentology	
2.1 Paleogeography and Sedimentary Basin.....	14
2.2 Stratigraphy and Subsurface Geology.....	19
2.2.1 Qamchuqa Formation in Type Locality.....	20
2.2.2 Qamchuqa Formation in the Subsurface.....	21
2.2.3 Upper Qamchuqa Formation.....	21
2.2.4 Upper Qamchuqa Formation in the Khabbaz oil field.	23
2.3 Lithological Units)	25
2.4 Microfacies Analyses	32
2.4.1 Limestone Microfacies (L)	34
2.4.2 Dolomitic Limestone Microfacies (DL).....	35
2.4.3 Dolostone Microfacies (D).....	37
Chapter Three: Reservoir Characterization	
3.1 Preface.....	47
3.2 Porosity	47
3.3 Permeability	52
3.4 Neutron-Density Cross Plotting	58
3.5 Pore Throat Type.....	66
3.6 Rock Fabric Type.....	70
3.7 Reservoir Unit Classification.....	74
3.7.1 Unit (A)	74
3.7.1.1 Reservoir Subunit (A1).....	77
3.7.1.2 Reservoir Subunit (A2)	78
3.7.1.3 Reservoir Subunit (A3)	78
3.7.1.4 Reservoir Subunit (A4).....	79
3.7.1.5 Reservoir Subunit (A5).....	80
3.7.1.6 Reservoir Subunit (A6).....	81
3.7.1.7 The Non Reservoir Subunits	81
3.7.2 Unit (B and C)	90
3.7.2.1 Reservoir Subunit B1.....	90
3.7.2.2 Reservoir Subunit B2.....	90
3.7.2.3 Reservoir Subunit B3.....	91
3.7.2.4 Reservoir Subunit C1.....	91
Chapter Four : Reservoir Fluids	
4.1 Introduction.....	95
4.2. Resistivity Logs	95
4.3. Estimation of Cementation Factor (m).....	96
4.4. Fluids Resistivity Correction	97

4.5 Water Saturation and Oil Saturation	99
4.5.1 Archie Water Saturations: S_w and S_{xo}	99
4.5.2. Bulk Volume Water	100
4.5.3 Residual and Moveable Hydrocarbons.....	106
4.5.3.1 Unit (A)	107
4.5.3.2 Unit (B and C)	111
4.6 Permeability Estimates From Φ and S_w	113

CHAPTER FIVE : Reservoir Geochemical Analyses

5.1. Introduction	114
5.2. Classification of Oil Field Water	115
5.3. Classification of the Formation Water in the Studied Wells	119
5.4. Crude oil composition	121
5.5. Oil Alteration Through Secondary Processes in the Reservoir	122
5.5.1. Biodegradation and Water Washing	122
5.5.2. Infilling Reservoir by Gases, Natural deasphalting.	123
5.6. Oil characterization of Khabbaz Field	124
5.6.1 Compositional Relationship	129
5.6.2 Bacteriological Examination.....	131
5.6.3 Origin of the Oils	132
5.6.4 Stable Carbon Isotopic Compositions	135
5.6.5 Maturity levels	137

CHAPTER SIX : Conclusion

Appendices	143
References	159

Figures

Fig. (1.1): Map of Iraq showing the location of the Khabbaz oil field.....	11
Fig. (1.2): The structural contour map on top of Upper Qamchuqa reservoir.	12
Fig. (1.3): Structural cross section along the Khabbaz field axis (A-B).....	13
Fig. (2.1): Aptian and Albian Paleogeography in Iraq.....	17
Fig. (2.2): Stratigraphic correlation chart of Early - Middle Cretaceous formations.....	19
Fig. (2.3): The Isochore map of Upper Qamchuqa Formation with.....	23
Fig. (2.4): General composite column of Upper Qamchuqa Formation.....	26
Fig. (2.5): The lithologic units of Upper Qamchuqa Formation from (GR and N-D) logs.	28
Fig. (2.6): (a) Core represent unit (A) in well Kz-2(b) core of unit (B) well Kz-11.....	29
Fig.(2.7):Core photograph represent unit C of U. Qamchuqa Formation from well Kz-11	30
Fig. (2.8): Limestone Microfacies.....	40
Fig. (2.9): Dolomitic Limestone Microfacies.....	41
Fig. (2.10): Dolomitic Limestone Microfacies.....	42
Fig. (2.11): Dolostone Microfacies.....	43
Fig. (2.12): Dolostone Microfacies.....	44
Fig. (2.13): Dolostone Microfacies.....	45
Fig. (2.14): Dolostone Microfacies.....	46
Fig. (3.1): Comparisons of N-D & Sonic Logs, with the core porosities in well Kz-16..	53
Fig. (3.2): Correlation of the core and log measured permeability.....	57
Fig. (3.3): Neutron-Density crossplot.	59
Fig. (3.4): The Neutron-Density crossplot of well Kz-1 section.....	60
Fig. (3.5): The Neutron-Density crossplot of well Kz-4 section.....	61

Fig. (3.6): The Neutron-Density crossplot of well Kz-5 section.....	62
Fig. (3.7): The Neutron-Density crossplot of well Kz-11 section.....	63
Fig. (3.8): The Neutron-Density crossplot of well Kz-14 section.....	64
Fig. (3.9): The Neutron-Density crossplots of well Kz-16 section.....	65
Fig. (3.10): Porosity permeability crossplot	66
Fig. (3.11): Porosity permeability crossplot, pore throat radius type of the six subunits.	69
Fig. (3.12): Carbonate Petrophysical Classification after Lucia, 1995.....	70
Fig. (3.13): Rock Fabric Classes. (after Jennings and Lucia, 2003).	71
Fig. (3.14): Rock Fabric Classes of the six porosity subunits (A1, A2, A3, A4, A5, A6).	73
Fig. (3.15): Reservoir and non-reservoir subunits, using N-D porosity logs (Kz-1	75
Fig. (3.16): Reservoir and non-reservoir subunits, using N-D porosity logs (Kz-11... ..	76
Fig. (3.17): Thin-section photomicrographs, Microfacies, subunit A1 and A2.....	85
Fig. (3.18): Thin-section photomicrographs, Microfacies, subunit A3 and A4.....	86
Fig. (3.19): Thin-section photomicrographs, Microfacies, subunit A4, complementary...	87
Fig. (3.20): Thin-section photomicrographs, Microfacies, subunit A5.....	88
Fig. (3.21): Thin-section photomicrographs, Microfacies, subunit A6.....	89
Fig. (3.22): Lithologic units (B and C) at wells Kz-1, Kz-2, Kz-4, and Kz-5	93
Fig. (3.23): Lithologic units (B and C) at wells Kz-11, Kz-13, Kz-14, and Kz-16	94
Fig (4-1): The cementation factor (m) from the Porosity-formation resistivity factor....	97
Fig (4.2): porosity vs. water saturation used to determine bulk volume water (BVW)...	102
Fig (4.3): Porosity versus water saturation in wells Kz-3, Kz-4, Kz-5, Kz-13, and Kz-14.	105
Fig.(4.4) :Water saturation, irreducible and movable oil saturation of the unit A.....	110
Fig.(4.5): Water saturation, irreducible and movable oil saturation of the unit B and C...	112
Fig. (5.1): Ternary plot of oil compositional fractions of the crude oils.	128
Fig. (5.2): Crude Oil Compositional Relationship API, S%, Ni, V, and Asphaltenes%...	130
Fig. (5.3): Crossplot between Ph/C18 and Pr/C17 of crude oil samples.....	133
Fig. (5.4): The trianary diagram of regular sterane C27, C28, and C29.....	135
Fig. (5.5): Relationship between the carbon isotopic of the saturate and aromatic.....	137
Fig. (5.6): Gas chromatographic analyses of oil samples n-alkanes in the C15-C35.....	140

List of Tables

Table 2.1: Top & Bottom and drilled thickness of U. Qamchuqa in the studded wells...	24
Table 2.2: Thickness of lithological Units of the Upper Qamchuqa in the studded wells.	32
Table 3.1: Classification of Porosity according to North (1985).....	48
Table 3.2: Classification of Reservoir Permeability (North, 1985).....	54
Table 3.3: Type of pores according to pore throat size.....	67
Table 3.4: The reservoir subunits, their intervals, thickness, and average porosity.	83
Table 3.5: Pore throat, porosity, and permeability of reservoir and non reservoir subunits	84
Table 3.6: The depth intervals, thicknesses, and average porosity, of (B1, B2, B3, C1) ...	92
Table 4.1: Correction of (Rmf, Rw), into formation temperature.....	99
Table 5.1: Coefficients characterizing the genetic type of water (Sulin, 1946).....	116
Table 5.2: Converting the ions in Khabbaz Formation water from ppm into epm.....	118
Table 5.3: The formation water classes of Khabbaz oil field.....	119
Table 5.4: Crude oil fraction ratios, heterogeneous compounds and oil API density.....	127
Table 5.5. The bacteriological tests of the crude oil samples.....	131
Table 5.6: The molecular ratios of Pr/Ph, Pr/C17 and Ph/C18.....	133
Table 5.7: Normalized ratio of C27, C28 and C29%.....	134
Table 5.8: Stable carbon isotopes in saturated and aromatic fractions of oil samples.....	136
Table 5.9: Aromatic hydrocarbon molecular ratios.....	138
Table 5.10: Analytical data for oil samples from the selected wells of Khabbaz oil field.	139

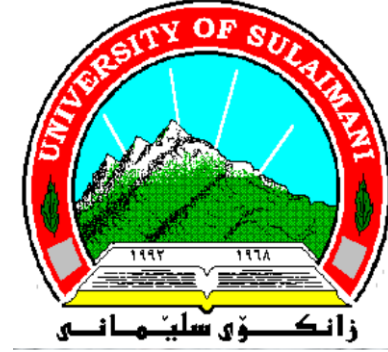
**Formation Evaluation of Upper Qamchuqa
Reservoir, Khabbaz oil Field, Kirkuk area,
Northeastern Iraq**



**Ph D. Thesis in Petroleum Geology
(2008) جیۆلۆجیاسی نقتوت**

Fuad M. Qadir فؤاد محمد قادر

**E-Mail: fuadqadir@yahoo.com
Fuad.qadir@univsul.net**



Chapter One

Introduction

1.1 Preface

Iraq is one of the world's petroleum-rich countries. In near future it could become one of the main producers, because it is endowed with multiple petroleum systems that include Paleozoic, Mesozoic and Cenozoic rocks. The majority of Iraq's oil fields are located in the Zagros-Mesopotamian Cretaceous-Tertiary petroleum system. The Middle–Lower Cretaceous carbonate sediments of Iraq (Qamchuqa Group) comprises one of its major reservoirs system.

The Khabbaz oil field is one of the giant Iraqi oil fields with its multiple pay zones similar to most of the northern Iraq oil fields, which produces from Tertiary (Jeribe reservoir) and Cretaceous(Qamchuqa Reservoirs), the Upper Qamchuqa unit is the goal of this study .

The Qamchuqa Formation is a shallow-water carbonate with wide spread distribution in the outcrop (North-Northeast Iraq) and subsurface of the foothill zone toward south Iraq, extending to Arabian Gulf. Vertical and lateral facies variations in the formation have resulted in a variety of stratigraphic subdivisions that have been compounded further by varying terminology used by operating oil companies.

Before 1972, there were three foreign oil companies working in Iraq, in addition to the Iraqi National Oil Company, each company has a defined concession by law, which should work within its boundaries. Consequently, at least three different names exist for the same formation in the three different parts of country.

This formation represents the important Cretaceous reservoir all over the Foothill zone oil fields i.e. (Jambour, Bai Hassan, Khabbaz, Ain Zalah,

Qarachuq, Hamrin etc..) In this area, it is divided into upper and lower Qamchuqa Formation. They are separated by a shaley, marly to dolomitic limestone unit which is represented by Nahr Umr or Upper Sarmord Formations. While the two units of Qamchuqa (Upper and Lower) represent the equivalent to the Mauddud and Shuaiba Formations respectively. The latter two formations are also well known as two pay zones of the southern Iraq oil fields.

1.2 Previous works

The original description of the Qamchuqa Formation was (according to Bellen et. al. 1959) by Wetzel, in 1950, who studied the sequence of the formation in the Qamchuqa gorge in the High Folded Zone in the north – northwest of Sulaimani City, and the formation was named after the gorge of Qamchuqa. According to the original definition the Qamchuqa Formation comprises the neritic limestones (often the strongly dolomitized) of the Hautrivian to Albian age.

In the type section, the formation is underlain by Sarmord Formation with conformable and gradational contact, while the upper contact with Kometan Formation is an erosional unconformity but without angular discordance (Bellen et. al. 1959).

The similar and the equivalent limestone in south and western Iraq were described as the Shuaiba (Aptian) and Mauddud (Albian) Formations. Later on Chaton and Hart.1960 (in Buday, 1980) divided the Qamchuqa Formation into lower unit of pre-Albian and upper unit of Upper Albian age. They considered the Shuaiba and Mauddud Formations as extensive individualized tongues of the lower and upper Qamchuqa Formation respectively (Buday, 1980).

The first well was drilled in the Kirkuk area targeting Qamchuqa reservoir as a pay zone from Baba Dome of Kirkuk oil field in 1951. Further explorations for the Cretaceous prospects which proved to be good promising reservoir comes from Jambour, Bai Hassan and then Khabbaz oil fields. (AL-Shakiry, 1977)

AL-Shakiry (1977), studied the petrology of part of the Qamchuqa Formations in Jambour oil field. The study encompassed parts of Upper Qamchuqa and Lower Qamchuqa Formations, with an intervening tongue of the Batiwa (Upper Sarmord) Formation. In his study he suggested two basic facies within the studied section, the first is a high energy facies represented by the shoal banks of the Upper Qamchuqa and the patchy reefs of Lower Qamchuqa. The second is low to relatively moderate- energy facies situated on the shelf. He concluded that the dolomitization affects the shelf facies of Upper Qamchuqa more than the high-energy facies.

AL-Sadooni (1978) in his sedimentology and petroleum prospects study of the Middle-Lower Cretaceous deposits, he suggested the term Qamchuqa Group of these sediments to include Mauddud, Shuaiba and Garague Formations in the neritic zone with the Jawan Formation which replacing the Mauddud in the lagoonal zone of the shelf. Also he suggested the term Ain Zalah Group to replace the Qamchuqa Group of Ain Zalah Field as described by Hart and Hay (1974), he thought that the Ain Zalah Group is for subsurface stratigraphic use only and it is partially correlative with Qamchuqa Group.

Sahar (1987) studied the dolomitization of Upper Qamchuqa Formation from four subsurface sections of northern Iraqi oil fields (Kirkuk-130, Chamchamal-2, Bautma-2, and Tal Hajer-1). He deduced that most of the studied sections are completely dolomitized except for a few parts of them remain with partial or no dolomitization. Also he concluded the depositional

environment of the formation as calm shallow marine, represented by mudstone and wackestone carbonate facies graded into high energy condition of packstone and grainstone facies.

AL-Shdidi et.al. (1995) divided the Qamchuqa reservoir of Jambour oil field laterally into three facies: the northwestern part which is neritic facies, the central part with basinal influence, and the southeastern considered as basinal mudstone type facies.

Allah-Werdi (2001) studied the sequence stratigraphy of the Lower Cretaceous formations (Garagu, Ratawi, Shuaiba, Batiwah and Mauddud), he was selected the subsurface sections from Bai-Hassan, Khabbaz and Jambour oil fields. He concluded that these successions were deposited in a variety of shallow marine ramp setting and basinal environment. Garagu Formation was deposited at the beginning in a homoclinal ramp setting and the overlying Ratawi (Middle Sarmord), Shuaiba (Lower Qamchuqa), Batiwah (Upper Sarmord) and Mauddud (Upper Qamchuqa) Formations were deposited later in a distally steepened ramp setting.

Al-Peryadi (2002) studied the sedimentology and reservoir characterization of Upper Qamchuqa and Jawan Formations from Bai-Hassan oil field; he divided the Upper Qamchuqa/Jawan succession into four lithological units for Upper Qamchuqa Formation and two units of Jawan Formation. From the view point of reservoir characteristics he divided the Upper Qamchuqa/Jawan succession into six porosity units.

Sadooni and Alsharhan (2003) in their study on Mauddud Formation (equivalent to Upper Qamchuqa) included stratigraphy, microfacies, and petroleum potential in the Arabian Gulf. They concluded that this formation includes the Albian–Cenomanian Orbitolina-bearing limestone and dolomites that cover most of the Arabian basin, and the Mauddud Formation represents a very shallow to shallow carbonate shelf with local basin margin

rudist buildups, which established following the shutdown of the clastic front of the Nahr Umr Formation. The Upper Jurassic and Cretaceous pelagic strata are probably the source rocks for the accumulated oil within Maaddud Formation in the central and northeastern Iraqi oil fields.

Ameen (2008) studied the sedimentology and lithostratigraphy of Qamchuqa Formation along some outcrop sections in northeastern Iraq. He divided the Qamchuqa Formation into eight units based on the lithology and fossil contents, and he concluded that the formation is deposited in low energy reef, backreef, forereef and lagoonal environments. In his study, he suggested the conformable contacts to the lower and upper boundaries of Qamchuqa Formation with the underlain (Sarmord) and overlain (Kometan and/or Dokan) Formations respectively. He does not agree with the ancient suggestion of unconformable relation to the overlaying unit.

The previous works studied the Qamchuqa Formation from the viewpoints of petrology, sedimentology, stratigraphy, microfacies, and sequence stratigraphy in different locations of Iraq, most of them attempt the formation with regional dimensions. Only one of them includes the reservoir characterization of Upper Qamchuqa Formation in Bai Hassan oil field. The present study attempt to evaluate the Upper Qamchuqa reservoir in Khabbaz oil field.

1.3 Aim of the study

The study of the Upper Qamchuqa reservoir in Khabbaz oil field of Kirkuk area is aimed to evaluate the following aspects:

- 1- Lithologic characters and microfacies distribution of the reservoir in this field which leads to the solution of the reservoir unit pattern.
- 2- Study the reservoir petrophysic characters including assessment of reservoir units and their porosity, permeability, and pore throat system.
- 3- Assessment of reservoir fluid saturations including water saturation (S_w), irreducible hydrocarbon saturation ($S_{h_{irr}}$) and finally moveable hydrocarbon saturations, to better understand reservoir fluid mobility.
- 4- The classification of the reservoir's formation water based on the salinities and the evaluation of its role on the crude oil geochemistry.
- 5- Putting some light on the origin (source rock), the oil maturation, the alteration and the correlation of the crude oil in the Qamchuqa reservoir.
- 6- Tackling some production problems related to recent heavy oil transformation of a certain well (Kz-4) of the Khabbaz oil field.

1.4 Methods of research

The collected data and the study methods of the Khabbaz oil field for the present study classified into three main groups:

A- Data existence in relation to petrophysical characteristics and reservoir fluid saturations, and they form the great part of the total data. This group of data collected from ten wells (Kz-1, Kz-2, Kz-3, Kz-4, Kz-5, Kz-7, Kz-11, Kz-13, Kz-14 and Kz-16), which include the following types:

- 1- Wireline logs of the ten well sections include, Dual Laterolog (Laterlog deep "LLD" and Laterolog shallow "LLs"), Induction logs (deep Induction log "ILD" and Induction log medium "ILm"), Microspherical log (μ SFL), Spontaneous (SP) Log, Compensated Neutron tool (CNT), Formation Density compensated (FDC), Sonic log (borehole compensated BHC type), Gamma Ray (GR) and caliper log.
- 2- More than 500 thin sections (made by N. O. C) from the studied reservoir in the selected wells were studied using polarizing microscope in order to classify the reservoir rocks into lithologic unit's microfacies as well as porosity type, origin and qualitative evaluation.
- 3- Lithologic description of core interval from seven wells (Kz-1, Kz-2, Kz-3, Kz-4, Kz-11, Kz-13, and Kz-14) including sedimentary structures, large scale textures Macro porosity (fracture, vugs) and oil show.
- 4- More than 120m core plugs having detailed laboratory measurements (porosity, permeability, resistivity) carried out by N. O. C. for each

30cm of the cored intervals, they used in petrophysical evaluation and log measurements calibration.

B- Data related to the formation water analyses:

These data are represented by geochemical parameters of formation water analyses of Upper Qamchuqa reservoir which were available from four wells (Kz-3, Kz-4, Kz-7 and Kz-23). They include the detailed geochemical analyses of their salinity: total dissolved solid (TDS), amount of each individual ion (cations and anions) in the water, and formation water resistivity (R_w).

C- Data related to crude oil composition:

In addition to the use of the massive geochemical data of crude oil which were analyzed by North Oil Company (N. O. C.) during the drilling operation of the wells, new samples of crude oil were selected from the five present day producing wells (Kz-4, Kz-12, Kz-21, Kz-23 and Kz-24) within the Upper Qamchuqa reservoir interval, and a sample from Lower Qamchuqa reservoir (well Kz-1). The samples were used for further detailed geochemical analyses and gas chromatography-mass spectrometry (GC-MS) measurements.

The bacteriological testing for two of the oil samples from wells (Kz-1 and Kz-4) were added to detect the probability if oil was exposed to biodegradation or not, due to some strange phenomenon properties of the oils (heavier oil) of Kz-4, as it was declared by the workers of the Producing Department of North Oil Company.

1.5 Khabbaz Field

The Khabbaz oil field represents a small subsurface asymmetrical anticline, its northeast limb dips more than the southwest limb. The structure is located between Jambour and Bai Hassan oil fields (Figure 1.1). The axis of the structure runs in the same direction of Jambour structure with slightly shifting from Bai Hassan. The first seismic investigation of the Khabbaz area (Kuna Rewi Valley) done by the Iraqi Petroleum Company (I.P.C) in 1955 indicated a subsurface structure plunging toward northwest. The second seismic survey operation began in July 1971 to the Khabbaz area and completed in 22 October 1971 which proved the presence of the structure and the first well (Kz-1) was drilled in August 1976. Geographically, the Khabbaz oil field is located **23** km to the west and northwestern of Kirkuk city in north Iraq, (Figure 1.1). Tectonically the field is located in the Foothill zone (Hamrin - Makhul Subzone) which belongs to the Folded zone of the Unstable Shelf (Buday and Jassim, 1987).

Structurally, this field represents the small subsurface anticline with around 20 Km length and 4 Km width at the top of Upper Qamchuqa Formation (Figure 1.2) and it is trending with the Jambour structure to its southeast with some shifting from the Bai Hassan structure to the northwest. In the past it was believed that this dome is an extension of the Bai Hassan structure, after the interpretation of the seismic section it was indicated as an independent enechelon structure. These three oil fields are located in a parallel manner to the southwest of the main Kirkuk structure (Figure 1.1).

About 30 wells were drilled on the Khabbaz oil field, although a large number of these wells were targeted to the Tertiary reservoirs, more than half of them penetrated the Upper Qamchuqa reservoir, and only a few wells reached the Lower Qamchuqa pay zone.

Figure 1.3 shows the geological cross section along the Khabbaz oil field from the top of Upper Qamchuqa Formation with two underlain units, Upper Sarmord and Lower Qamchuqa Formations. The section from the northwest to the southeast direction and it is denoted by A (NW) – B (SE). Also the

figure illustrates the normal fault to the right side of the section with around of 100m displacement of Upper Qamchuqa Formation in well Kz-7.

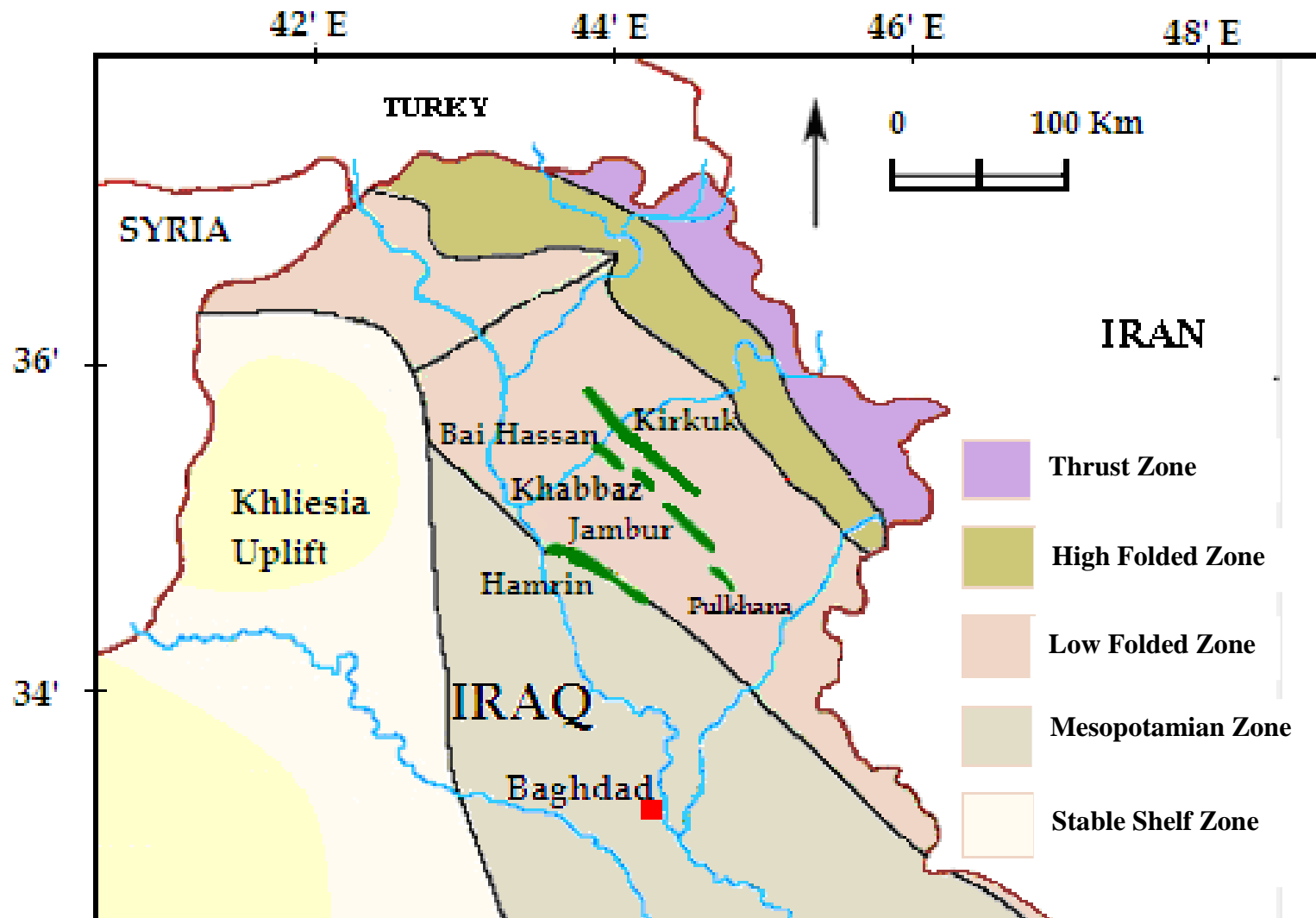


Figure 1.1: Map of Iraq showing the location of the Khabbaz oil field, with tectonic subdivisions (after Buday and Jassim, 1987).

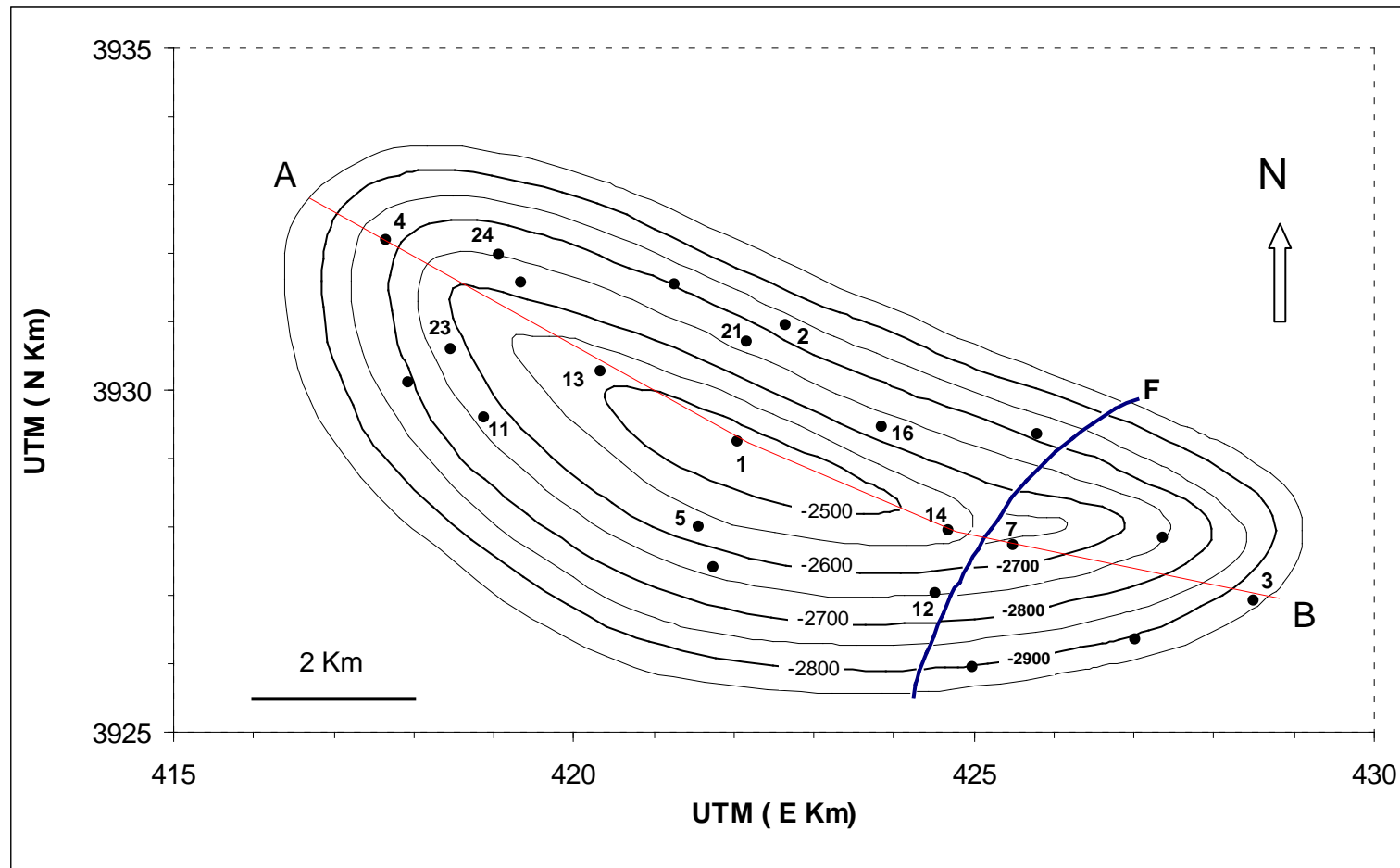


Figure 1.2: The structural contour map with (m) on the top of Upper Qamchuqa reservoir in Khabbaz oil field.

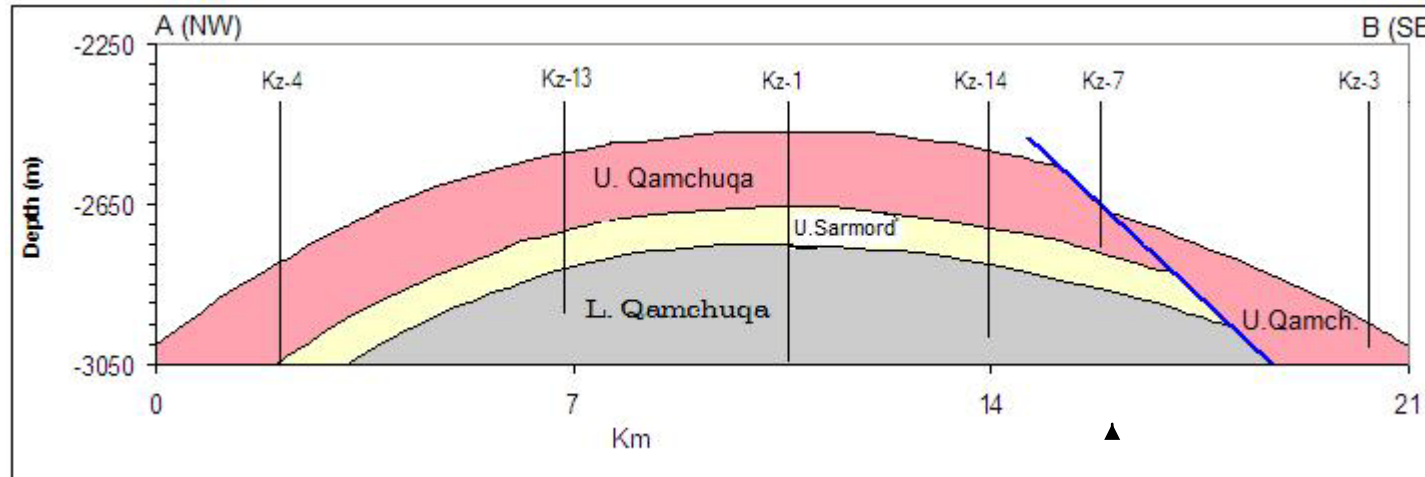


Figure 1.3: Structural cross section along the Khabbaz field axis (A-B), which shows the three formations; Lower Qamchuqa, Upper Sarmord, and Upper Qamchuqa Formations. (See Figure 1.2 for location of the section).

Chapter Two

Stratigraphy and Sedimentology

2.1 Paleogeography and Sedimentary Basin

During the Cretaceous time, the Middle East area was divided tectonically and stratigraphically into three positive features (Wilson, 1975; Al Shakiry, 1977), the first feature is the Arabian shield in the west, the second is the Qatar- Surmah high to the south, which is a large uplift of the Mesozoic age, and acted as a nucleus for carbonate sand and rudist development, the third positive feature is the Mosul Block in the north. Along with the above positive area, two major troughs exist to the east of Arabian shield. The northern basin was a part of the Zagros geosyncline, with its east side there was sediment starved and deep from Jurassic to Cretaceous, while its southwestern part (generally termed the Basrah Basin) was the site of accumulation of as much as 1000 meters of mixed terrigenous and limestone sediments (Wilson, 1975).

During the Early and Middle-Albian age, the siliclastic sediments had spread to the whole platform, except the narrow belt in the northeast side (possibly Dhok-Chemchemal ridge), which separates this platform from the Balambo basin, (Murriss, 1980; in AL-Karadaghi, 2001). The Balambo basin represents the extension of the Lurestan basin (Garau Formation) of the Iranian territory, which is separated by a shallow mixed – carbonate shelf from the Khuzestan sub-basin (Murriss, 1980 in AL-Karadaghi, 2001; Tagavi, et.al. 2007).

At Middle-Albian the sea level rises gradually, causing the Qamchuqa ridge (Buday and Jassim, 1987) which runs roughly along NW-SE direction; by the time this ridge grows vertically and laterally to the west and westward. Facies change occurs from the sandy sediments of Sarmord (or Nahr Umr) Formation to the carbonate shoal facies of Qamchuqa Formation, causing the development of lagoonal environment of evaporite facies represented by

Jawan Formation (Al Khirsan et al, 1992 in AL-Karadaghi, 2001). Facies changes were recorded essentially on some parts of the Foothill Zone, northwest of the line roughly connecting Tikrit – Samarra area with Jambour (Buday, 1980).

The underlying shale (Sarmord, Batiwa and Nahr Umr Formations) that deposited on the platform extends southward, parallel to Qamchuqa limestone ridge, then showing intertonguing with the Kazhdumi Formation in Iran, (AL-Karadaghi, 2001). While Chaton and Hart (1960) stating (in Al-Karadaghi, 2001) that "the Batiwa Formation is a lateral transition between the Nahr Umr sandstone and shale to the massive neritic limestone of the Qamchuqa Fformation".

During the Albian, the carbonate facies moved westward onlapping the restricted platform facies (i.e. the neritic and the lagoonal facies) hence the marine transgression caused the development of Mauddud formation (Upper Qamchuqa equivalent). The lagoonal belt to northeast of the line connecting Samarra-Dujaila-Ammara was replaced by neritic belt of Mauddud Formation (Homci, 1975 in Buday, 1980). In fact the transgression extended for a short time episode and is terminated by a regression at the most late Albian age (Al-Karadaghi, 2001).

Cretaceous deposits of Iraq in general, are distinguishable from sediments of other periods by the exceptionally great thickness of these sediments (Al Sadooni, 1978) compared to those above and below. Formations with several hundreds of meters of thickness were deposited in the Cretaceous basin, for example, Balambo Formation is 792 meters, Sarmord 455 meters and Qamchuqa (Upper and Lower) is 799 meters thick. These sediments, except the Balambo, were deposited in shallow to medium and to deep water, which indicate the high rate of subsidence of the depositional shelves during the Cretaceous (Al Sadooni, 1978).

The depositional history during the Lower and Middle Cretaceous period in northern Iraq characterized by some tectonic and depositional features

divided by Chatton and Hart (1961-unpublished report) in Al Saadooni (1978) to the following sectors or territories (Figure 2.1):

- A- The permanent basin: a basin is the most negative area in Iraq occupying the area from Sulaimani city to the Naft-Khana by the eastern borders along axis passing by Pulkhana (Figure 2.1). It was characterized by continuous sedimentation during all the middle and lower Cretaceous time, and mainly represented by globigerinal, basinal biomudstone of the Balambo Formation.
- B- The Neritic area: this area was situated to the west of the permanent basin. It is confined between the Pulkhana-Jambour-18 axis and the K-116 - Hamrin north. The area is characterized by neritic deposition during all the Early to Middle Cretaceous period where Garagu, Shuaiba and then Upper Qamchuqa (Mauddud) Formations were deposited.
- C- The Lagoonal – Supratidal zone: At this area the two types of deposits are recognized. On the eastern part of the sector, lagoonal evaporite and pelletal limestone of Jawan formation were formed, whereas on the extreme westward side of the basin supratidal conditions were common, with an area of interdigitation between both facies. The emerged areas are arranged into two sectors.
- D- The Mosul Block: This is the most positive area during the Cretaceous period. It occupied the area from Rawandoz in the east and all the present day Mosul area.
- E- The Gaara-Khlesia High: This is also a positive tectonic area (non deposition).

F- The last zone is constituted of siliclastic sediments that come from the rim of the African shield (Delfaud, 1986 in Al Shdidi, et. al., 1995).

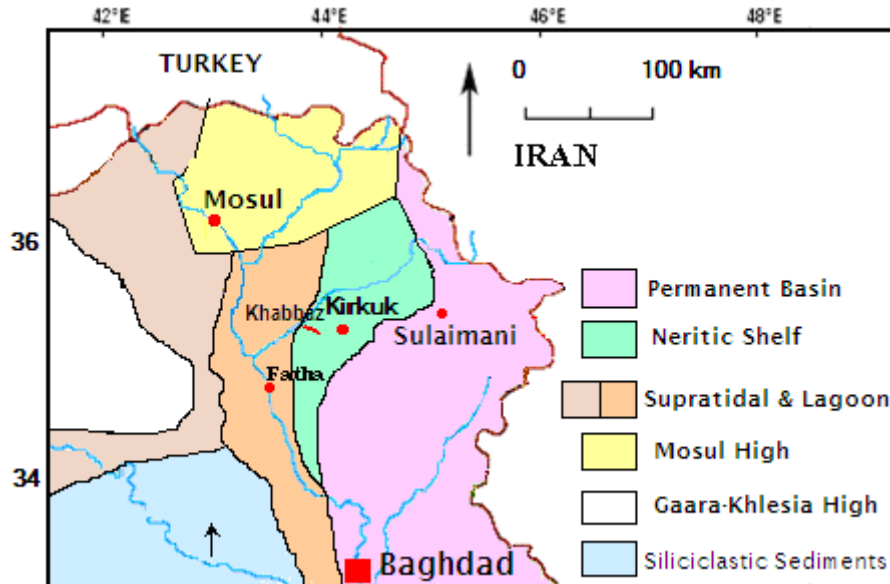


Figure 2.1: Aptian and Albian Paleogeography in North Iraq. (after Al Shdidi, et.al, 1995.)

Based on (Dunnington, 1958; Chatton and Hart, 1960) in Al Shakiry, (1977) the Early Cretaceous in Iraq is divided into two depositional cycles:

- 1- The Tithonian – Aptian cycle: In order from shore to basin, (generally from west to east and northeast), includes the following basic formations: Zubair, Ratawi, Yamama, Lower Qamchuqa, Sarmord, Chia Gara and Balambo. In the Kirkuk area, the lower Cretaceous sediments are subdivided lithologically into the following four units:
 - a- The Lower Qamchuqa Formation (Hautrivian – Aptian).

- b- The Middle Sarmord (Rattawi) Formation (Hautrivian - Late Valanginian).
- c- Garagu (Yamama) Formation (Hautrivian - Late Valanginian)
- d- Lower Sarmord Formation (Hautrivian – Late Valanginian).

In the eastern part of the area, the Lower Cretaceous deposits are of bathyal facies and they gradually pass westward into the Lower and Middle Sarmord marl and marly limestones, the Garagu oolitic limestone and the Qamchuqa neritic limestone.

The boundary between this cycle and the Albian cycle in the Kirkuk area is considered to be transitional (top of Lower Qamchuqa), (Gaddo, 1966 in Al Shakiry, 1977).

2- The Albian cycle: which includes the basic rock unit successions from shore to basin: Nahr Umr sands, Nahr Umr shales, Upper Qamchuqa, and Balambo Formations.

In Kirkuk area, the middle Cretaceous sediments are represented by the following units based on a study by Al Shakiry (1977):

- a- Kometan Formation (Turonian).
- b- Gulneri Formation (Turonian).
- c- Dokan Formation (Cenomanian).
- d- Upper Qamchuqa Formation (Albian).
- e- Upper Sarmord (Batiwah) Formation (Albian).

During the Albian, the eastern parts of Iraq were occupied by the Balambo facies. Toward the north and west, it grades from the neritic marly limestone and marls of Upper Sarmord, neritic limestone and dolomite of the Upper Qamchuqa formation, into the deeper marly limestone and shales of the Dokan, Gulneri and Komitan Formations

2.2 Stratigraphy and Subsurface Geology

Qamchuqa Formation represents one of the important rock units of Iraq, which consists of massive dolostone and dolomitic limestone. This formation is exposed extensively in the folded zone, it is known as a continuous single rock unit, and laterally changes toward southwest into two units: Upper Qamchuqa (equivalent to Mauddud formation), and Lower Qamchuqa (equivalent to Shuaiba formation), (Figure 2.2). They represent a potential oil reservoir in the subsurface in many oil fields of both the Foothill Zone and Mesopotamian Plain.

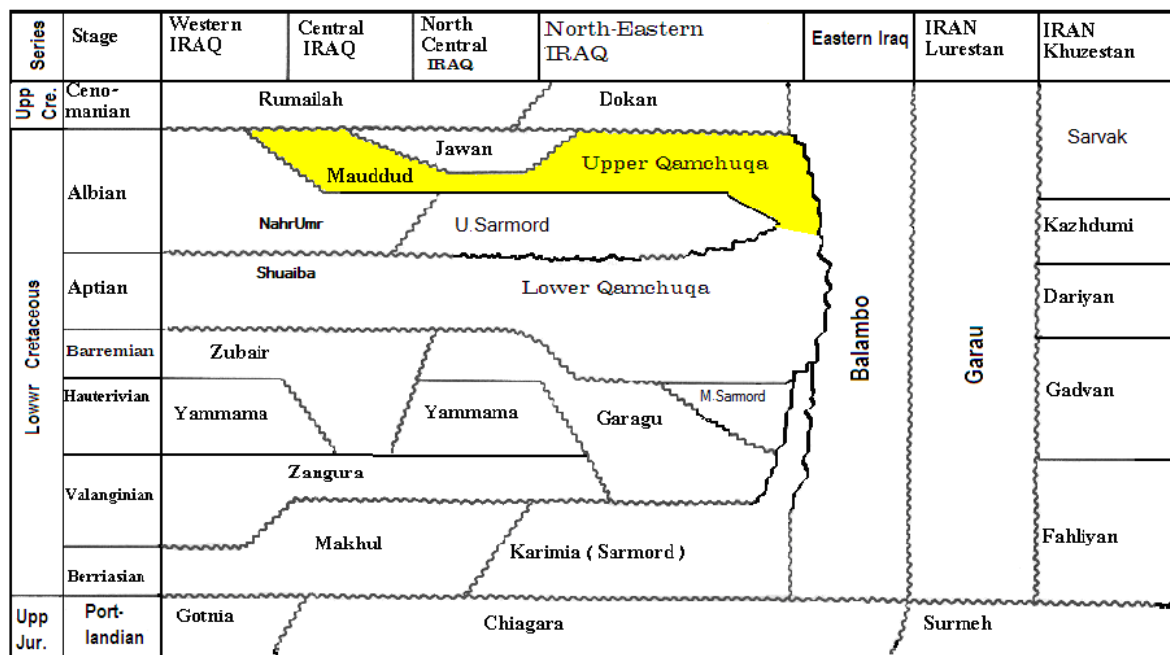


Figure 2.2: Stratigraphic correlation chart of Early - Middle Cretaceous formations, after (Allah-Werdi. 2001).

2.2.1 Qamchuqa Formation in Type locality:

The Qamchuqa Formation was described for the first time in 1950 by R. Wetzels in Bellen et al (1959) from Qamchuqa village (Type locality), east of Dokan dam site to the NE of Sulaimani city in northern Iraq. The section runs along the gorge to Sarmord. The formation was named after the gorge of Qamchuqa. The lower contact is conformable and gradational with Sarmord Formation, while the upper contact with Kometan Formation is an erosional unconformity but without angular discordance in the type section. In a new study by Ameen 2008, he concludes that the upper boundary of Qamchuqa Formation with overlying formations is conformable. According to Bellen et al (1959), adopted Wetzels definition for the formal recognition of the Qamchuqa Formation with 799 meters thickness, comprises the neritic limestones (often strongly dolomitized) of the Hauterivian till Albian time space. He subdivided the type section into the following units from the top to base, with brief description of each unit:

a- Upper Dolomite Unit (192m thick), comprising generally coarsely crystalline, granular, rhombic and mosaic dolomites replacing neritic, organic limestones with molluscan detritus.

b- Upper Limestone Unit (28m thick), comprising detrital limestones, locally argillaceous, locally dolomitized, with *Cuneolina pavonia var. parva*.

c- Middle Dolomite Unit (316m thick), coarsely crystalline, mosaic or saccharoidal dolomite with some interstitial calcite.

d- Middle Limestone Unit (147m thick), comprising massive rather argillaceous limestones, partial-dolomitized, macrofossil debris and *Choffatella decipiens* and *Orbitolina cf. discoidea*.

e- Lower Dolomite Unit (55m thick), comprising very coarsely crystalline dolomite without significant vestiges of original fauna.

f- Lower Limestone Unit (61m thick), comprising massive limestone with rather argillaceous matrix, abundant macrofossil detritus; microfauna includes *Choffatella decipiens*.

2.2.2 Qamchuqa Formation in the Subsurface:

Qamchuqa Formation forms an important reservoir rock in northeastern Iraq oil field especially Kirkuk and surrounding areas (Kirkuk, Jambour, Bai Hassan, Khabbaz oil fields etc...). In 1953, Kirkuk deep well No. 109 was drilled and the Qamchuqa Formation was encountered between 1274.9 and 1795 meters, during 1959 another deep well was drilled, which is well K-116. McKinly (1959) unpublished report in Al-Sadooni (1978) divided the Qamchuqa section into two main formations; (1) Qamchuqa –Jawan Formation, (2) Lower Qamchuqa Formation. Later in 1963, Well K-130 was drilled, and the stratigraphic nomenclature has been changed to be more correlated with the Middle-Lower Cretaceous sediments of the southern Iraq. The Upper and Lower Qamchuqa have been renamed Mauddud and Shuaiba Formations respectively, and the name Nahr Umr or Upper Sarmord Formation was suggested to the marly limestone and shale unit between them.

Since that time, the Qamchuqa Formation (Upper and Lower parts equivalent to Mauddud and Shuaiba Formations respectively) become well-known all over the Low Ffolded Zone oil fields as a good Cretaceous reservoir, including Hamrin, Jambour, Khabbaz, Bai Hassan, Kirkuk(Baba Dome), Taq Taq, Ain Zala. Also a massive limestone of the equivalent age in NE Syria was defined (Andrew and Al Sadooni, 2006)... etc.

The equivalent unit of the formation is well known in southwest Iran and called Sarvak Formation which is a good carbonate reservoir of Khuzestan district oil fields (Tagavi, et. al. 2007).

2.2.3 Upper Qamchuqa Formation

The Upper Qamchuqa (or equivalent Mauddud) Formation is the most widespread Lower Cretaceous deposits which extend over most parts of the Arabian basin, and it represents a very shallow to shallow carbonate shelf with local basin margin rudist buildups that was established following the

shutdown of the clastic of the Nahr Umr Formation (Sadooni and Alsharhan, 2003).

In Iraq its thickness varies due to lateral facies change and erosional truncation (Sahar, 1987). The formation extends over the Stable shelf and in the Foothill and High Folded Zones of the Unstable Shelf.

The isochors map (Figure 2.3) shows that the Upper Qamchuqa basin which has the general trend of northwest to southeast, and the thickness decrease around the Mosul Block, and it shows the rapid increase westward of Sinjar basin, whereas its thickness reaches 125m in well Bautma-1 and 198m in well Tal-Hajr-1.

The thickness also increases northeastward of Kirkuk area, the average thickness of Upper Qamchuqa in Khabbaz field is around 168m which increases toward the central part of the Qamchuqa basin where it reaches 237m in well kirkuk-130 and 250m in well chamahmal-1

The lower contact of the Upper Qamchuqa (Mauddud) Formation is conformable and gradational with the Upper Sarmord, or Nahr Umr or Lower Balambo Formations. The upper contact is marked by a break and it is either nonsequential or unconformable (Bellen et al, 1959; Sahar, 1987; Jassim and Goff, 2006).

The Upper Qamchuqa (Mauddud) Formation passes into the Balambo Formation on the northeast part of the High Folded Zone, while on the Mosul High the formation passes into the Jawan Formation.

In Syria, in the Palmarides and central Syria, the neritic dolomitic limestones of the upper part of the Asafir Formation are equivalent to the Upper Qamchuqa Formation (Jassim and Goff, 2006). In southwest of Iran the Albian part of the Sarvak Formation is also equivalent to the Upper Qamchuqa (Mauddud) Formation (Jassim and Goff, 2006; Tagavi, et. al. 2007).

In Kuwait the Burgan Formation (shallow inner shelf environment) equivalent of Maaddud (Upper Qamchuqa) Formation (Jassim and Goff, 2006).

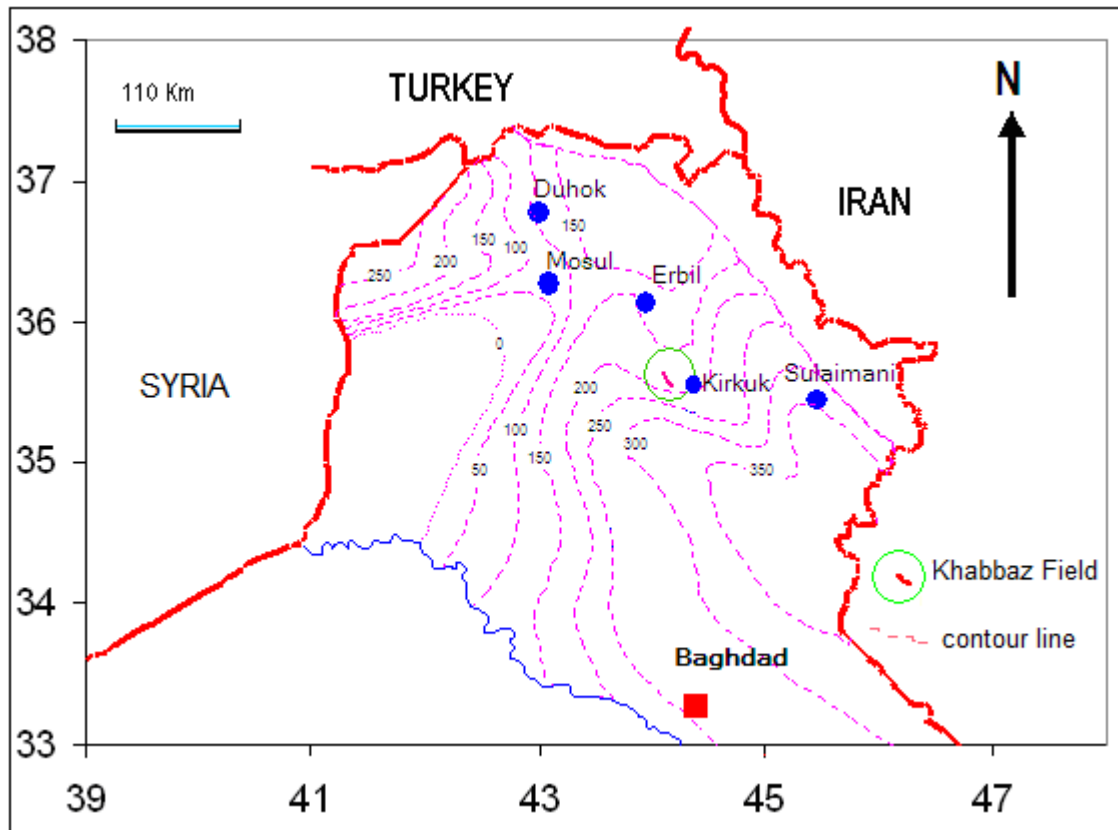


Figure 2.3: The Isochore map of Upper Qamchuqa Formation with 50m contour intervals, after Sahar, 1987.

2.2.4 Upper Qamchuqa Formation in the Khabbaz Oil Field:

Structurally, the Khabbaz oil field represents a small subsurface structure (asymmetrical anticline) located between Jambour and Bai Hassan oil fields (Figures 1.1&1.2). Its axis runs on the same trend of Jambour structure and slightly shifted from Bai Hassan structure. The upper contact of the Upper Qamchuqa Formation in Khabbaz oil field is unconformable with the overlying Dokan Formation; this is indicated clearly from log curves, especially **GR** log that shows the abrupt increasing along the contact through the well sections all over the field (Appendices A1-A9).

This phenomenon is also observed in Bai Hassan oil field (AL-Peryadi, 2002). On the other hand, the sonic transit time (Δt $\mu\text{s}/\text{ft}$) curve shows a low value along the dense rock of Dokan limestone, which rapidly increases opposite the underlying porous part of Upper Qamchuqa (Figure 2.4).

The lower boundary of Upper Qamchuqa Formation with underlying Upper Sarmord Formation is conformable, where the GR log shows the gradational increasing from the top of the formation toward the lower part which is influenced by Upper Sarmord shale dominant (Figure 2.4 and Appendices A1-A9). On the other hand the porosity logs (Neutron, Density, and Sonic) show the gradational decreasing of porosity toward the base of Upper Qamchuqa Formation (Figure 2.4). This unit is gradationally changed into the underlain Upper Sarmord unit with about 120m of shale, marl and argillaceous limestone

The Upper Qamchuqa Reservoir of Khabbaz oil field has the thickness ranging between 156 to 180m (with an average of 167.63m), (Table 2.1), and mainly consists of dolomite, dolomitic limestone, limestone and marly limestone..

Table 2.1: Illustrates top & bottom depths and drilled thickness of Upper Qamchuqa in the studded wells.

Wells		Kz-1	Kz-2	Kz-3	Kz-4	Kz-5	Kz-7	Kz-11	Kz-13	Kz-14	Kz-16
U. Qamchuqa	Top m.	2752.5	3025.5	3202	2979	2832	2931	2885.5	2805.5	2811.5	2905
	Bott. m.	29241	3205	3250	3150	2991	3010	3057	2982	2968	3061
	Thick. m	71.5	179.5	48 *	171	159	79*	171.5	176.5	156.5	156

*** Partially penetrated.**

2.3 Lithologic Units

The Upper Qamchuqa Formation shows variable lithologic characters which could be recognized by examining core (and cutting) samples from ten studied wells (Table 2.1). Wireline log interpretations assist lithologic interpretation of uncored or poorly sampled intervals as well as help in the determination of thickness of these units in different wells. Final well report documentations of some of these wells (Kz-1, Kz-2, Kz-3, Kz-4, Kz-11, Kz-13, and Kz-14) are also considered in reviewing the general lithologic characters of the reservoir. The lithologic characters of the formation are generally consisting of dolostone and dolomitic limestone with intercalation of marly limestone and shale, and in all studied wells these lithologies are distinguished in three parts or units. (Figure. 2.4) Illustrates these three lithologic unit divisions, the upper part (unit A), the middle part (unit B) and the lower part (unit C).

These subdivisions are found to be generalized and persistent over most of the studied wells. Below a brief description of each unit:

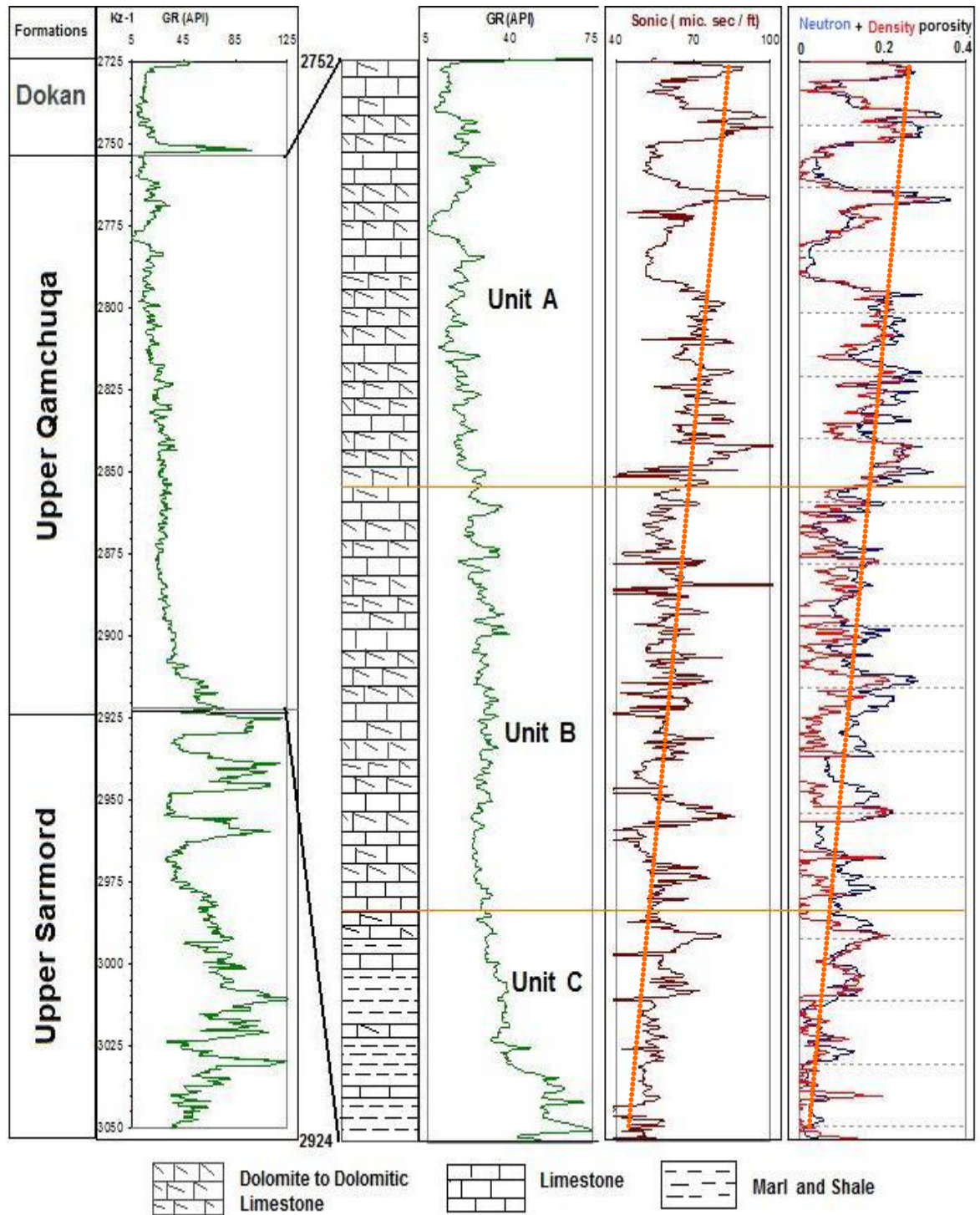


Figure 2.4: General composite column of Upper Qamchuqa Formation, in Khabbaz oil field, well (Kz-1), showing log responses (GR, Sonic, Neutron porosity red color and Density porosity blue color) to major lithologic unit characters and boundaries. (The labeled numbers denoted to depth with meters), porosity logs show downward decreasing of porosity denoted by orange dashed lines).

UNIT (A)

This unit represents the upper lithologic part. It ranges in thickness from 62 to 69.5m with maximum thickness in well (Kz-13) at the central part of the field, where it reaches 69.5m, (Table 2.2). This unit is easily recognized from the Neutron-Density combination porosity (N-D) logs, which is characterized by high porosity intervals (Figure 2.5), and this unit includes principal reservoir subunits. This unit is generally characterized by alternation of light gray hard, dense, fossiliferous and occasionally bioturbated limestone with buff brown medium to soft sucrosic to fine crystalline dolomite, and dolomitic limestone (Figure 2.6 a). The dolomite horizons are dominant, usually oil-stained to saturated, and occasionally characterized by vuggy porosities. These horizons are frequent and exceeds six in numbers in some cases and commonly associated with most porous and permeable parts of the unit.

UNIT (B)

Unit (B) represents the middle and thickest part of the Upper Qamchuqa Formation. It ranges in thickness between 66.5 and 79.5m, with maximum thickness in well Kz-11 (Table 2.2). It consists of alternation of dolostone, dolomitic limestone and limestone with secondary intercalation of marly limestone. The dolostones are represented by irregular horizon of buff, medium, hard, sucrosic to coarse crystalline dolomite. It is commonly associated with vugs and saturated with oil (Figure 2.6b). The limestone and the dolomitic limestone are generally gray to light gray in color, hard, bioturbated and intercalated with dark green fissile shale or marl. Occasionally, white irregular patches of anhydrite inclusions are recognized within the dolomitic part (Figure 2.5b).

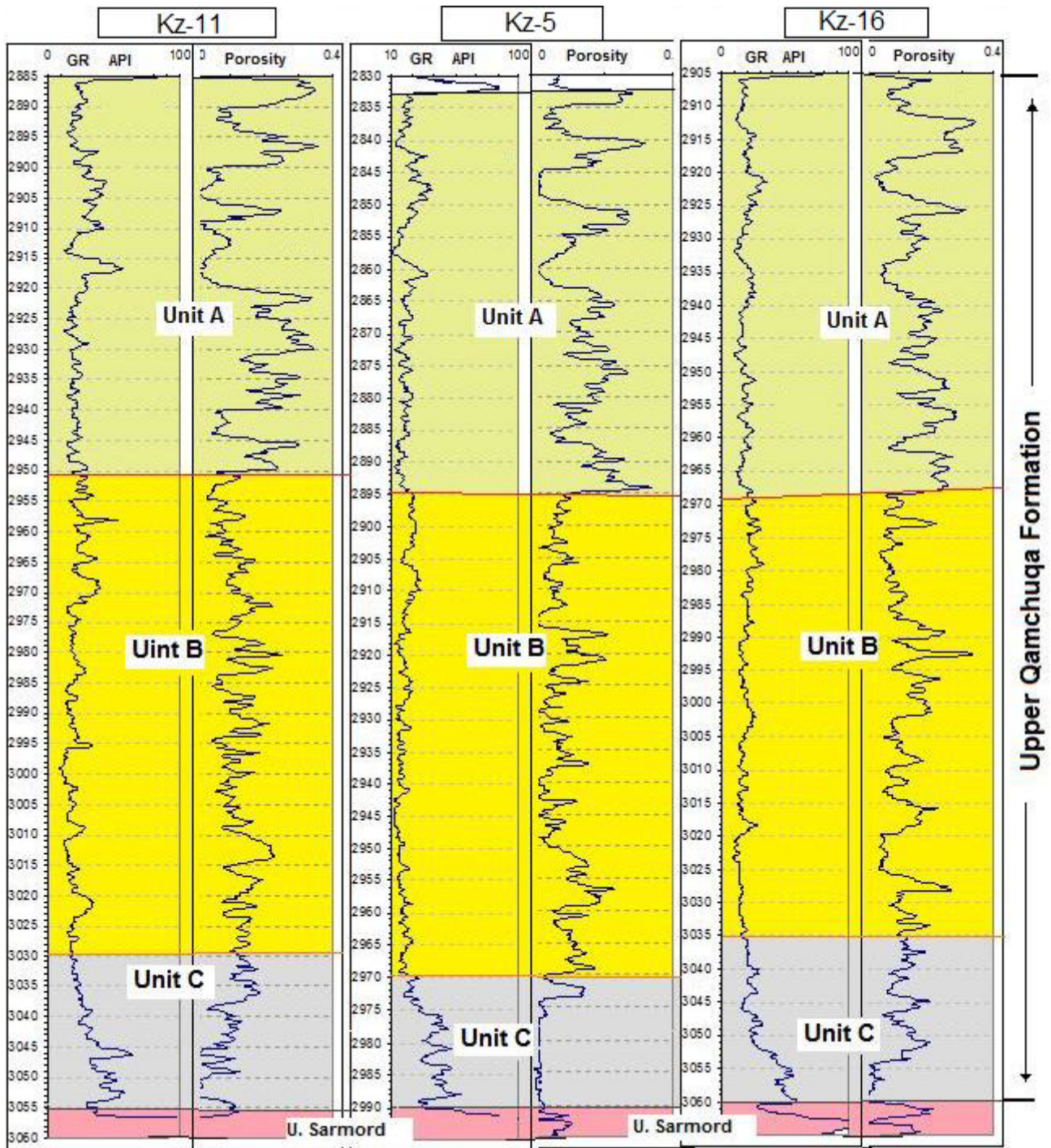


Figure 2.5: Shows the correlation of different logs (GR and N-D porosity) against the lithologic units of Upper Qamchuqa Formation in three wells, Kz-5, Kz-11 and Kz-16, over the axial trend of the field.

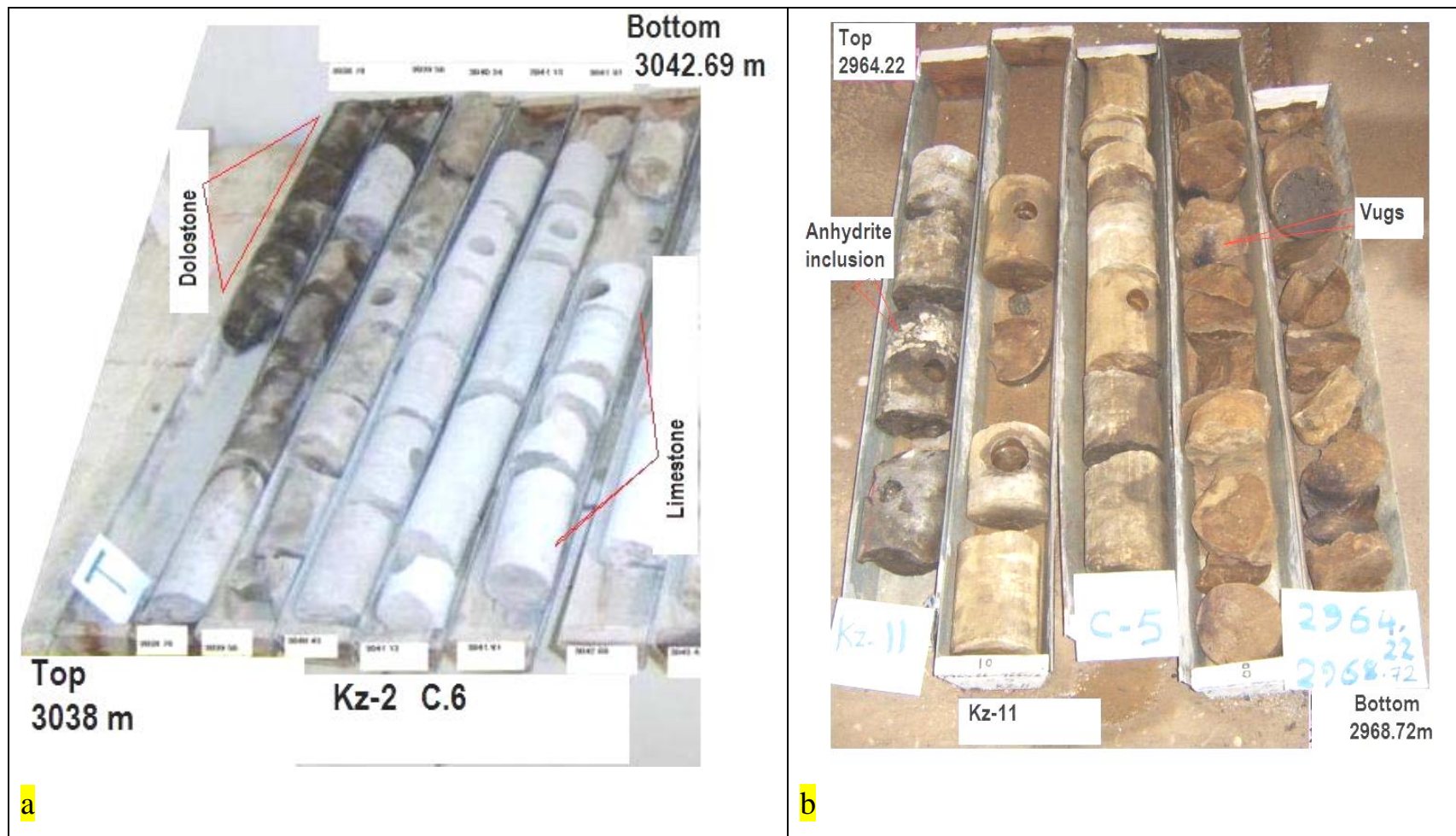


Figure 2.6: (a) Core (with 2 $\frac{1}{4}$ inch diameter) represent unit (A) in well Kz-2 showing alternating light color grey hard limestone, and dark color oil saturated porous dolostone (b) core (with 3 $\frac{1}{4}$ inch diameter) sample of unit (B) in well Kz-11 showing irregular alternating dolostone, dolomitic limestone and bioturbated limestone. The brown colors belong to the oil staining of the core.

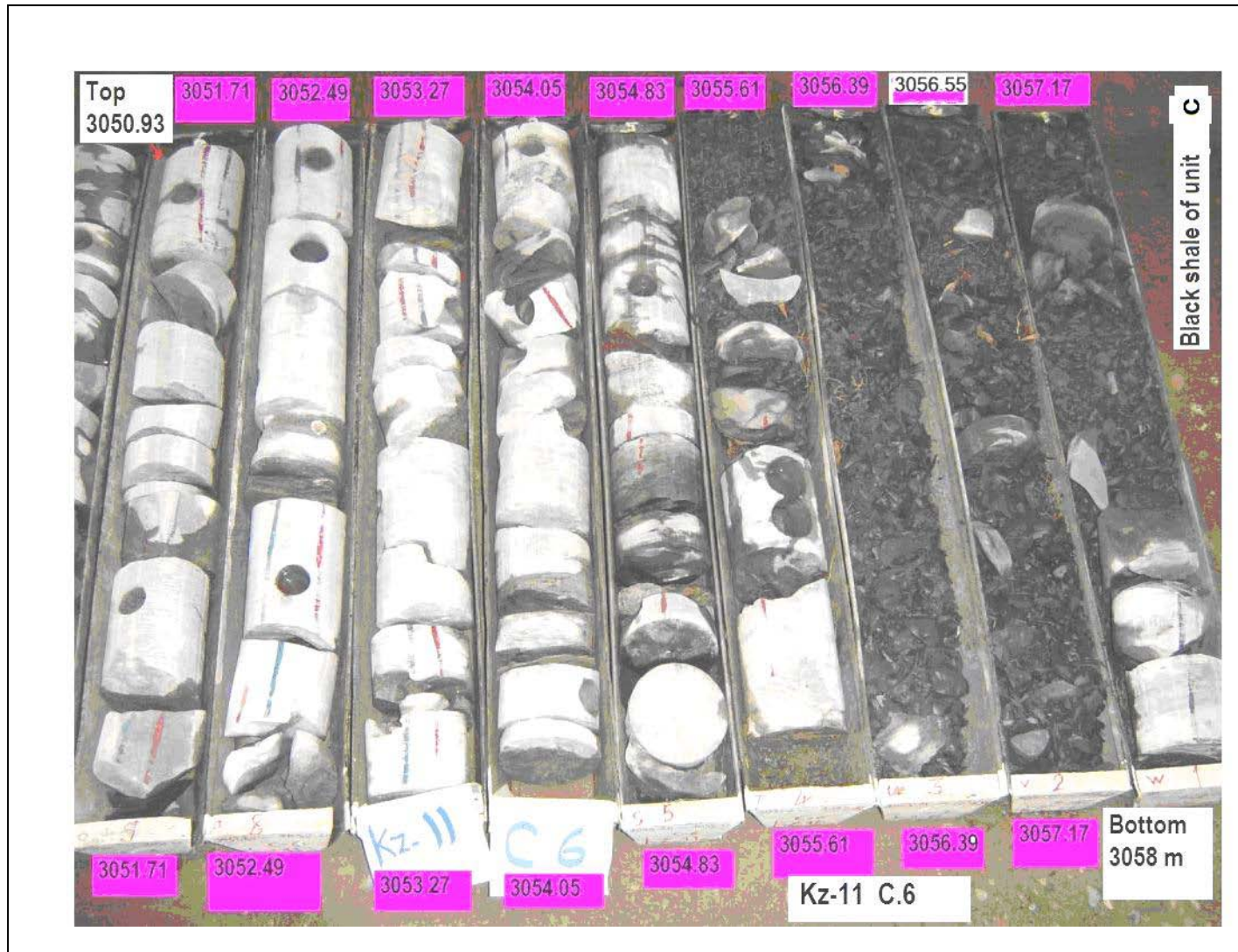


Figure 2.7: Core photograph of Upper Qamchuqa Formation from well Kz-11 (core No.6 with 3 1/4 inch diameter) represent unit C, showing typical lithologies of light grey bioturbated limestone, and dolomitic limestone dolostone with dark fissile shale (right hand side).

UNIT (C)

It represents the lower part of the Upper Qamchuqa Formation; this unit generally consists of alternation of light gray to whitish gray hard, bioturbated, fossiliferous, and occasionally marly or dolomitic limestone. It shows fine crystalline limestone or dolomitic limestone (Figure 2.7), with dark gray to black fissile, friable shale or marlstone. The shale portion is usually variable but generally increased downwards. The thickness of this unit is greatly variable and ranges between 19.5 and 42m (Table 2.2). The shaleness of this unit indicates the influence of Upper Sarmord Formation. Microfractures filled with dried bitumen, some pyrite crystals observed in some intervals.

Table 2.2: Top/bottom and thickness of lithological Units of the Upper Qamchuqa Formation in the studded Wells of the Khabbaz Oil Field.

wells	U. Qamchuqa Interval & Thickness m	Units	Units interval (m)	Units thickness (m)
Kz-1	2752.5 – 2924 171.5	A	2752.5 - 2821	68.5
		B	2821 - 2888	67
		C	2888 - 2924	36
Kz-2	3025.5 - 3205 179.5	A	3025.5 - 3091.5	66
		B	3091.5 - 3163	71.5
		C	3163 - 3205	42
Kz-3	3202 – 3250 48	A	3202 - 3250	48
		B	----- Non penetrated -----	
		C	----- Non penetrated -----	
Kz-4	2979 - 3150 171	A	2979 - 3047	68
		B	3047 - 3120	73
		C	3120 - 3150	30
Kz-5	2832 – 2991 159	A	2832 - 2895	63
		B	2895 - 2969	74
		C	2969 - 2991	26
Kz-7	2931 – 3010 79	A	----- Displaced by the fault	
		B	2931 - 2975	44
		C	2975 - 3010	35
Kz-11	2885.5 – 3057 171.5	A	2885.5 - 2950.5	65
		B	2950.5 - 3030	79.5
		C	3030 - 3057	27
Kz-13	2805.5 – 2982 176.5	A	2805.5 - 2875	69.5
		B	2875 - 2947	72
		C	2947 - 2982	35
Kz-14	2811.5 – 2968 156.5	A	2811.5 - 2873.5	62
		B	2873.5 - 2948.5	75
		C	2948.5 - 2968	19.5
Kz-16	2905 – 3061 156	A	2905 - 2968.5	63.5
		B	2968.5 - 3035	66.5
		C	3035 - 3061	26

2.4 Microfacies Analysis

Microfacies include those characteristics and distinctive aspects of a sedimentary rock which are visible and identifiable under a low power magnification microscope (Bate and Jackson, 1980). It is the total of all paleontological and sedimentological criteria which can be classified in thin-

sections, peels, and polished slabs (Flügel, 1982). The microfacies analysis is attempted here to investigate:

- a) Type and distribution of microfacies to define specific rock types and sedimentary facies identification.
- b) To recognize the type and the influence of various diagenetic processes on reservoir quality.
- c) To identify the type and the distribution of pore spaces and its relation to sedimentary facies.
- d) To evaluate relations between pore throat system and reservoir flow units.

The analysis is conducted using petrographic studies of about 500 thin sections selected for core and cutting samples from 10 wells for the examined interval. Staining of dolomitized samples were attempted following Dickenson (1966) to differentiate between limestone (calcite) and dolomite. Identification of microfacies of the studied sequence is assisted using previous related studies such as: Al-Sadooni 1978. Al-Shadidi et al. 1995. AL- Peryadi 2002., Sadooni and Al-Sharhan 2003.

Nomenclature of microfacies followed Dunham schema (1962) with slight modification especially for dolomitized samples. Textural description of dolomite and terminology is conducted following Sibley and Gregg (1982). Attempts were made to restore original fabric and sedimentary microfacies of dolomitized samples by using relict fabric within original undolomitized components. Terminology of pore types and classification is adopted after (Choquette and Pray, 1970), (Reeckmann and Friedman, 1982), and Pittman (1992) in addition of final well reports of studied wells carried out by North Oil Company.

Microfacies analysis is done for the three basic rock types: Limestone (L1, L2, L3,), Dolomitic Limestone (DL1, DL2, DL3,) and Dolostone (D1, D2, D3,). Symbols were used as such to simplify references to different microfacies in diagrams and texts.

Below is the discussion of the different microfacies:

2.4.1 Limestone Microfacies (L)

(L1) Bioclastic Wackestone to Packstone

Grains of this microfacies are dominated by fine sand to silt size skeletal fragments and debris, commonly of rudist bioclasts (Figure 2.8a).

Other bioclasts include molluscan, miliolids, algae, and usually of finer size. Matrix is recrystallized micrite, sometimes clayey, or replaced partially to completely by sparry calcite. This facies prevails in most limestone intervals through lithologic units, especially upper parts of Unit "A".

Porosity is generally low and is characterized by dissolution intergranular spaces, intraskeletal vugs and rarely moldic.

(L2) Peloidal – Bioclastic Wackestone to Packstone

Peloids and pseudopeloids are the characteristic grain types of this microfacies. Other grains of less abundant include lumps, molluscan bioclasts and miliolids (Figure 2.8.b). Matrix is dominated by micrite. Sometimes, grain matrix ratio is increased to grainstone type especially with rounded bioclasts of algal fragments (Figure 2.8.c). This facies is shown in lower part of Unit "A" within the limestone patches.

Porosity is mainly leached intergranular and sometimes moldic.

(L3) Milioline- Peloidal Packstone to Grainstone

Miliolids and peloidal grains are commonly associated together to form packstone to grainstones rock types (Figures 2.8.d, e, f, and g). Miliolids often show micritization. Other types of grains include bioclasts of gastropods and other types of benthic foraminifera. Matrix is less commonly leached micrite and commonly of micritic origin. In other cases, sparry calcite replaces part of the micritic matrix. This rock is occasionally stylolitic (Figure 2.8.h). Also this facies is encountered through most of limestone intervals.

Intraskelatal porosity is the common type along with the leached intragranular spaces (Figures 2.8, d, f).

Other less common porosity type is moldic and intercrystalline of dolomitized burrow fills, oil show of this microfacies can be seen either in isolated pores or along stylolite. (Figure 2.8.h)

(L4) Foraminiferal Mudstone Wackestone to Packstone

This is a typical basinal or deep marine microfacies. Characteristic features include: abundant planktonic foraminifera, skeletal debris of ostracods, echinoids and mollusks in a marly to clayey micritic matrix (Figure 2.9.a). Mostly this facies is consequent in the lower part of the Upper Qamchuqa Formation (Unit C), which is influenced by the Upper Sarmord Formation.

2.4.2 Dolomitic Limestone Microfacies (DL)

(DL1) Bioclastic Dolowackestone to Dolopackstone

This microfacies is represented by partially to completely dolomitized bioclastic limestone. Bioclasts are of shell fragments origin, mainly of rudist debris and other molluscs (Figure 2.9b). Dolomite is characterized by fine crystalline (10-20 μ), planar-e to planar-s type. Dolomitization which selectively affects the matrix along the stylolite (Figure 2.9c), or occurs as coarser crystalline mosaic (> 100 μ) when limestone is of bioclastic packstone (Figure 2.9d). This facies appears in unit "A" and "B" along the dolomitic limestone intervals.

Porosities in the dolomitic parts are clearly intercrystalline (Figure 2.9c), and in the nondolomitized parts are intergranular and intragranular (Figure 2.9d).

(DL2) Miliolid – Bioclastic Porphyrotopic Dolowackestone to Dolopackstone

Allochem type of this microfacies is dominated by miliolids and/ or bioclasts of rudist and other benthic forams. Matrix is neritic with slight recrystallization (Figure 2.9.f). Dolomite is distributed as fine to medium crystalline (10- 40 μ), euhedral rhombs of planar-p type (Figures 2.9.e and f).

Both matrix and grains are affected by this type of dolomitization but grains are of low intensity (Figure 2.9.e). This facies seems some intervals in lower part of unit "A" and upper part of unit "B".

(DL3) Peloidal – Bioclastic Dolowackestone to Dolopackstone

Pellets bioclasts are the dominant grain types with partially to completely dolomitized matrix, algal grains are locally concentrated (Figure 2.9.g). Dolomite occurs either as selectively replacing matrix and forming a fine crystalline mosaic, or as isolated euhedral, planar-p dolomite rhombs. The facies noticed in the middle part of the unit "A".

Oil shows are recognized occasionally by saturating dolomitized matrix of medium crystalline mosaic (Figure 2.9.h). Leached matrix formed the best intergranular type of porosity (Figures.2.9.g and h)

(DL4) Peloidal- Foraminiferal Dolowackestone to Dolopackstone

Allochems of this microfacies characterized by peloides and foraminifera mainly of miliolids (Figures 2.10.a and b). Other grains include skeletal debris.

In other cases, dolomite is pervasive and occurs as medium crystalline mosaic (20-100 μ), (Figures 2.10 c and d). Dolomite covers most of the micritic matrix with fine crystalline dolomite mosaic of planar-s type, or follows the weak fractured and stylolite zones and invaded them completely (Figure 2.10 e). Sometimes dolomitization is so intensive that only ghost of foraminifera can be recognized (Figures 2.10 c and d). Also this facies is alternated in the dolomitic limestone intervals especially in the middle part of the unit "A" and unit "C".

Porosity of this microfacies is either intercrystalline especially in the intensively dolomitized parts (Figure 2.10 e), or intergranular spaces (Figures 2.10.b, c). Oil

shows usually stains dolomitic intercrystalline pore-system along fracture or stylolite which are intensively dolomitized (Figure 2.10.e), or filled the moldic pores (Figures 2.10.a, and b).

(DL5) Fenestral Doloboundstone

The origin of this microfacies is seemingly stromatolitic boundstone of tidal flat environment. The unusual effective dolomitization of this facies yield an intensively dolomitized microfacies with relics of the original biogenic fabric (Figure 2.10f), porphyrotopic dolomite occasionally recognized overprinting biogenic fabric.

Porosity is commonly of fenestral stromatolitic boundstone of dolomitic facies type (Figure 2.10f).

(DL6) Foraminiferal-Bioclastic Mudstone- Dolowackestone to Packstone

Planktonic foraminiferids are the characteristic skeletal grains of this microfacies. It is usually embedded in clayey micritic matrix .Other skeletal grains include fine bioclasts (Figure 2.10g). Lamination sometimes can be recognized in thin-sections. Coarse bioclasts occasionally concentrated yielding excessive moldic porosity. This facies related to the unit "C" which is affected by Upper Sarmord Formation.

Dolomite is represented by floating rhombs of medium crystalline mosaic (Figure 2.10h); some isolated moldic pores are occasionally filled by dry bitumen.

2.4.3 Dolostone Microfacies (D)

(D1) Dolomudstone

This microfacies is characterized by very fine crystalline dolomite (< 10 μ) of dolo-mudstone type. Allochemical grains are rare. Occasional microvugs and/or fractures are the main type of porosity which is frequently stained by oil (Figure 2.11a).

(D2) Fine Crystalline Planar-s cloudy dolomite mosaic

The dolomite of this microfacies is characterized by fine crystalline (10-20 μ) and generally less than (20 μ) of type planar-s. Mosaic is commonly cloudy and occasionally includes ghosts of fine shell bioclastic or fragments (Figures 2.11.b, c, d). Dolomite crystals sometimes are anhedral in shape especially when it is too fine (<10 μ). Other special form of dolomite associated with this microfacies is coarse crystalline (> 100 μ) euhedral layer which is developed around pore spaces (Figure 2-11e). Common porosity type is intercrystalline (Figure 2.11f), vuggy, moldic or sometimes microfractures (Figure 2.11e).

(D3) Medium Crystalline Planar-e-s Dolomite Mosaic

This dolofacies is characterized by medium crystalline (20-100 μ), planar-e to planar-s mosaic. Relics of original micritic matrix can be recognized as fogged or cloudy mosaic (Figures 2.11. h, g), or other forams (Figure 2.12.a). Ghosts of skeletal grains such as orbitolinds (Figure 2.12.b), in other cases relics of the original micrite developed as a pseudopelletal fabric (Figure 2.12.c) or miliolids (Figure 2-12d), or skeletal debris (Figures 2.12.e, and f). This microfacies belongs to the lithologic unit "A" in most well sections, especially in the reservoir subunits A1, A2, and A3 and it has a positive role on the reservoir properties which make these subunits the main pay zones in most wells.

(D4) Medium Crystalline Planar-a Dolomite Mosaic

Planar-a dolomite type is the characteristic features of this microfacies. Crystal size commonly is medium and ranging between fine to medium (Figures, 2.12.f, g, h and 2.13.a). Fabric is dense with general low intercrystalline porosity. Mosaic sometimes is cloudy (Figure 2.12.g) or with micritic relics (Figure 2.13. b). In some cases vein-filling calcite are fractured and partly replaced by coarse crystalline dolomite of late diagenetic origin (Figure 2.12.h).

Oil staining is commonly associated with medium crystalline fraction which usually shows continuous intercrystalline pore network (Figure 2.13b), or

stylolites (Figures 2.13.a, and c). Leached porosity of intraskeletal origin developed into isolated moldic or vuggy porosity.

(D5) Coarse Crystalline Planar-e-s Dolomite Mosaic

It is characterized by coarse ($>100 \mu$), euhedral to subhedral dolomite crystals of type planar-e to planar-s with low intercrystalline but high vuggy porosity (Figures 2.13.d) Mosaic is sometimes cloudy. Mosaics some times occur as planar-a type with cloudy center which show no oil stains (Figures 2.13.d and 2.13 h). Common oil shows are associated with finer fractions which occupy intercrystalline porosity (Figures 2.13.e, and f). Other types of porosity are microvugs which show oil staining (Figure 2.13.g.). Dolomite Rhombs sometimes are too coarse and show progressive dissolution (Figures 2.14.a) Some times it coats dissolution vuggs and occurs as coarse euhedral planar-e layer (Figure 2.14.b). Undolomitized bioclasts can be occasionally recognized (Figures 2.14.c, d). In general, this microfacies (D5), is abundant consequently in the lithologic unit "B" from most well sections, and it has a negative function on the reservoir properties.

(D6) Planar- a, Dolomite Cement

This is a special type of dolomite with local occurrences. It is characterized by very coarse crystalline, clean, sometimes cleaved dolomite which replaces carbonate material (Figure 2.13.e). It is similar to the saddle dolomite of Sibley and Gregg (1982). And in many cases it replaces a skeletal grain forming irregular large dolomite patches (Figures 2.14.e.f). Also this microfacies belongs to the lithologic unit "B" in most well sections and it has a negative role on the reservoir properties.

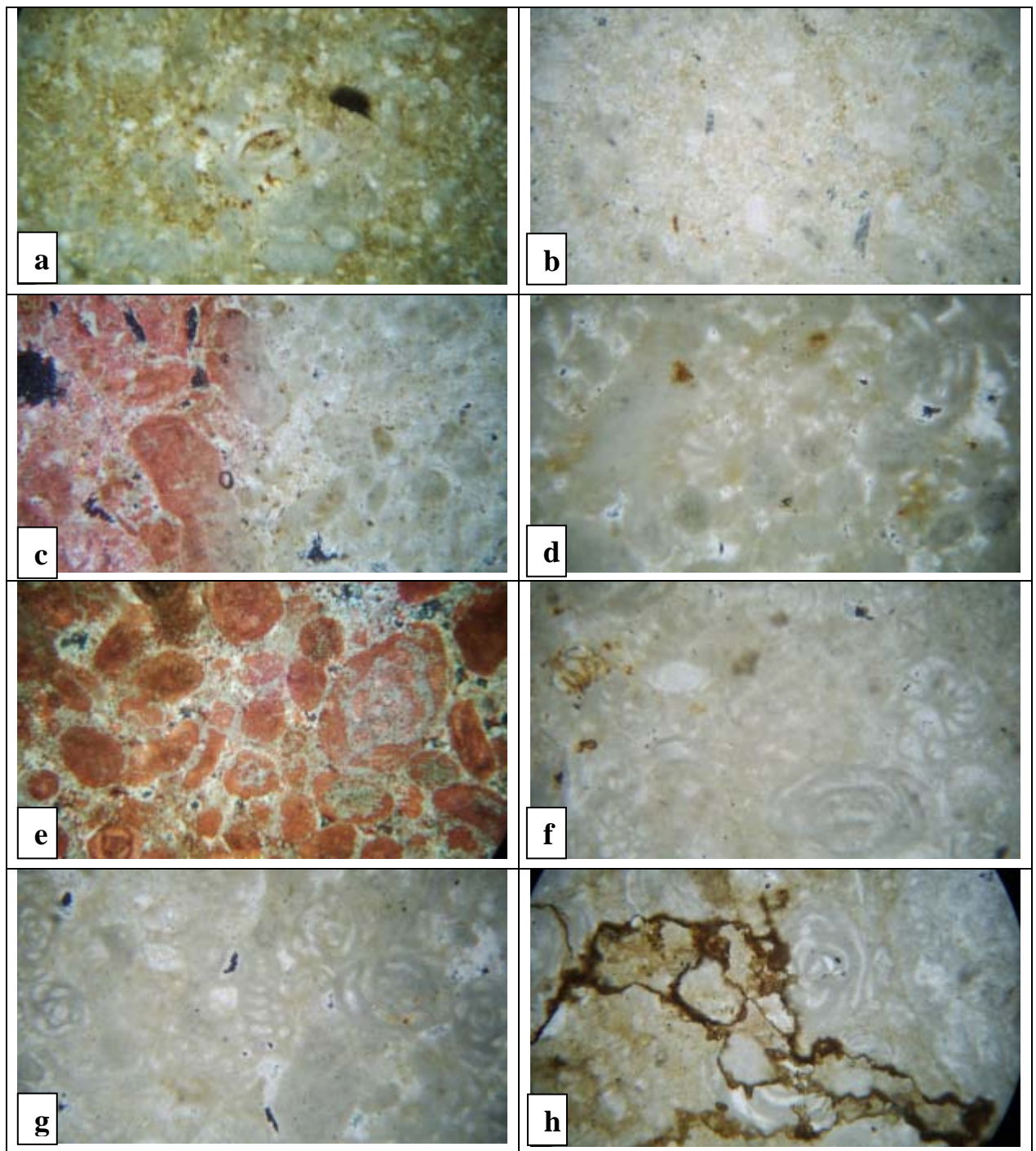


Figure 2.8: Limestone micro facies, (a) Kz-16/2911m, bioclastic packstone with dominant fragments of rudists. (b & c) Kz-16/2916.9 and 2936.25m, Peloidal- bioclastic wackestone to packstone,. (d, e, f, & g) Kz-16/2923, 2926, 2946.1m, and 2957 Miliolid-Peloidal packstone to grainstone, respectively. (h) Kz-16/ 2967m Mililoid bioclastic wackestone to packstone, the stylolite filled with oil. (all photos width is around 2mm and cross nickoled).

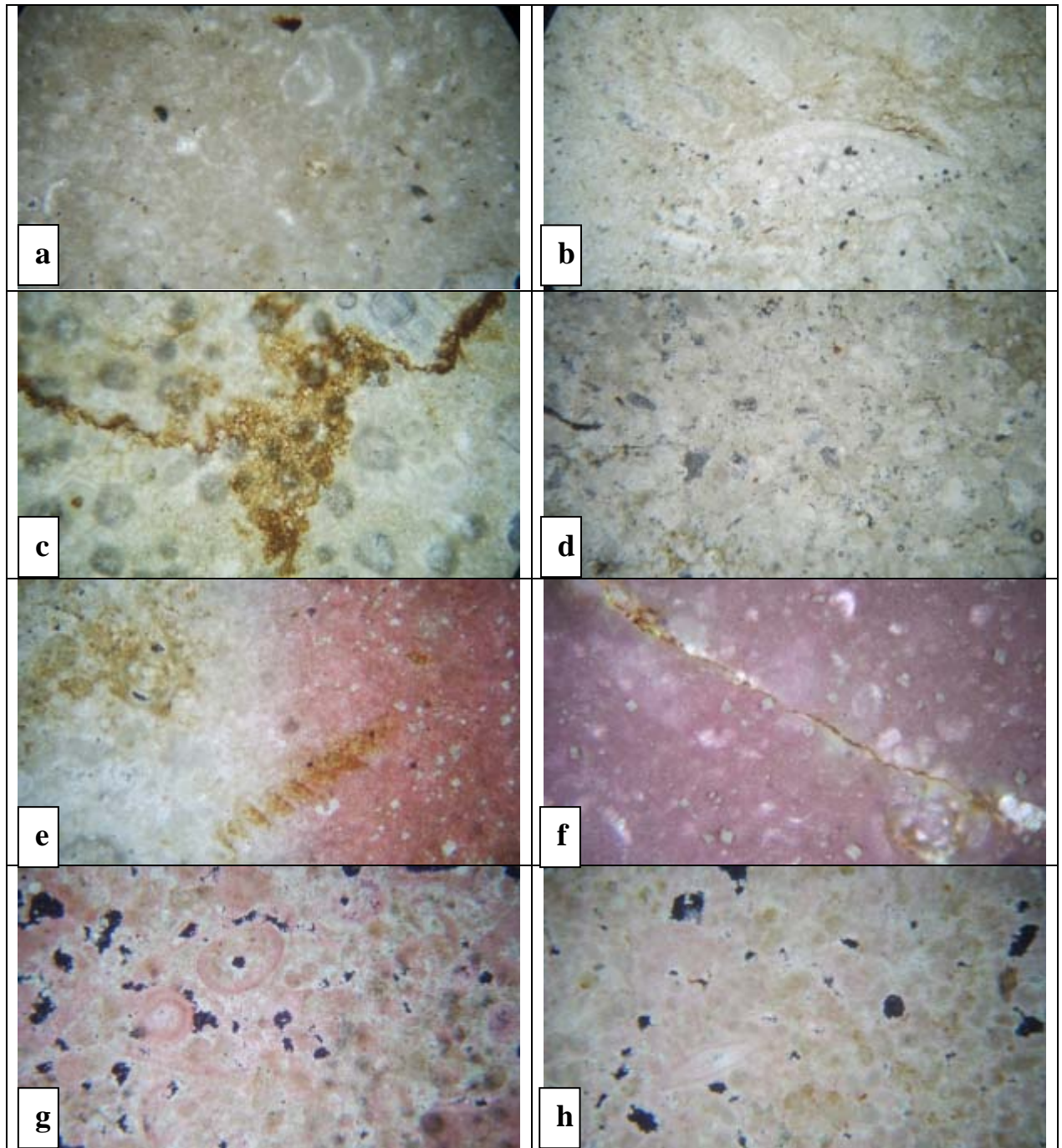


Figure 2.9: (a) Kz-16/3061-62m, Basinal Foraminiferal marly wackestone to packstone. (b & c) Kz-16/2920,2927.58, bioclastic dolowackestone to dolopackstone facies the latter shows selective dolomitized along the stylolite which is oil stained. (d) Kz-4/3094-95m, Bioclastic dolowackestone to dolopackstone facies. (e & f) Kz-16/ 2945.85, 2975.1m, Miliolid- bioclastic porphyrotopic dolowackestone to dolopackstone the oil followed ghost of Miliolid and other molds. (g & h) Kz-16/2938.85, 2939.4m, Peloidal-bioclastic dolowackestone to dolopackstone. (all photos width is around 2mm and cross nickoled).

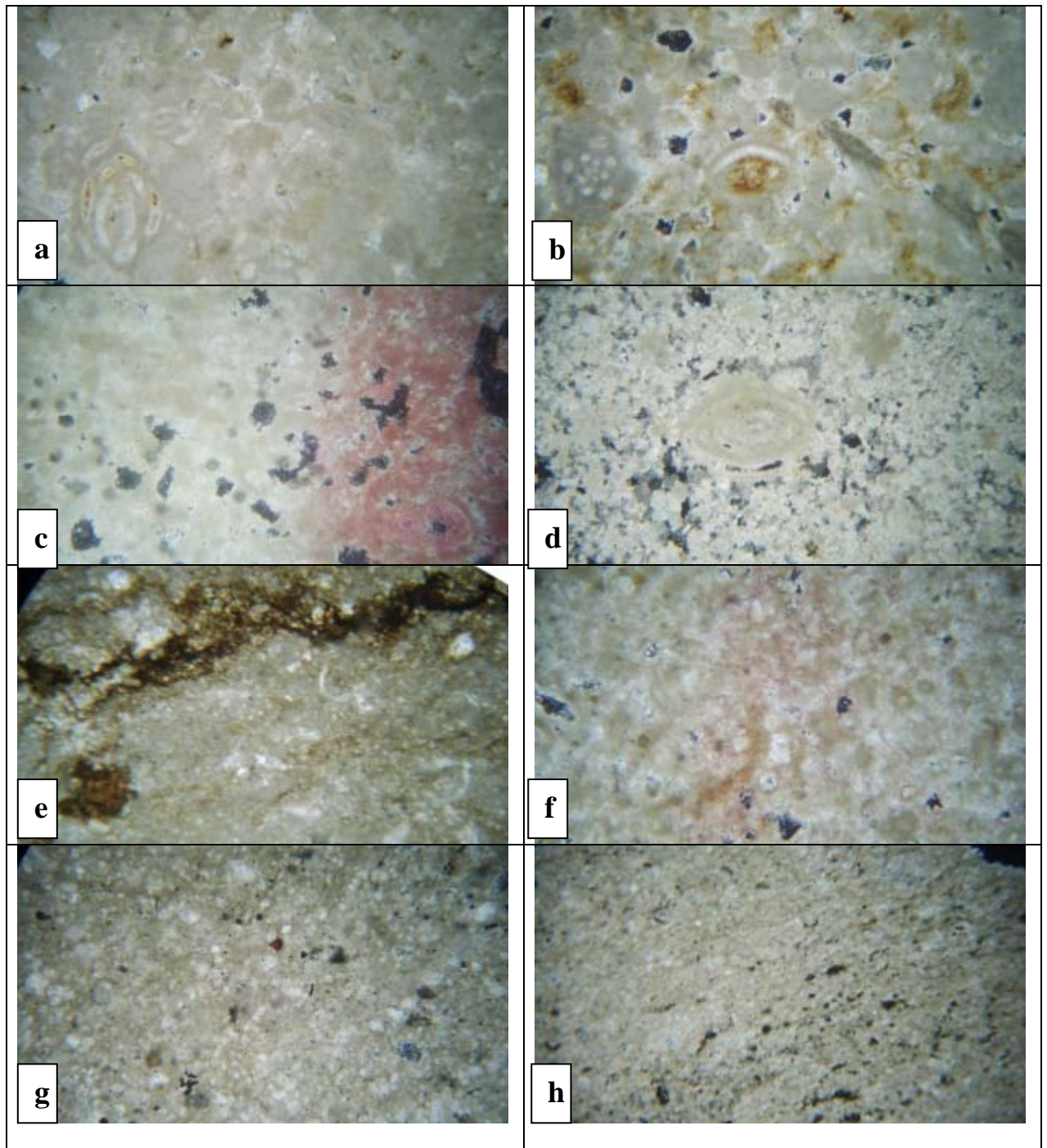


Figure 2.10: (a, b, c, & d) Kz-16/ 2929, 2930, 2941, 2942m, Peloidal-Foraminiferal dolowackestone to dolopackstone facies the moldic porosity stained by oil. (e) Kz-4/3145m, Foraminifera and bioclast, selective dolomitized, oil stained especially along the fracture. (f) Kz-16/ 2953.85m, Fenestral doloboundstone. (g) Kz-11/3049 and (h) Kz-16/3061; Foraminiferal-bioclastic marly dolowackestone to dolopackstone, (all photos width is around 2mm and cross nickoled).

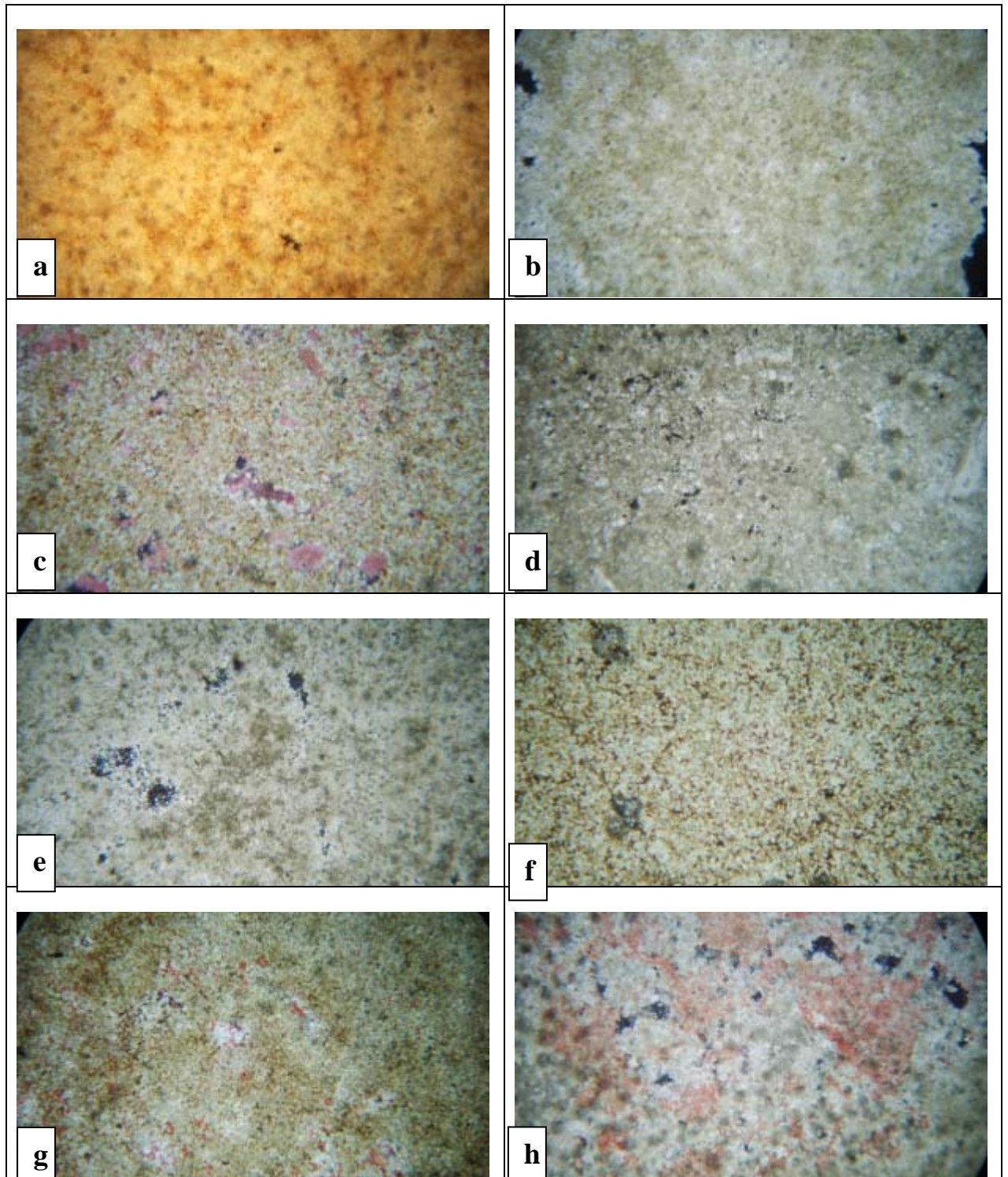


Figure 2.11: Dolostone microfacies. (a) Kz-16/ 2995, Very fine crystalline dolomudstone, impregnated with oil. (b, c, d, e, & f) Kz-16/ 2910, 2915.7, 2918, 2959.1, and 2992m respectively, the photos show fine crystalline planar- s cloudy dolomite mosaic, they are show oil impregnation. (g, & h) Kz-16/ 2967and 2940m, medium crystalline planar-e-s dolomite mosaic, this facies has the good reservoir characteristics. (all photos width is around 2mm and cross nickoled).

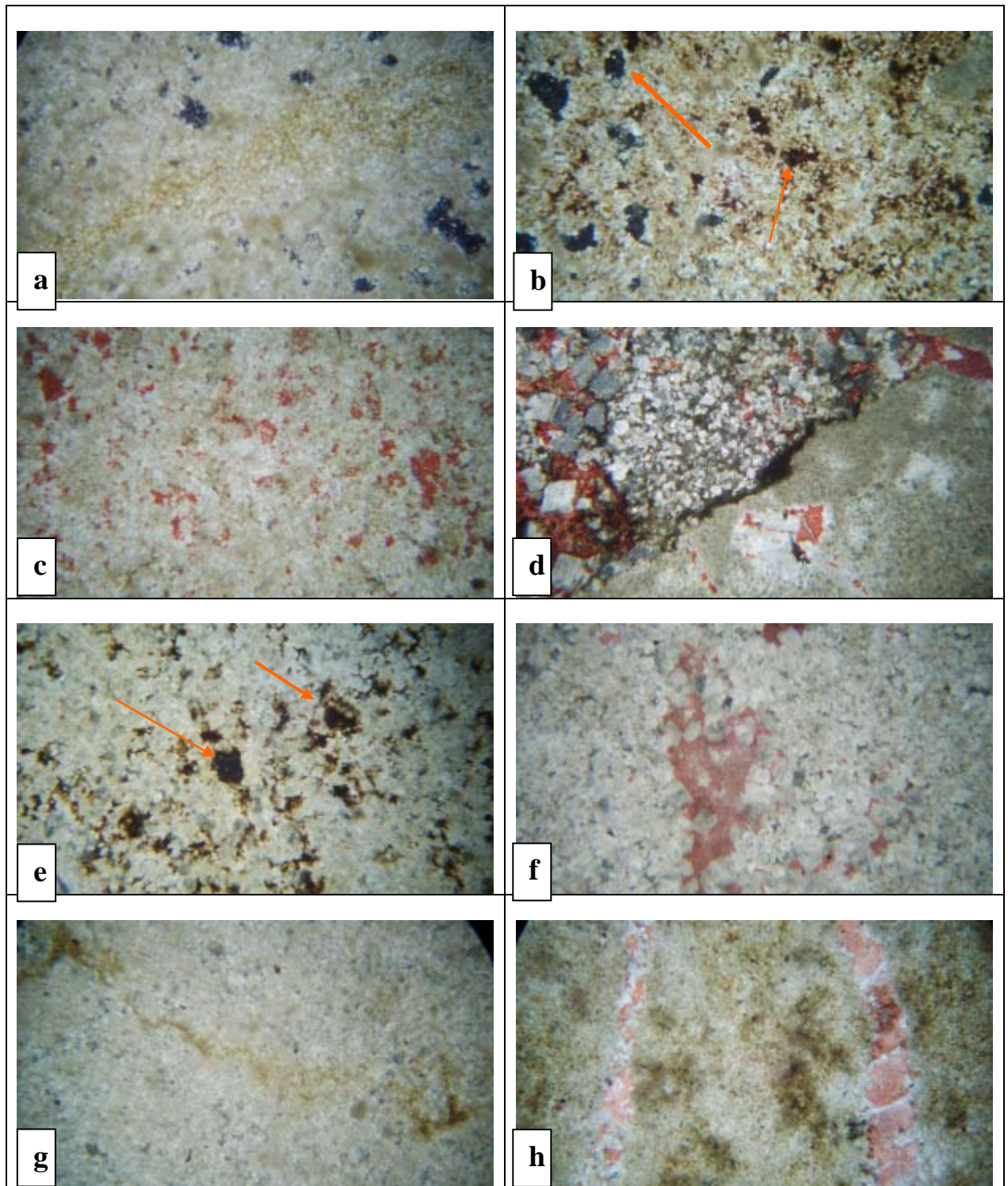


Figure 2.12: (a, b, c, d, e, & f) Kz-16/ 2950.01, 2950.03, 2951, 2973.3, 2988, 2958.2m, these photos include medium crystalline planar-e-s dolomite mosaic, all of them show oil stained, in their intercrystalline porosities, in addition to micro vugs (denoted by rows) figure (b and e), figure (d) represent the polymodal mosaic dolomite; medium crystalline (lower right part), oil stained, while the upper right part includes euhedral coarse crystalline and very coarse Porphyrotopic floating on the calcite cement. (g, and h) Kz-16/2960.42, -2966.85 Medium Crystalline Planar-e-a Dolomite Mosaic (all photos width is 2mm and cross nickoled).

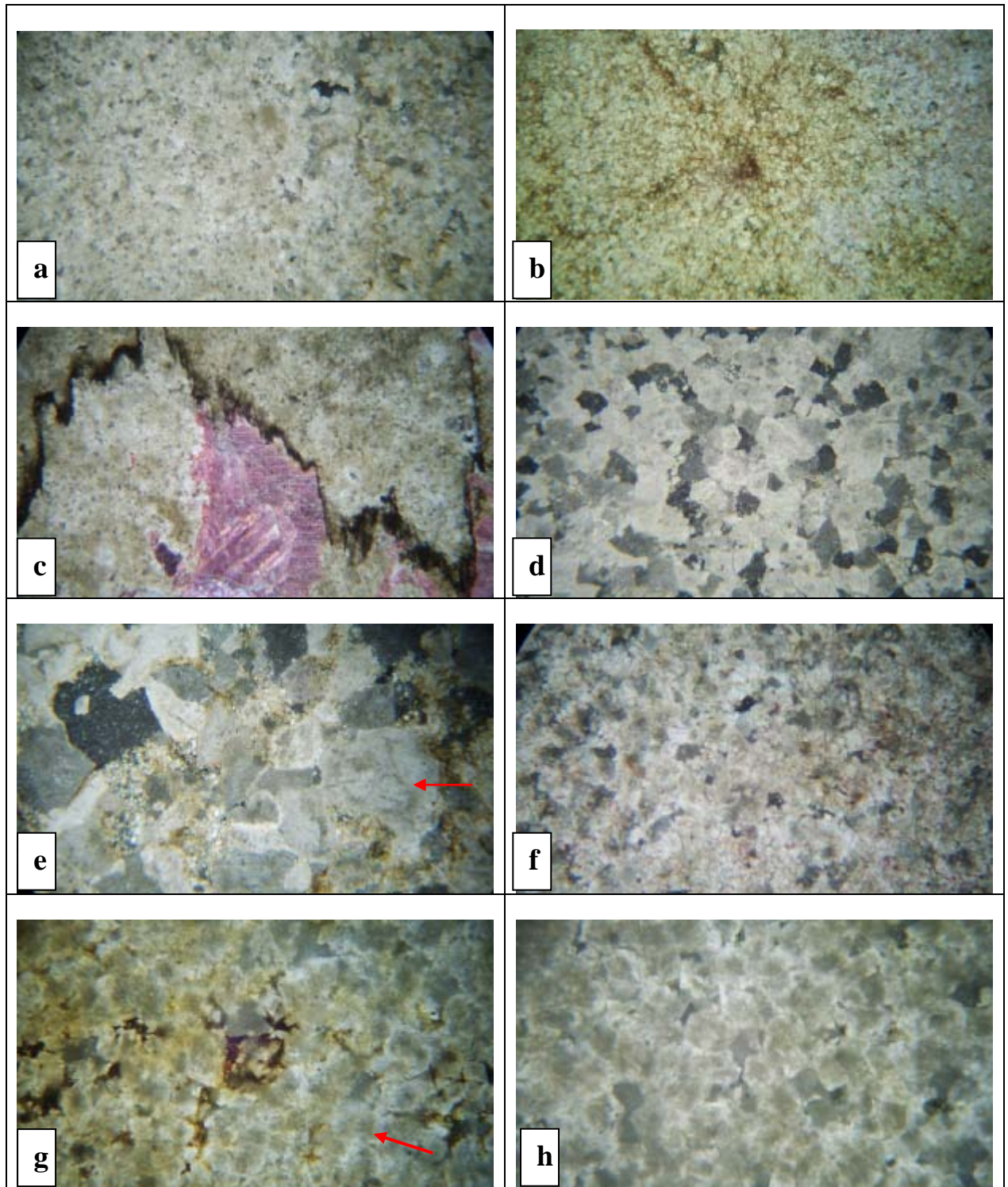


Figure 2.13: Dolostone microfacies, (a, b, & c) Kz-16/2956, 2971.06, 2976.1 Medium Crystalline Planar-a Dolomite Mosaic, in general this facies in low porosity, but along some weak zone the medium crystalline planar-e-s dolomite are growth which the later characterized by high inter crystalline porosity. (d & e) Kz-16/2997, Kz-4/3090, Coarse crystalline planar-e-s dolomite, the fine crystalline zone has intercrystalline porosity. (f, g, & h) Kz-16/2982, 2986, 2985 m also Coarse Crystalline Planar-e-s Dolomite Mosaic (all photos width is around 2mm and cross nickoled).

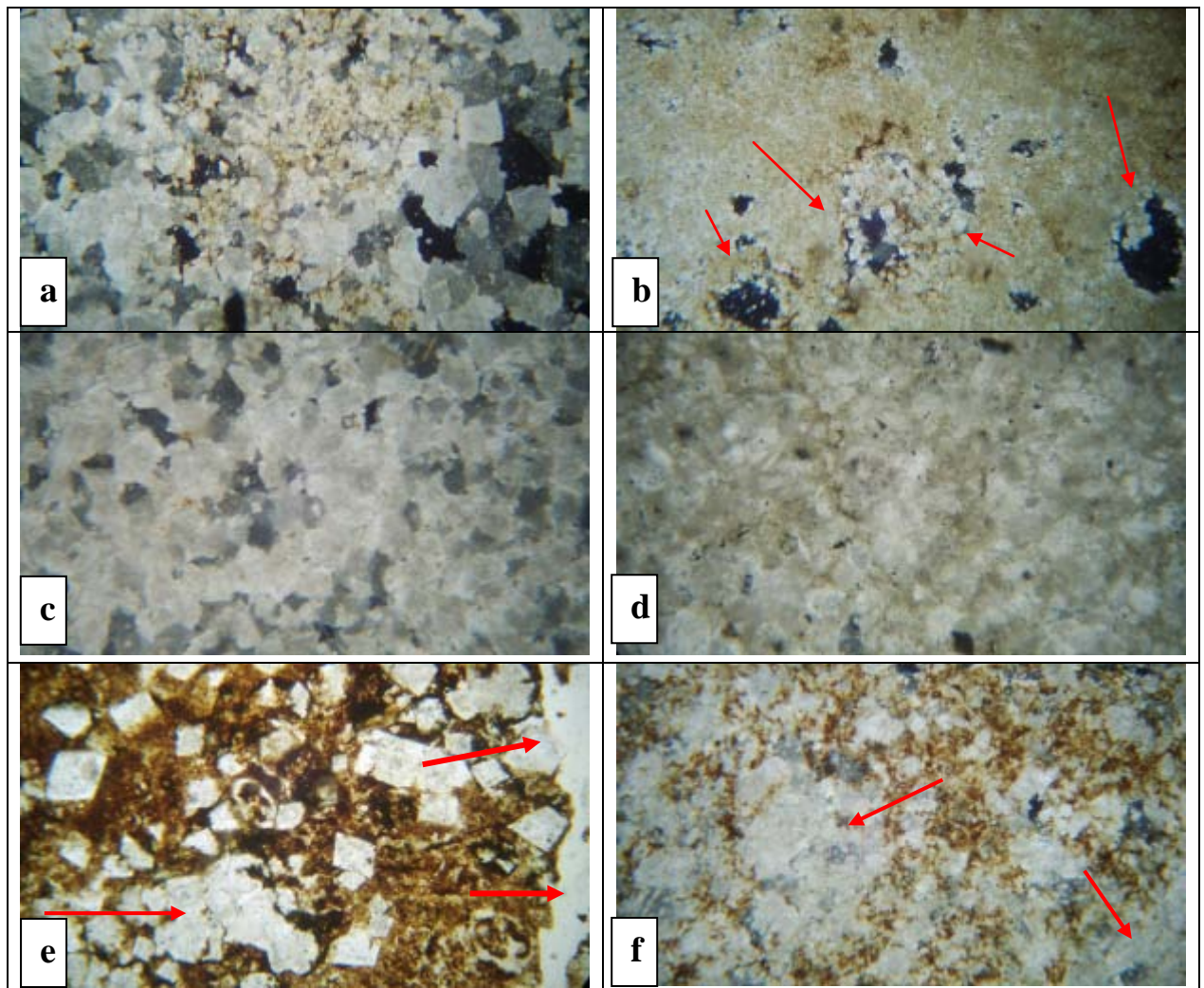


Figure 2.14: Dolostone microfacies, (a) Kz-11/3041, very coarse dolomite crystals show progressive dissolution, (b) Kz-11/ 2895-96, coarse crystalline dolomite coats dissolution vugs, (c & d) Kz-16/ 3035-36 and 3075-76, Coarse Crystalline Planar-e-s Dolomite Mosaic, the latter belongs to the Upper Sarmord Formation. (e & f) Kz-11/ 2967 and 2965m, Planar- a, dolomite cement denoted by rows, the brown area represent the vugs and fine to medium dolomite crystalline with high porosity filled by oil. (all photos width is around 2mm and cross nickoled).

Chapter Three

Reservoir Characterization

3.1 Preface

This chapter is concerned with the nature and internal properties of the Upper Qamchuqa reservoir. It begins with describing the porosity and permeability from wireline logs and comparing them with laboratory porosity-permeability measurements from available cored plug analyses.

In this chapter Neutron-Density combination logs are used to predict the porosity and lithology to distinguish between dolomite and limestone rocks with their role on reservoir characterization.

The chapter combines lithologic properties and petrophysical data of the reservoir with log analysis and processing to ultimately recognize potential reservoir units and subunits. Other lithologic units with less potentiality are also discussed to integrate the overall reservoir characters.

3.2 Porosity

The porosity is the first of the two essential attributes of a reservoir; porosity is the percentage of the total volume of the rock that is pore space. Total porosity consists of primary and secondary porosity (Selley, 1998). Porosity varies greatly within most reservoirs; both laterally and vertically. Effective porosity is the measure of the interconnected void space that is filled by recoverable oil or gas (North 1985), it is commonly 5-10 percent less than the total porosity, and in carbonate rocks the dolomitization creates more effective porosity because its rhombs provide planar grain surfaces and polyhedral pores (Levorsen, 1967).

Rock porosity can be obtained from the sonic log, density log, neutron log and newly tools Nuclear Magnetic Resonance log (MNR) (Asquith and Krygowski, 2004). For all these devices the tool response is affected by the formation porosity, fluids content and matrix. If the fluids and matrix effects are known or can be determined, the tool response can be related to

porosity. The results of log porosities must be compared with the laboratory core analysis. The best method for direct porosity measurement is obtained from core plug analysis; it is measured commonly every thirty centimeters. The porosity of most reservoir ranges from 5 to 30 percent, and it is most commonly between 10 and 20 percent. Carbonate reservoirs generally have slightly less porosity than sandstone reservoirs, but the permeability of carbonate rocks may be higher (North, 1985). A reservoir with porosity less than 5 percent is generally considered noncommercial or marginal unless there are some compensating factors, such as fractures, fissures, vugs, and caverns, that are not revealed in the small sections of the rock cut by the plugs (Levorsen, 1967; North, 1985). According to them a rough field appraisal of porosities (in percent) is clear in the table 3.1:

Table 3.1 Classification of porosity according to North (1985).

Type of porosity	%
Negligible	0-5
Poor	5-10
Fair	10-15
Good	15-20
Very good	20-25

Results: Ten wells are selected for this study which penetrate Upper Qamchuqa Formation except for wells Kz-3 and Kz-7 partially penetrate it. Most of the wells were partially cored and there are continuous core data of the most of the section from one well (Kz-16) (Appendix B). Porosity and permeability data are measured from plugs of these wells (provided by N.O.C. they used the **Boyle's Law** Method), and these core data were used for validation of the predicted data from well logs, all core data were depth shifted to match log depths. There are conventional well logs from all wells

including gamma ray, density, neutron, sonic, spontaneous potential and resistivity. Using the program "getdata222.exe" the hardware log graphs of ten wells were converted to digitize data with six points per meter (or 16 cm interval) for each log graph. The total derived data for six log types (GR, Neutron, Density, Sonic, Deep resistivity, and Shallow resistivity) were reached 6100 digitize points to each well (Appendices A1 to A9), and they were arranged in combination according to their relations to derive the principal reservoir parameters.

The porosity measured from three types of log including Sonic, Density, and Neutron logs, the following are the short identification of each one:

Sonic Log...The Sonic log is a porosity log that measures interval transit time (Δt) of compressional sound wave traveling through the formation along the axis of the borehole. Interval transit time Δt in microsecond per foot, $\mu\text{sec}/\text{ft}$ (or microsecond per metre, $\mu\text{sec}/\text{m}$) is the reciprocal of the velocity of sound. The borehole-compensated (BHC) devices were used in Khabbaz oil field and the Wyllie time-average equation (Asquith and Krygowski, 2004), was utilized:

$$\Phi_S = \frac{\Delta t_{\log} - \Delta t_{ma}}{\Delta t_{fl} - \Delta t_{ma}} \quad \dots\dots\dots 3.1$$

Where:

Φ_S = Sonic derived porosity.

Δt_{ma} = interval transit time in the matrix (Δt limestone is used)

Δt_{\log} = interval transit time in the formation (measured by log)

Δt_{fl} = interval transit time in the fluid in the formation (freshwater mud = 189 $\mu\text{sec}/\text{ft}$; saltwater mud = 185 $\mu\text{sec}/\text{ft}$), this term chosen according of type of used drilling mud in each wells.

Density Log...The Density log is measured in gram per cubic centimeter, g/cm^3 , and is indicated by Greek letter ρ (rho). The bulk density (ρ_b) is the density of the entire formation as measured by the logging tool. The formula for calculating density porosity is:

$$\Phi_D = \frac{\rho_{ma} - \rho_b}{\rho_{ma} - \rho_{fl}} \quad \dots\dots\dots 3.2$$

Where:

Φ_D = density derived porosity

ρ_{ma} = matrix density (in this study used standard limestone 2.71 g/cm^3)

ρ_b = formation bulk density (the log reading)

ρ_{fl} = fluid density (according to the type of drilling mud; 1.0 or 1.1 g/cm^3 for fresh and saline drilling mud respectively).

Neutron Log...The Neutron log is porosity log that measured liquid (water or oil) filled porosity; the neutron porosity denoted by Φ_N , the neutron curve displayed in porosity unit and referenced to a specific lithology. In the Upper Qamchuqa reservoir, the standard limestone lithology was considered.

Neutron-Density combination porosity: the combination of the neutron and density measurements is the most widely used for the estimation of the average neutron-density porosity Φ_{N-D} , this gives a more accurate porosity (Selley, 1998; Asquith and Krygowski, 2004), various combination formula are used such as:

$$\Phi_{N-D} = \frac{\Phi_N + \Phi_D}{2} \quad \dots\dots\dots 3.3 \quad \text{or} \quad \Phi_{N-D} = [(\Phi_N^2 + \Phi_D^2)^{1/2}]/2, \quad \dots\dots\dots 3.4$$

or in some cases the two porosities averaged with different ratio such as

$$\Phi_{N-D} = \frac{1}{3} \Phi_N + \frac{2}{3} \Phi_D \quad (\text{in gas zone}), \quad \dots\dots\dots 3.5$$

The first formula (3.3) was used in this study.

The derived porosities result from above well logs were compared with the laboratory core measured porosity in well (Kz-16), the results indicate that the neutron-density derived porosities (Φ_{N-D}) will give the most reasonable matching with the core derived porosities (Figure 3.1.A), which made us to trust these log's evaluation values. Also the result indicates that the Φ_{N-D} porosity shows the best matching without any correction from shale effect, because the Upper Qamchuqa Formation is clean, particularly its upper part which represents the main reservoir unit.

Figure 3.1.B illustrates the correlation between sonic log derived porosity with the core measured porosity which shows less matching than that of with N-D derived porosity. The last column of Figure 3.1.C represents the correlation between derived porosity from sonic log with N-D derived porosity; the figure shows good matching between the two porosities along the entire section, with notice that the N-D porosity is greater than the sonic porosity. This pattern was expected because the sonic porosities represent the primary (interparticles) porosity, excluding the secondary porosities (fracture, vug, mold, etc.) which are measured by N-D tool in addition to primary porosity.

Although the neutron-density combination logs are well-known as a good technique for the identification of gas zone, gas in the pores causes the density porosity (Φ_D) to be too high and causes the neutron porosity (Φ_N) to be too low (Selley, 1998; Asquith and Krygowski, 2004). But this technique could not be able to indicate the presence of the gas cap in the Khabbaz oil field due to the domination of the dolomite rock which has the inverse effect on the logs, especially density log which measures low porosity against the dolomite rock, (Selley, 1998; Asquith and Krygowski, 2004). This phenomenon depleted the effect of gas; hence, both dolomite and gas compensate each other's effect.

The application of this method of analysis shows that the upper lithologic unit (unit A) is characterized by the higher porosity values as compared to other units.

Correlation of the porosity values of unit (A) in most of the studied wells shows the occurrence of six continual porosity subunits named from the top A1, A2, A3, A4, A5, and A6. These porosity subunits are isolated by five nonporous intervals denoted by N1, N2, N3, N4, and N5.

The depth intervals, average porosity and thickness of these subunits in the studied wells were illustrated in (Tables 3.4 and 3.5).

3.3 Permeability

Permeability is the ability of porous medium to conduct fluids, permeability controls how fluid can migrate through the reservoir. The permeability is a key parameter in reservoir development and management because it controls the production rate. In general, the permeability increases with increasing porosity, increasing grain size and improved sorting (Selley, 1998; Tagavi, 2005). In carbonates rocks connectivity between pores is the main control for the permeability. Heterogeneity occurs in carbonate reservoirs due to variation in depositional environment and subsequence diagenetic processes.

The permeability of a reservoir can be measured in three ways: First is by means of a drill stem test or production test from reservoir, depends on the rate of flow and drop in pressure. The second way is from Wireline logs it is possible to identify permeable zones from in a qualitative way from SP and Caliper logs. The third way is by means laboratory core plug measurement. (Selley, 1998).

The best method for direct permeability measurement is obtained from core plug analysis; it is measured commonly every thirty centimeters. Also coring is very expensive and time consuming with limiting such measurements. Another problem with core plug measurements is the scale. Small scale heterogeneities that might not affect flow on a reservoir scale are measured, and these need to be upscaled (Tagavi, 2005).

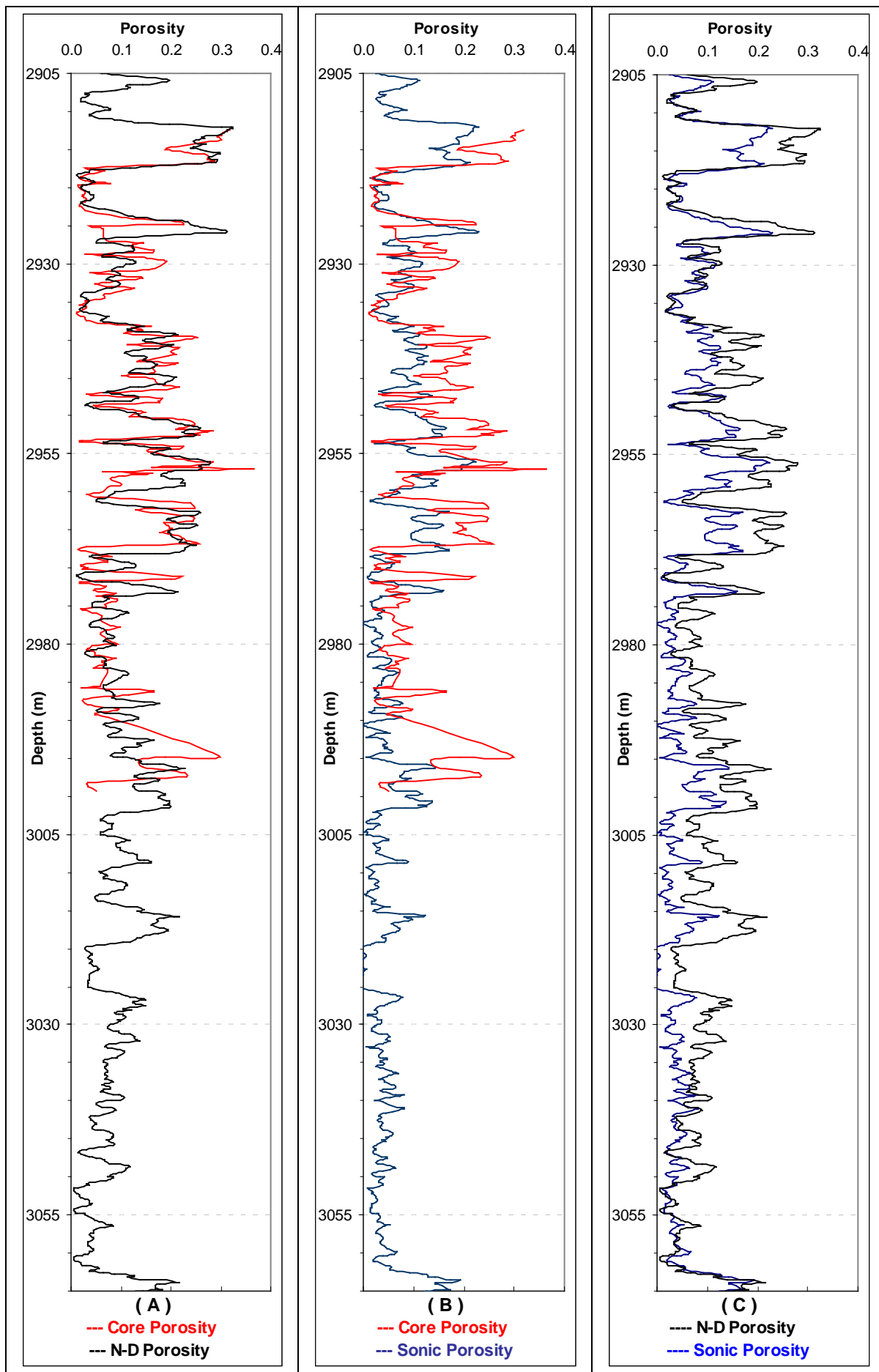


Figure 3.1: Comparisons of derived porosity from N-D & Sonic Logs, with the core measured porosities in well Kz-16.

The permeability of average reservoir rocks generally range between 5 and 1000 millidarcys {a millidarcy (md) = 0.001 darcy}, commercial production has been obtained from rocks whose permeabilities were as low as 0.1 md, but such rocks may have highly permeable fracture systems that are not revealed in the standard laboratory analysis (Tagavi, 2005). Permeability, along with porosity, varies greatly laterally and vertically in the average reservoir rock, a reservoir rock whose permeability is 5 md or less is called *tight sand* or a *dense limestone* (Levorsen 1967; North, 1985). Table 3.2 reveals the classification of reservoir permeability according to North (1985):

Table 3.2: Classification of Reservoir Permeability (North, 1985)

Type of permeability	Range of permeability
Poor to fair	< 1.0 -15 md
Moderate	15 - 50 md
Good	50 - 250 md
Very good	250 -1000 md
Excellent	> 1000 md

Results

In this work measured porosity and permeability data from plugs of the available core intervals were provided by N.O C. laboratories (Appendix B), and these core data were used for validation of the predicted data from the logs. Also an alternative to estimate the permeability is from Wireline logs. The challenge in permeability prediction is that permeability is related more to the pore throat size rather than pore size, which is difficult to be measured by logging tools directly without calibration with measured data. Numerous methods for predicting permeability have been attempted, and several equations have been suggested which relate porosity to permeability. The challenge for estimation of the permeability from the porosity is that the permeability is not dependent on the porosity alone. It

also depends on grain size, sorting and pore throat size. The permeability estimation is unsuccessful in carbonates when porosities occur as separate vugs or as moldic pores. In such cases the porosity values may be high but the permeability may be very low, because of lacking connection between the pores. Figure 3.1 shows the derived porosity from sonic log which is responsible of primary porosity or interparticle (grains or crystals) porosities, on the other hand the total porosity measured from Neutron-Density combination logs, and the two curves show the neglected separation. This indicates the dominance of interparticle porosities (Asquith and Krygowski, 2004), in such cases the well log derived permeability gives a reasonable result.

In this study, Multilinear regression (MLR) method has been used to predict permeability from well logs (Tagavi, 2005) to non-measured intervals. MLR technique is a mathematical method for permeability prediction which incorporates several input data. This method is based on averaging of the input well log data (Appendices A1 to A9) which is associated with the permeability (K) in md. Gamma ray (GR) with API, density (Den) in g/cm³, neutron (Neut) with porosity unit (p.u) and sonic logs (Δt) in $\mu\text{sec}/\text{ft}$ were used as input values in this model with the following equation (Tagavi, 2005):

$$\text{Log (K)} = (-2.488 - 0.0073 \cdot \text{GR} - 0.619 \cdot \text{Den} + 11.128 \cdot \text{Neut} + 0.050 \cdot \Delta t) \dots\dots 3.6$$

Though any reservoir has its environment and the measurements of the log tool affected by the reservoir conditions, it is not possible to use the above formula directly, where the results of the predicted permeability from the equation are compared to measured core permeability from a selected key well (Kz-16), and the result shows that the log derived permeability is slightly higher than the core measured (actual) permeability, particularly in low permeable intervals (Figure 3.2.A). Then after some trials on the log relations, a new equation is suggested which gives more reasonable matching with the core measured permeability (Figure 3.2.B).

The suggested equation is as follows:

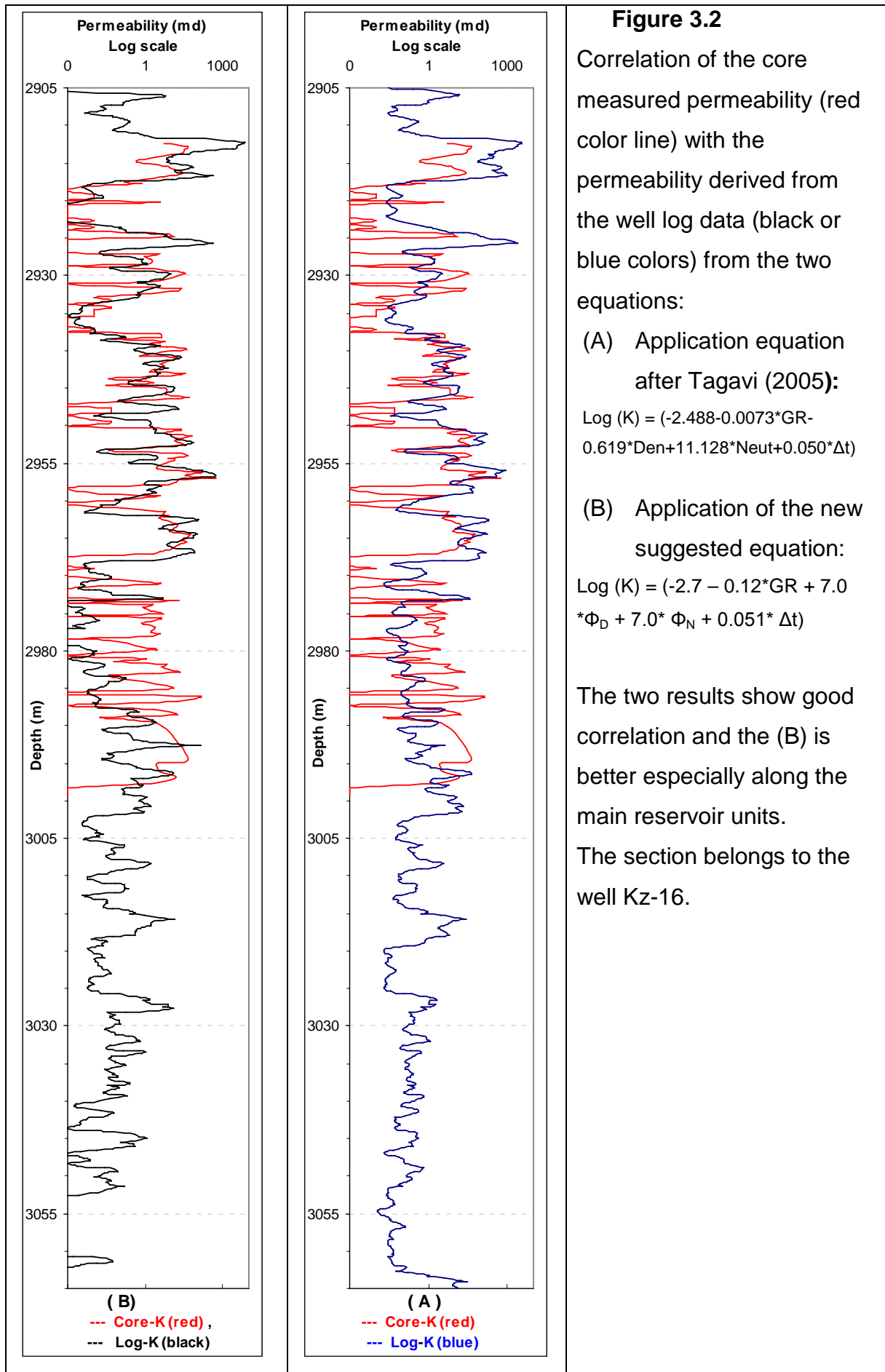
$$\text{Log (K)} = (-2.7 - 0.12 \cdot \text{GR} + 7.0 \cdot \Phi_D + 7.0 \cdot \Phi_N + 0.051 \cdot \Delta t) \dots \dots \dots 3.7$$

And the permeability (**K**) with md = $10^{(-2.7 - 0.12 \cdot \text{GR} + 7.0 \cdot \Phi_D + 7.0 \cdot \Phi_N + 0.051 \cdot \Delta t)}$

Where: Φ_D and Φ_N are derived porosity from density and neutron logs respectively.

The two equations include several input data derived from the log measurements (Appendices A1-A9), based on their relations with permeability the equation was created; GR log refers to shale volume in the reservoir rock, which has negative (inverse) effect on the permeability and makes it to act as negative (-) parameter in the equations, while all other three logs: Density, Neutron, and Sonic, which are porosity logs, and they have normal (direct proportion) relation with the permeability and act as positive (+) parameters in the equation with the labeled factor to each one. From the application of the new equation, the permeability was derived for nine well sections (Kz-1, Kz-2, Kz-3, Kz-4, Kz-5, Kz-11, Kz-13, Kz-14, and Kz-16), (Appendices C1 to C3). The results show that the upper unit of the Upper Qamchuqa reservoir (Unit A) characterized by higher permeability all over the well sections and it is decreases downward along other two units (B and C)

The permeability is also could be derive from indirect well data associations, for example the relation between water saturation (S_w) and the porosity (ex. Neutron-Density porosity), this method will be discussed in chapter four.



3.4 Neutron-Density cross plotting

Since the reading of the porosity logs (Sonic, Density, and Neutron) depends on porosity and lithology, the evaluation of porosity from a single log is possible only if lithology remains constant, while when the lithology changes, porosity can be determined by the reading of the two logs. The best combination is Density + Neutron logs. By themselves, both the neutron and density logs are difficult to use for gross lithology identification, the combination of two becomes the best available indicator of lithology and porosity (Schlumberger, 1972; Rider, 2000). Cross-plot for Schlumberger, 1972, 1979, Formation Density Compensated (FDC) and Compensated Neutron Log (CNL) cross plot, in fresh water and apparent limestone was used to detect the lithology and actual porosity from two log's data (Figure. 3.3). The horizontal axis represents the compensated neutron log apparent limestone porosity; while the vertical axis represents the formation density compensated apparent limestone porosity. The two terms were shortened into N-porosity and D-porosity respectively and conventionally they are more shortened to N-D crossplot. The theoretical standard values of pure sandstones, limestones and dolomites are computed with a range of porosity. These trends can be drawn on the appropriate crossplot graph (Figure 3.3) to act as boundary end members (Doveton, 1986).

Figure 3.3 illustrates the N-D crossplot of the averaged neutron- density data of the unit A (the total data of each subunit in single well averaged into one point) to the each of six porosity subunits (Tables 3.4 and 3.5), the six subunits (A1 to A6) denoted by solid dots and five interlayers non-reservoir zones (N1 to N5) denoted by open triangles, the figure shows that all points of the porosity subunits fall between the dolomite and limestone fields, with more closer to the dolomite line, and most of them fall with the field of porosity between 15% and 30%. While the points of non-reservoir layers concentrated around the limestone field and most of their porosity fall

between zero and 10%. . This indicates that the dolomitic facies play as good reservoir characteristics in Upper Qamchuqa formation.

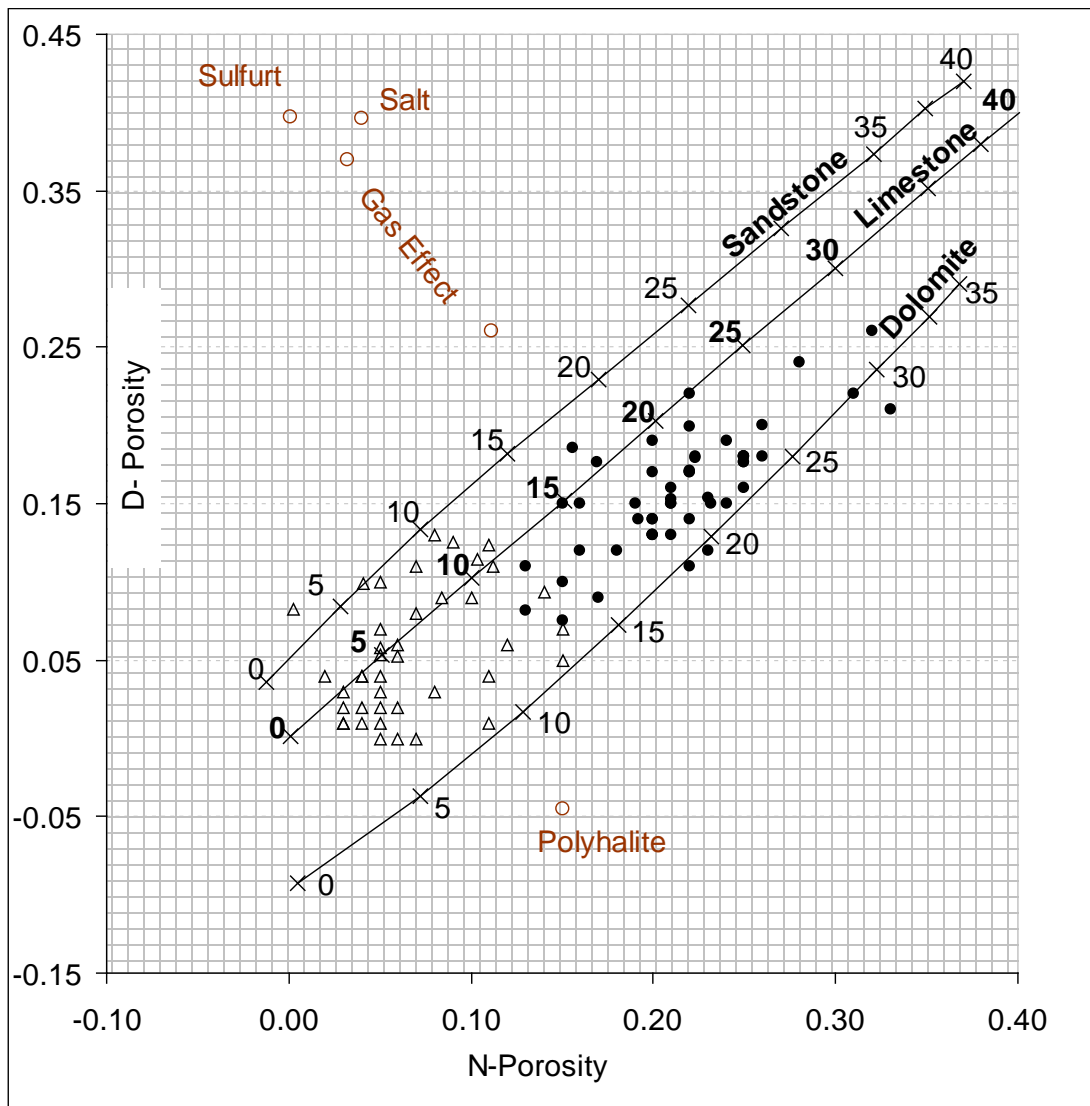


Figure 3.3: Neutron-Density crossplot, solid dots represent the porosity subunits (A1 to A6) they fall to the dolomite to dolomitic limestone lithological area and average porosity 15-30%; and open triangles are non or low porous inter-layering (N1 to N5) fall to the limestone to dolomitic limestone zone with low porosity ranged from zero to 10%. (The total data of each subunit in single well averaged into one point to the each of six porosity subunits)

Also Figures 3.4, 3.5, 3.6, 3.7, 3.8, and 3.9 illustrate in detail the lithology and averaged porosity of the six porosity subunits in each wells.

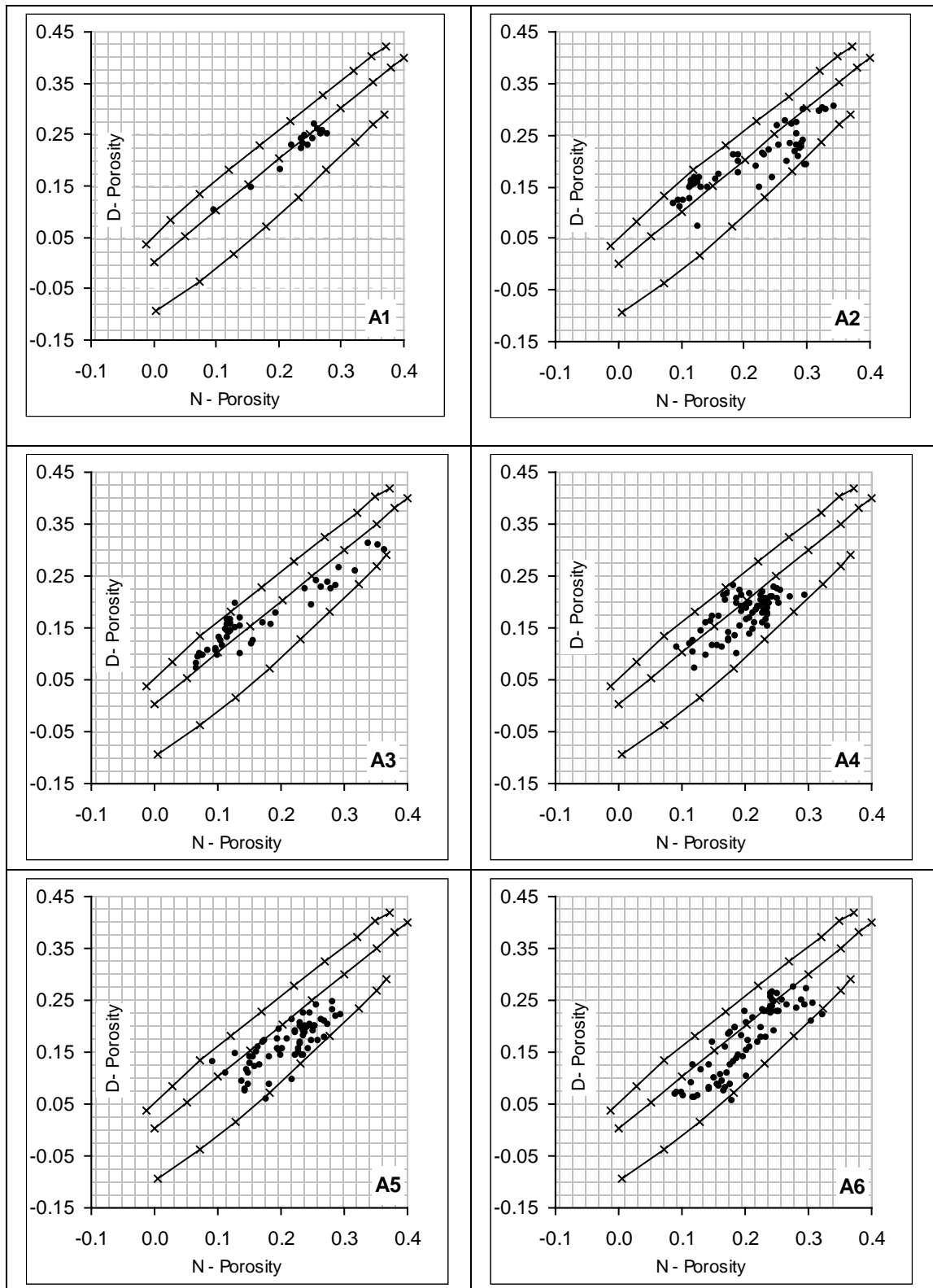


Figure 3.4: The Neutron-Density crossplot of well Kz-1 section.

(A1) subunit, limestone with around 25% Φ ; (A2) subunit is limestone to dolomitic limestone with Φ of 10-30%; (A3) subunit, limestone to dolomitic limestone with Φ of 10-30%; (A4) subunit dolomitic limestone with Φ of 15-25%; (A5) subunit, dolomitic limestone with Φ of 15-25%; and (A6) subunit is dolomitic limestone with Φ of 10-30%.

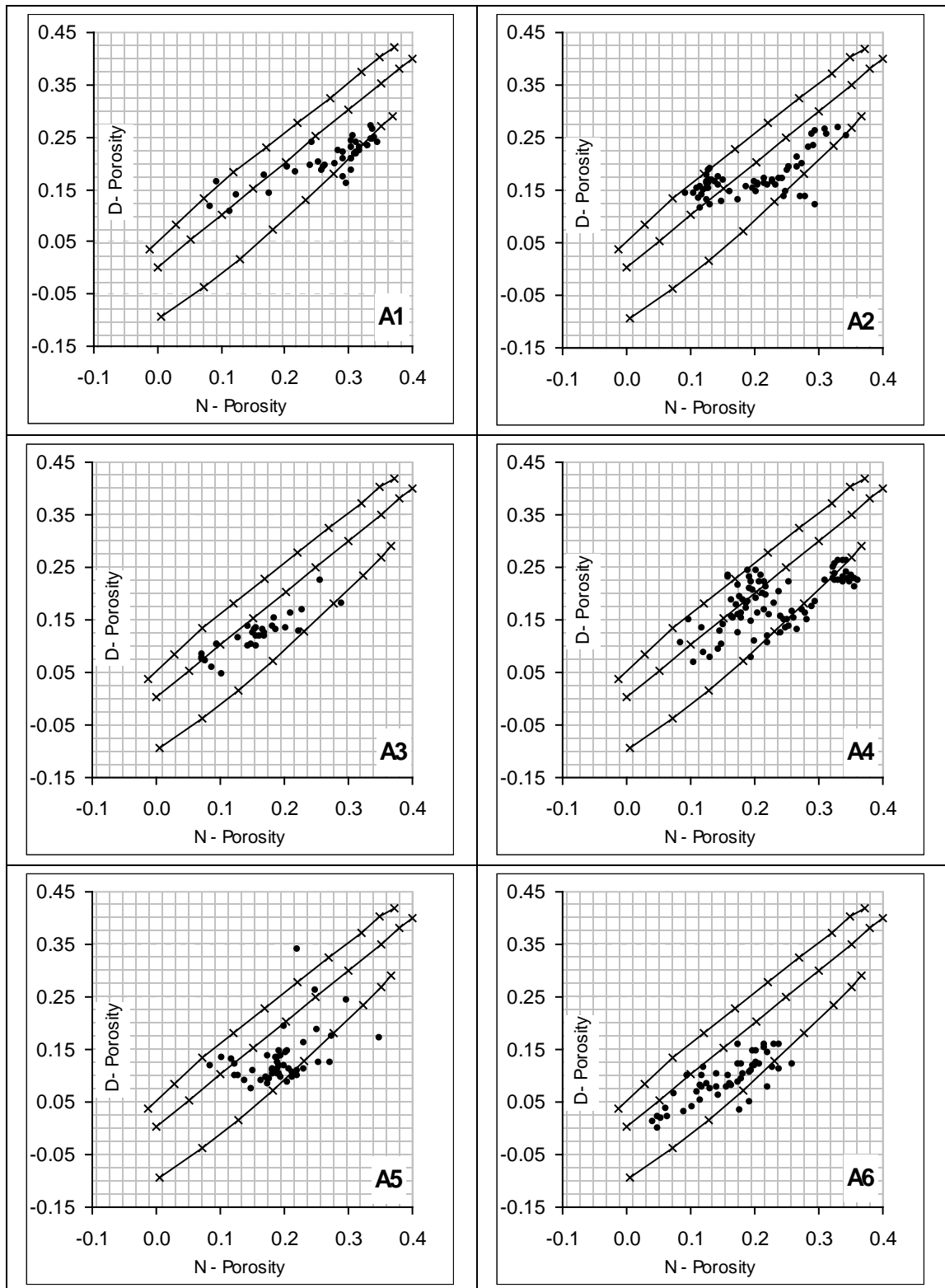


Figure 3.5: The Neutron-Density crossplot of well Kz-4 section.

(A1) subunit, dolomite with Φ of 25-30%; (A2) subunit is limestone to dolomitic limestone with Φ of 10-30%; (A3) subunit is dolomitic limestone with Φ of 8-25%; (A4) subunit, limestone – dolomite with Φ of 10-30%; (A5) subunit, dolomitic limestone with Φ of 10-25%; and (A6) subunit is dolomitic limestone with Φ of 5-25%.

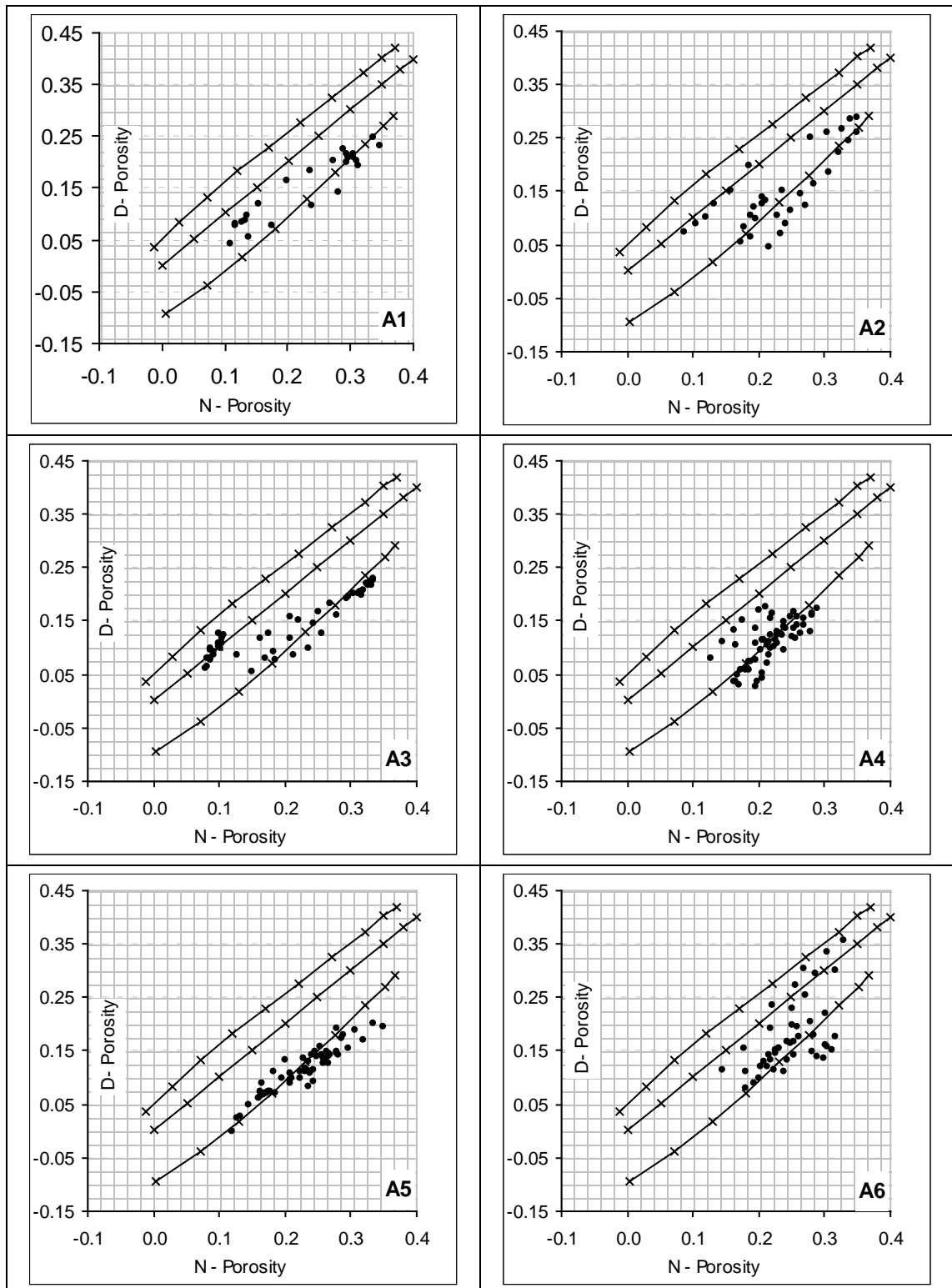


Figure 3.6: The Neutron-Density crossplot of well Kz-5 section.

(A1) subunit, dolomitic lst. with Φ of 10-30%; (A2) subunit, dolomite to dolomitic limestone with Φ of 10-30%; (A3) subunit, dolomite - limestone with Φ of 10-30%; (A4) subunit, dolomite with Φ of 12-25%; (A5) subunit, dolomite with Φ of 10-30%; and (A6) subunit, dolomite to dolomitic lst. with Φ of 15-30%.

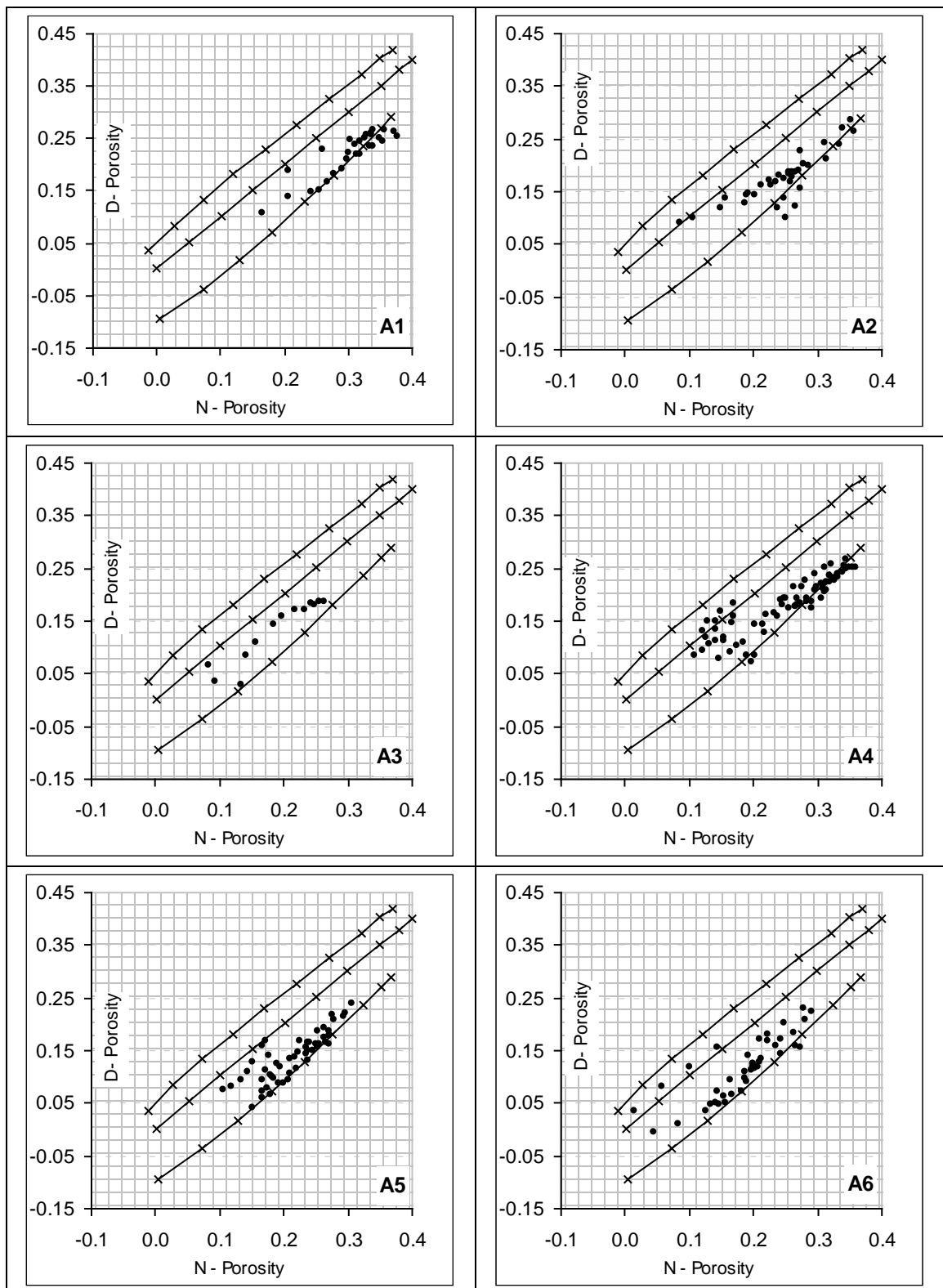


Figure 3.7: The Neutron-Density crossplot of well Kz-11 section.

(A1) subunit, dolomitic lst. with Φ of 25-30%; (A2) subunit, dolomite to dolomitic limestone with Φ of 20-30%; (A3) subunit, dolomitic limestone with Φ of 10-25%; (A4) subunit, is dolomite to dolomitic lst. with Φ of 10-30%; (A5) subunit, dolomite with Φ of 10-25%; and (A6) subunit, dolomite to dolomitic lst. with Φ of 10-25%.

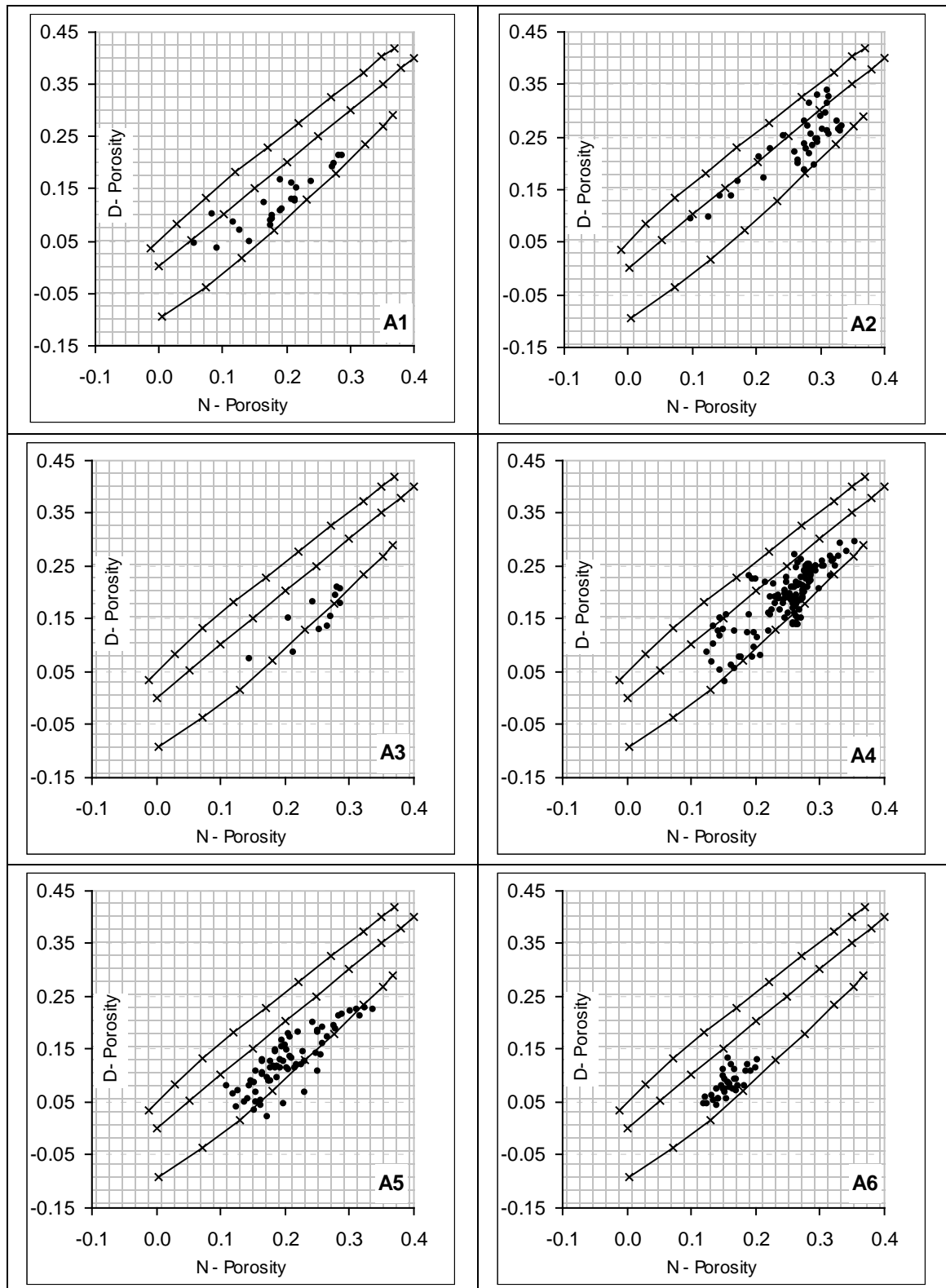


Figure 3.8: The Neutron-Density crossplot of well Kz-14 section.

(A1) subunit, is dolomite with Φ of 15-25%; (A2) subunit, limestone to dolomitic limestone with Φ of 15-30%; (A3) subunit, is dolomite with Φ of 15-25%; (A4) subunit, is dolomite to dolomitic lst. with Φ of 15-30%; (A5) subunit, dolomite with Φ of 10-25%; and (A6) subunit, is dolomite to dolomitic lst. with Φ of 10-20%.

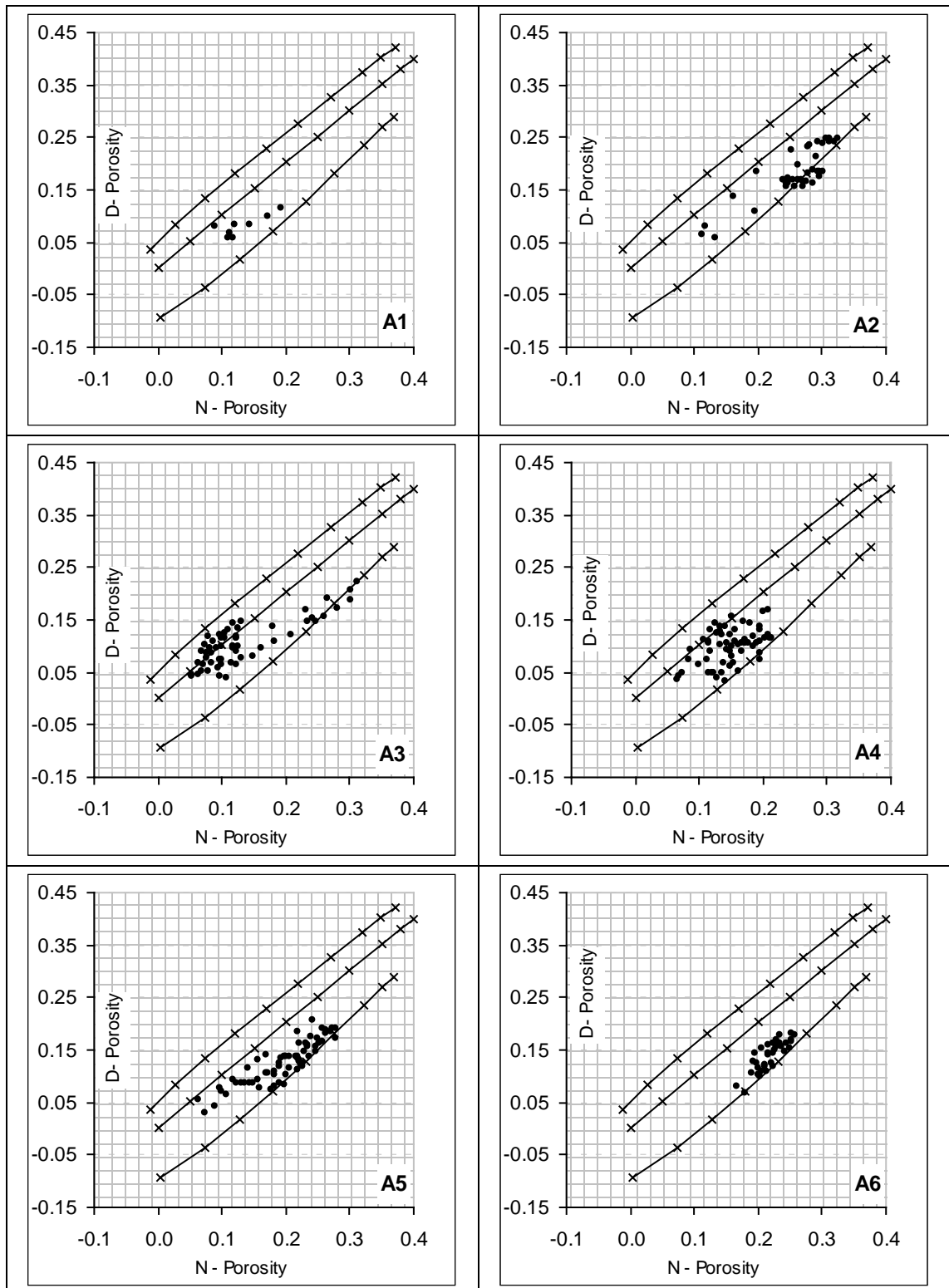


Figure 3.9: The Neutron-Density crossplots of well Kz-16 section.

(A1) subunit is dolomitic lst. with Φ of 10-17%; **(A2)** subunit, dolomite to dolomitic lst. with Φ of 15-27%; **(A3)** subunit, is limestone to dolomitic lst. with Φ of 8-25%; **(A4)** subunit, dolomitic limestone with Φ of 10-20%; **(A5)** subunit, is dolomite to dolomitic limestone with Φ of 10-27%; and **(A6)** subunit, is dolomite to dolomitic lst. with Φ of 17-25%.

3.5 Pore throat type

Ports or pore throats are the mean radius of the pore throats connecting the pores (doors through which the fluids flow from one pore to another). It is estimated from porosity-permeability relation (derived from plugs or logs) in term of (R35), which refers to size of pore throats radius at 65% water saturation or 35% pore volume (Martin et al, 1997). The R35 method is a powerful petrophysical technique for characterizing the productivity of a nonvuggy carbonate (Lucia, 1999), when separate vug pore occurs as a portion of the matrix porosity, the R35 is still an approximate indicator of flow (Martin et. al., 1999). Figure 3.10 show three fields of porosity-permeability relationship: The area of low porosity and high permeability indicates to fractured rocks. The area with high porosity and relatively low permeability belongs to the matrix porosity. While the third area is characterized by proportional relations between porosity and permeability, this field represents the interparticles porosity enhanced by small fractures and vugs. (Martin et al, 1997, and Martin et. al., 1999).

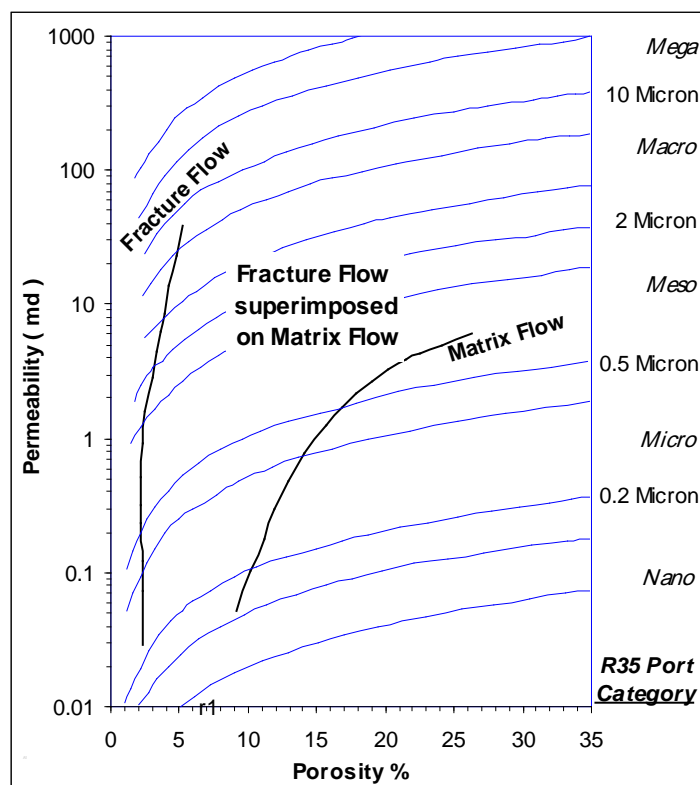


Figure 3.10 : Porosity-permeability crossplot show three fields of flow according to pore throat (R35).

By interrelating and coordinating the engineering and geologic approaches it is possible to learn much more about the role played by the size and shape of the pore system in determining the production capability of a carbonate rock. Thus, also one can use mercury capillary pressure tests to determine the general pore geometry of specific rocks types (Jodry, 1972).

Oil displaces water from pore spaces in a rock matrix, and the hydrocarbon column in a reservoir depends on pore throat sizes and capillary pressure. Large pore throats at the base of a reservoir are in general filled with oil, and oil may also fill smaller pore throats above with increasing capillary pressures (Taghavi et al, 2007 and Pittman, 1992). Fluid saturations are controlled by the pore geometry responding to the reservoir capillary pressure which is a function of the height above the free water level.

By increasing the differential pressure, smaller pore throats are invaded by oil. Capillary pressure tests can be used in conjunction with porosity and permeability measurements to describe the pore structure of carbonate reservoir.

The pore throat size of the sample have a direct impact on the flow capacity of the rock interval represented by the sample. When pore throat size is reflected by the rock fabric, which is the result of both deposition and diagenesis (Martin et al. 1999). Four petrophysical flow units with different reservoir are distinguished performances by the ranges based on the factor R35, table (Table 3.3) (Martin et al, 1997, Martin et al. 1999, Lucia, 1999).

Table 3.3: Type of pores according to pore throat size (Martin et al. 1999).

Pore throat Type	Size Range
Mega	>10 Microns
Macro	2 to 10 Microns
Meso	0.5 to 2 Microns
Micro	0.1 to 0.5 Micron
Nano	< 0.1 Micron

In this study the porosity-permeability diagram (Figure 3.11) was used to predict the pore throat size of the six porosity subunits (A1, A2, A3, A4, A5,

and A6), and classified their pore throat types according to the table 3.3. The following are the description of the results:

Figure (3.11A1) shows that all pore throat sizes of Subunit A1, the data fall within the range of 0.2 to 10 microns with an average of 2.08 microns, which is classified as macro pore throats. This subunit has the average core porosity of 0.17 (Table 3.5), comparatively lower than porosity of the next subunit (A2), but its pore throat size is larger. This result will be related to the situation of this subunit which is located to the top of Upper Qamchuqa Formation. Under the unconformity surface, it is possible to have been exposed to weathering, washing, and enlarging of the pore throats.

The pore size of Subunit A2 illustrated by (Figure 3-11A2), the points fall within the range of 0.2 to 4 microns with an average of 1.5 microns, which they classified as meso pore throats. The core measured porosity (Table 3.5) shows high porosity of this unit with an average of 0.28.

Figure (3-11A3) shows that most of the pore sizes of Subunit A3 fall within the range from 0.2 to 4 microns with an average of 0.67 microns, they classified as meso pore throats.

Subunit A4 has the pore throat size within the field of 0.5 to 4 microns (Figure 3-11A4) with an average of 1.3 microns, they classified as meso pore throats too.

Figure (3-11A5) shows that most of pore sizes of Subunit A5 fall within the range of 0.2 to 10 microns with an average of 2.2 microns, classified as macro pore throats.

Subunit A6 has the pore size within the field of 0.5 to 5 microns (Figure 3-11A6) with an average of 2.2 microns, which it is classified as macro pore throats.

The latter three Subunits (A4, A5, and A6) considered the best reservoir zones, in addition to their good reservoir properties, they are combined in most well sections and they form a single thick unit with extended continuously over the field.

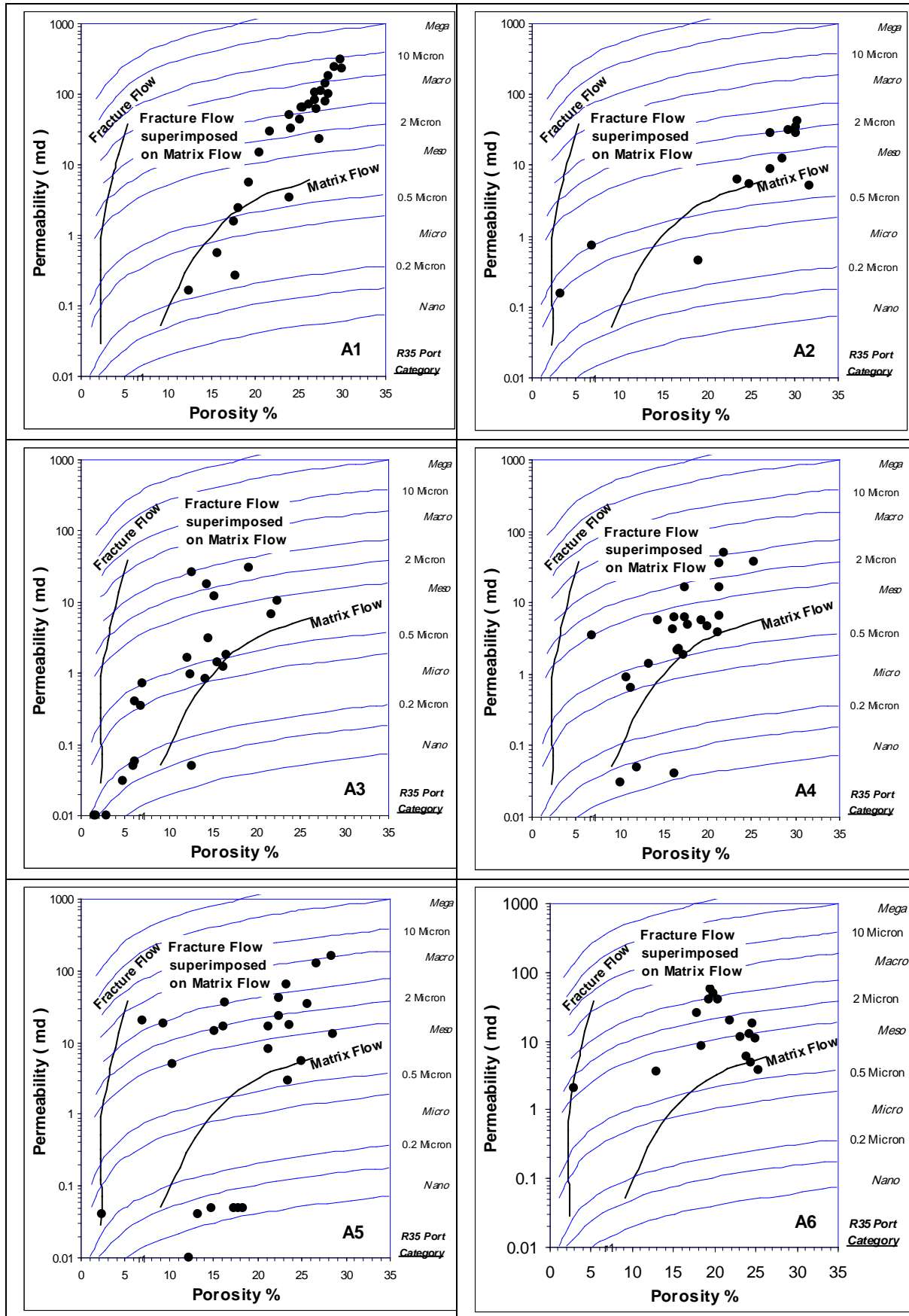


Figure 3.11: Porosity permeability crossplot, showing the pore throat radius type of the six porosity subunits, all units locate to the matrix to fracture superimposed flow field zones. (A1) fall to zone of Macro port, (A2, A3, and A4) classified as Meso pores, while (A5 and A6) fall on the Macro port type.

3.6 Rock Fabric Types

Rock-fabric parameters (particle size, sorting, interparticle porosity, separate vug-porosity, touching vugs) define pore-size distribution and their relations to rock fabrics which reflect the geologic processes that define the geologic model required to construct a realistic reservoir model (Lucia, 1999; Lucia et al., 2001; Holtz et al., 2002). They used a slightly modified Dunham classification (Figure 3.12), which discriminates between grain-dominated and mud-dominated rock fabrics as opposite to grain-supported and mud-supported texture (Ruf and Aigner 2004).

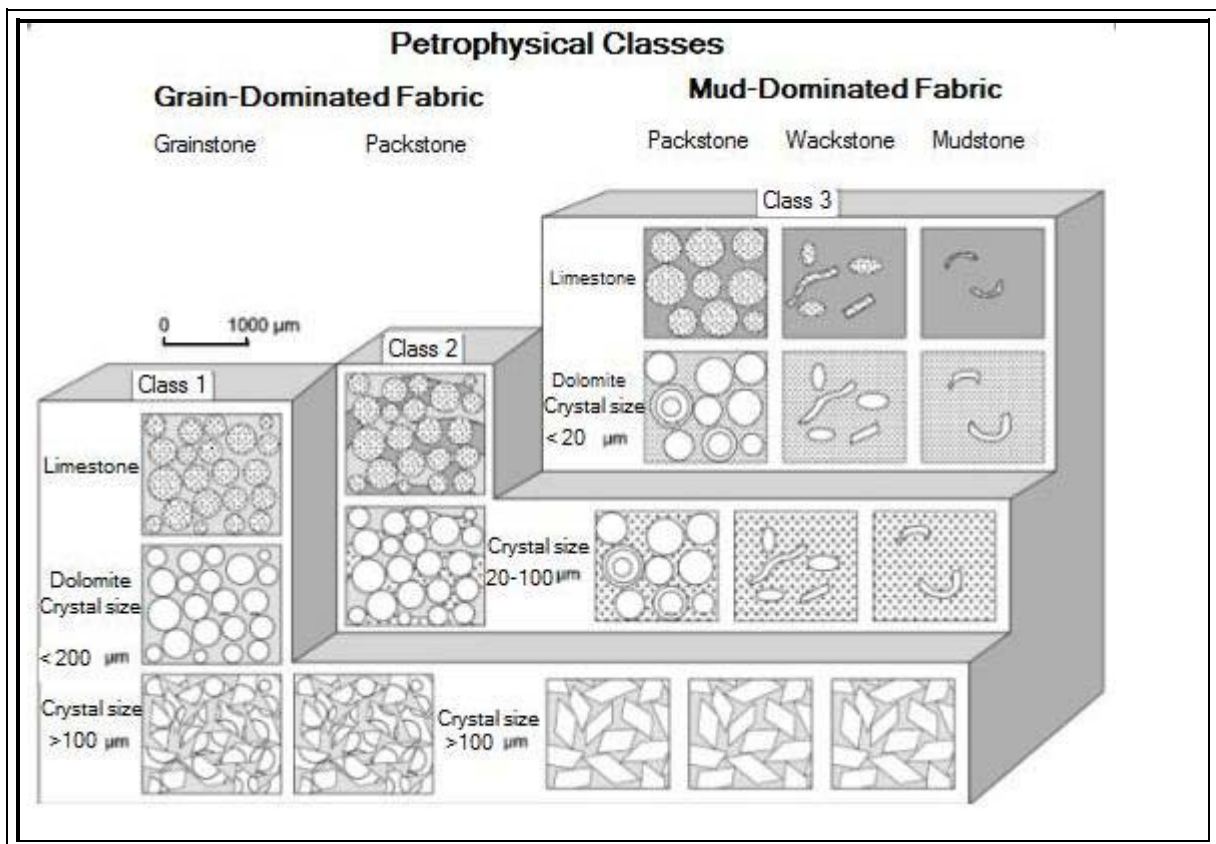


Figure 3.12: Carbonate Petrophysical Classes (grain-dominated and mud-dominated rock fabrics), after Lucia, 1995.

In comparing the rock fabric fields with crossplot of porosity-permeability, and R35 pore size (Figure 3.13), uniform pore size cut off across the rock fabric fields is shown.

These rock fabrics were initially classified into three categories called rock-fabric petrophysical classes on the basis of porosity/permeability and capillary pressure (Jennings and Lucia, 2003) (Figure 3.13).

- Class 1 - is composed of grainstone, dolograins and large crystalline dolostone, with lower porosity but high permeability.
- Class 2 - is composed of grain-dominated packstones, fine and medium crystalline, grain-dominated dolopackstones, and medium crystalline, mud-dominated dolostone, with moderate porosity and permeability.
- Class 3 - includes mud-dominated limestones and fine crystalline, mud-dominated dolostone, with high porosity, but lower permeability.

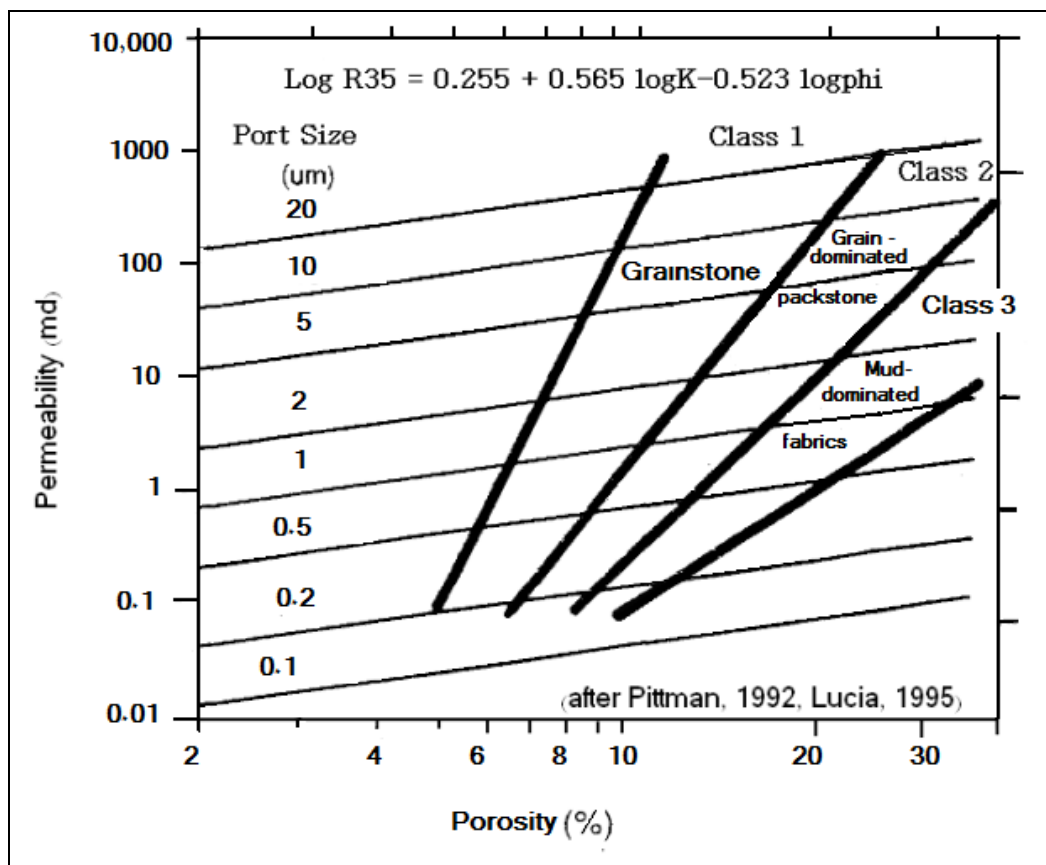


Figure 3.13: Porosity permeability crossplot, to classify the rock into three rock fabric classes (Jennings and Lucia, 2003).

The permeability of limestone increases with increasing intergrain porosity and increasing grain size and sorting. Mud-dominated limestone (mud-dominated packstones, wackestone, and mudstone) have the least permeability and generally fall on a porosity/permeability crossplot within a field associate with rock fabric class 3.

Grain-dominated packstones have higher permeability values and generally fall within the class 2 field. Grainstones have the highest permeability and generally fall within the class 1 field (Jennings and Lucia, 2003).

Permeability in dolostone also increases with increasing intergrain porosity with increasing grain size and with sorting of the precursor limestone. The permeability of mud-dominated dolostone increases with both increasing dolomite crystal size and intercrystalline pore space. Fine crystalline, and mud-dominated dolostone have permeability characteristics of class 3 limestone. Medium crystalline, mud-dominated dolostones have characteristics of class 2 limestones. Large crystalline mud-dominated dolostones have characteristics of class 1 limestone.

The figure (3.14) shows that most of the data of the reservoir Subunits fall to the area of the class 2 and class 3. This indicated that the rock fabrics can be described as grain-dominated packstones, fine and medium crystalline, grain-dominated dolopackstones, medium crystalline, mud-dominated dolostone with effect of mud-dominated limestones fine crystalline, mud-dominated dolostone. By the other term, it is possible to say that the most porosity of unit "A" of the Upper Qamchuqa reservoir in Khabbaz oil field, including A1, A2, A3, A4, A5, and A6 subunits belong to the inter particle (inter crystalline and inter granular) dominant porosities. This result also agrees with the derived porosities from sonic log and Neutron-Density porosity, which show the slight separations (Figure 3.1C). Because in case of domination of secondary porosities (caves, fractures, vugs, channels, molds etc.), the two log's derived porosities show high separations, where the Neutron-Density porosity is higher than the Sonic derived porosity.

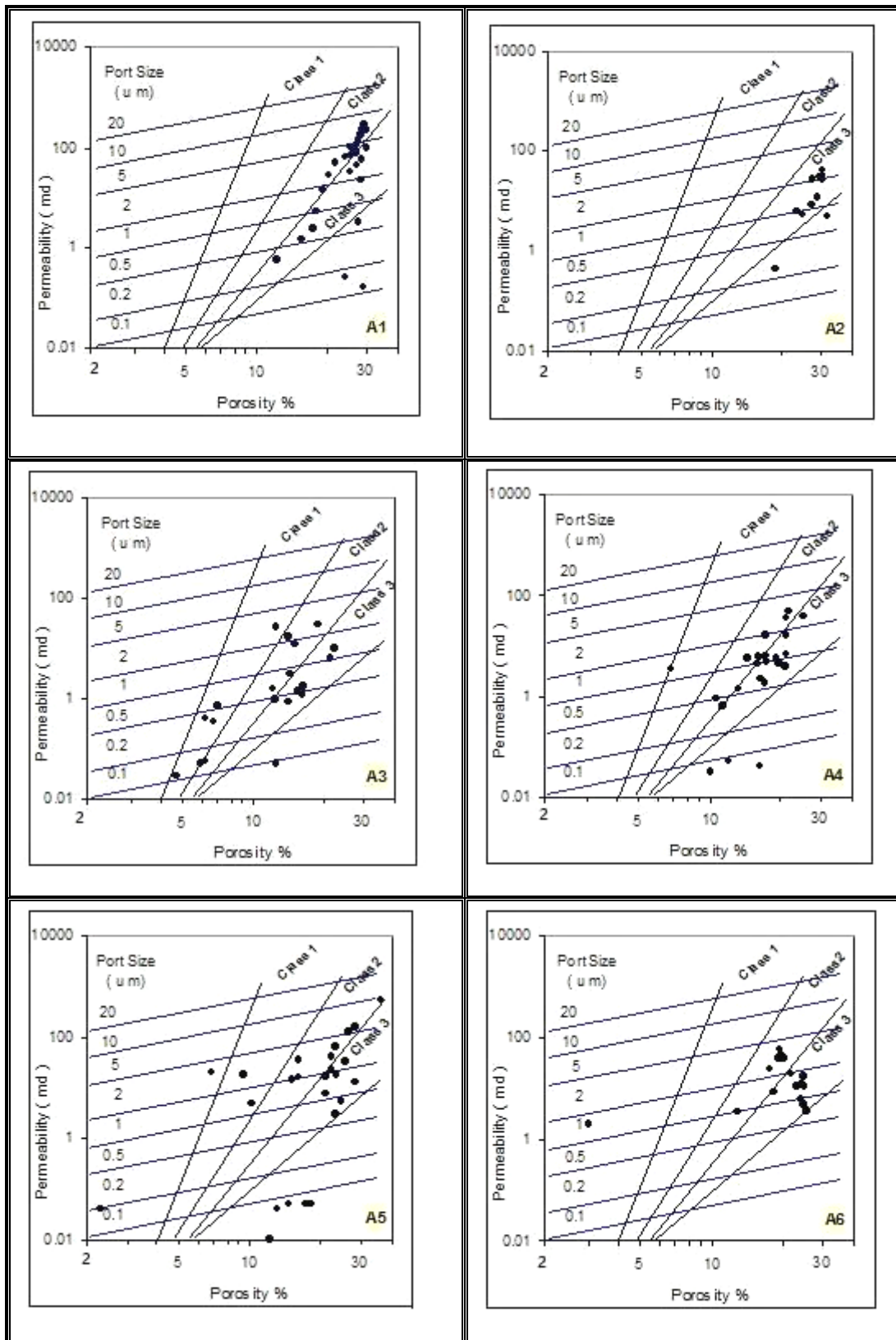


Figure 3.14: Porosity permeability crossplot, shows the R35 and rock fabric classes of the six porosity subunits (A1, A2, A3, A4, A5 and A6), most of the data fall to the class 2 and class 3 rock fabric types (packstone to mudstone).

3.7 Reservoir Unit Classification

The Upper Qamchuqa Formation is subdivided into three lithologic units in the Khabbaz oil field, named as lithologic unit A, B, and C (Chapter two). Based on the previously discussed petrophysical parameters the most important reservoir unit of the Upper Qamchuqa Formation is the most upper zone of the formation represented by unit "A" which shows the regular extended within the field with good reservoir properties. The formation shows downward regression (weakening) of the reservoir characteristics, which makes the other two units "B" and "C" to be considered as less important reservoirs. Below is a general review of these units with their distinctive petrophysical properties:

3.7.1 Unit (A).

Based on the reservoir characteristics, which was illustrated by some tools, especially Neutron-Density combination porosity, it was shown that the upper unit of the Upper Qamchuqa Formation (Unit A) represents the essential reservoir unit all over the field, which is subdivided vertically in each well from the top into six reservoir petrophysical subunits, named A1, A2, A3, A4, A5, and A6 (Figures 3.15 and 3.16). Each subunit is identified from an interrelated series of petrophysical cross plots, thin section slides study, and from the calculation of pore throat radii at the 35% pore volume (R_{35}), using both Winland's equation from core porosity(Φ) and permeability(K) data (Martin et al, 1997) and Aguilera & Aguilera equation (in Aguilera, 2004). The latter was given more reasonable results:

$$R_{35} = 2.665 [K / (100^\Phi)]^{0.45} \dots\dots\dots 3.8$$

The subunits are separated by five non reservoir layers named N1, N2, N3, N4, and N5. Figures 3.15 and 3.16 illustrate the correlation of these subunits (reservoir and non reservoir) along eight well sections.

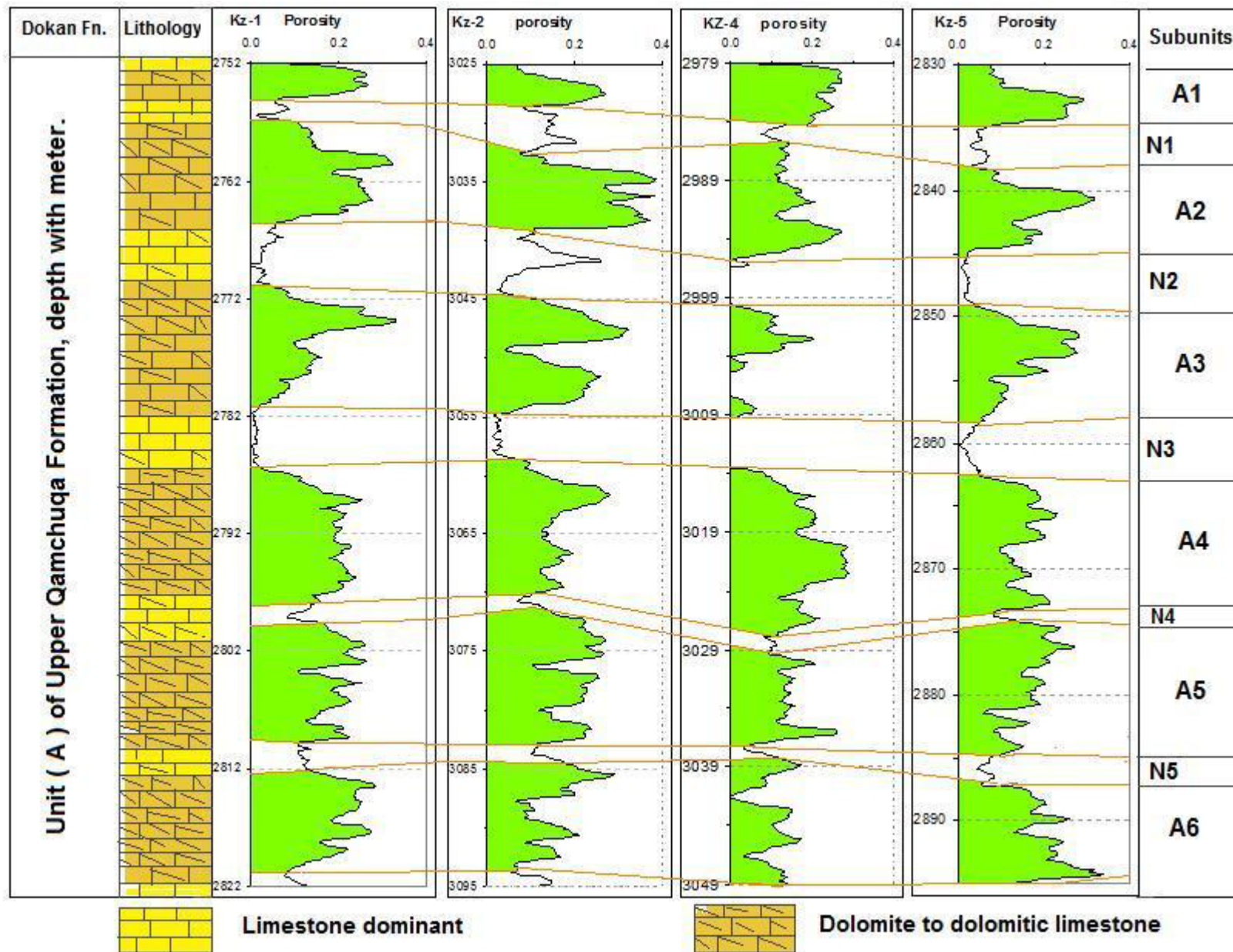


Figure 3.15: Lithologic unit (A) at wells Kz-1, Kz-2, Kz-4, and Kz-5 showing alternation of reservoir and non-reservoir subunits, using N-D porosity logs

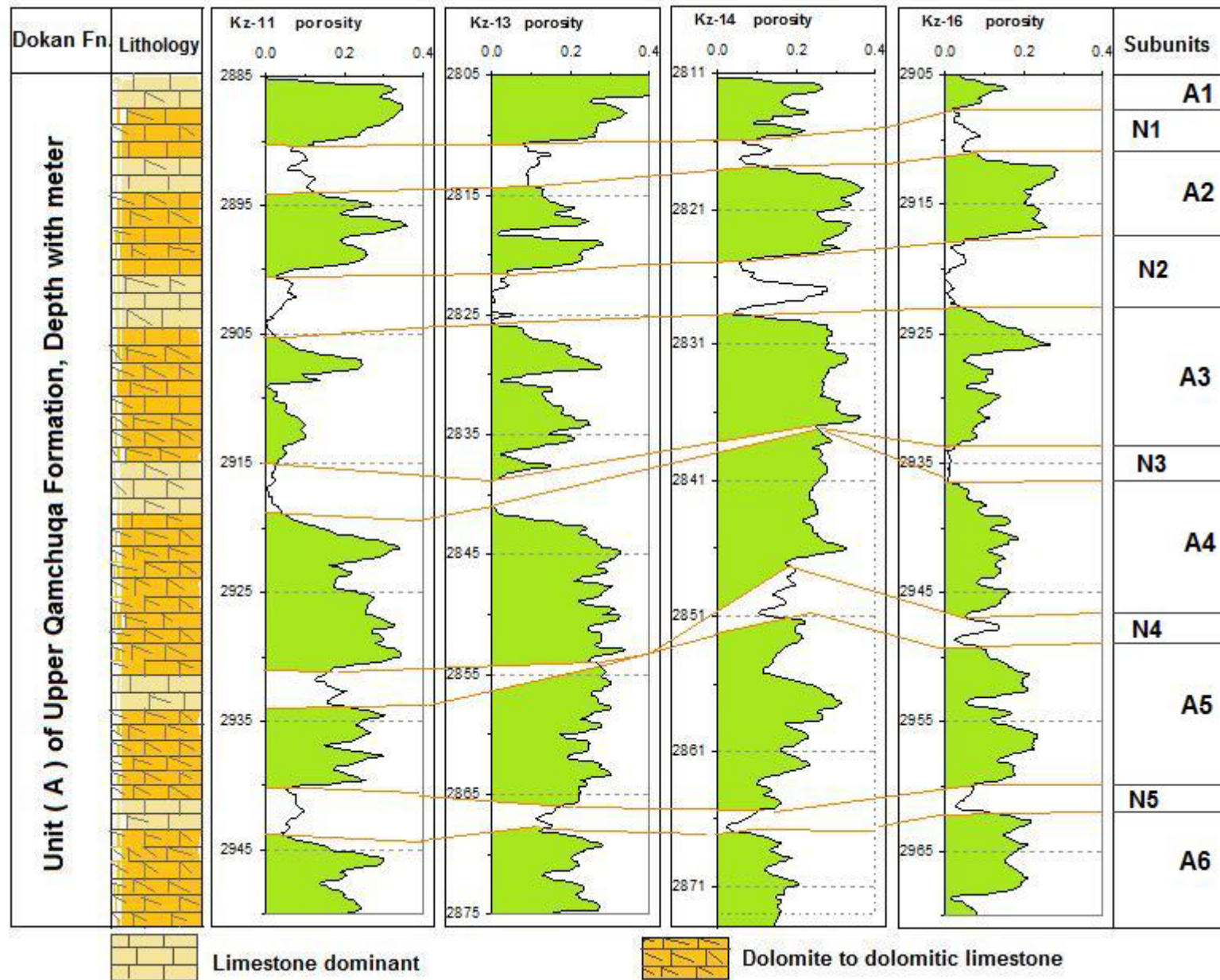


Figure 3.16: Lithologic unit (A) at wells Kz-11, Kz-13, Kz-14, and Kz-16 showing alternation of reservoir and non-reservoir subunits, using N-D porosity logs.

The following are the description of the reservoir subunits of unit (A):

3.7.1.1 Reservoir Subunit (A1)

The Subunit (A1) represents the upper most part of Upper Qamchuqa Formation, under the unconformable contact with Dokan Formation. The thickness of this subunit ranges between 2 and 5 meters, with an average of 3.2m (Figures 3.15 and 3.16). This unit has thickness of around 4m in the SE end of the Khabbaz structure in wells Kz-3 and Kz-14, while the thickness is reduced in the central part of the field (Kz-1, Kz-2, Kz-5 and Kz-16) which drops down into around 2m (Table 3.4). The NW end of the field shows increasing thickness of this subunit, which reaches 5m in Kz-11, and Kz-13 (Table 3.4), but its maximum thickness in well Kz-4 at the northwestern end of the field when combined with underlain subunit (A2). This unit is characterized by good porosity ranging between 0.14 and 0.25 (Table 3-4). The N-D diagrams (Figures 3.4A1, 3.5A1, 3.6A1, 3.7A1, 3.8A1, and 3.9A1) show that most of the data fall between the dolomite and limestone lines which they suggest the dolomitic limestone of subunit A1. While in well Kz-1 the points are concentrated near the limestone line, in well Kz-11, it is inverse case, most of the data fall on dolomite line. According to rock fabric classes of Jennings and Lucia (2003), this unit falls on Φ/k cross plot with the class "2" and "3" which is associated with mud dominated limestones and/or fine crystalline dolostone (Figure 3.14).

The microscopic study of these subunit shows that it mainly consists of dolomudstone facies with very fine crystalline dolomite (Figure 3.17a).

The pores are well sorted, and connections between pores are good. Pore throat sizes are generally large but variable (0.01 μm to 9.95 μm), with an average of 2.08 μm (Table 3.5) which is classified as macro pore. Table 3.5 illustrates high permeability (70 md), this may refer to the presence of fractures and channels, since it directly underlains the unconformity surface and these characteristics (fractures and channels) are expected due to weathered surface and diagenetic effects.

3.7.1.2 Reservoir Subunit (A2)

The Subunit (A2) underlies the Subunit A1 (Figures 3.15 and 3.16), both are separated by a non-reservoir layer named N1. The Subunit A2 ranges in thickness between 5 and 8m, having maximum thickness in the central part of the field and decreases toward the margins. This subunit is combined with the overlying Subunit (A1) in Kz-4 and underlying Subunit (A3) in Kz-3. N-D diagrams (Figures 3.4A2, 3.5A2, 3.6A2, 3.7A2, 3.8A2, and 3.9.A2) illustrate the lithology of this unit ranging from limestone, dolomitic limestone to pure dolomite. According to rock fabric classes of Jennings and Lucia (2003), this unit falls on Φ/k cross plot within the class 3 which is associated with mud dominated limestone and fine crystalline mud dolostone (Figure 3.14). Examination of thin section samples of this subunit reveals that it is dominated by dolomudstone facies (Figure 3.17b) to bioclastic wackestone to packstone, and often oil stained (Figure 3.17c). Dolomite is fine to medium crystalline, planar-s-e dolomite mosaic (Figure 3.17d, e, and g), and medium crystalline planer-e-s dolomitic mosaic (Figure 3.17f).

The A2 subunit has very good porosities ranged from 0.13 to more than 0.27 from log derived porosity (Table 3.4), the core derived porosity record higher values. The average permeability is 18.25 md. (Table 3-5) The moderate pore throat size (1.5 μm) with limited range (0.26-2.55 μm), also moderate permeability relatively, and very high porosity indicates well sorted, meso pore throat, intergranular or intercrystalline porosity.

3.7.1.3 Reservoir Subunit (A3)

The (A3) subunit has the average thickness of around 8.2m, the maximum thickness encountered in well Kz-13 is over 12m and its net thickness is reduced in Kz-11 into 3m (Figures 3.15 and 3.16).

The N-D plots (Figures 3.4A3, 3.5A3, 3.6A3, 3.7A3, 3.8A3, and 3.9A3) illustrate the dolomite, dolomitic limestones to limestone of this subunit. The rock fabric classes of this subunit falls on Φ/k cross plot with the class 1 to class 3(Figure 3.14), also thin sections study shows that this subunit

consists mainly of bioclastic mudstone to wackestone (Figure 3.18a, b); to medium crystalline planer-e-s dolomitic mosaic (Figure 3.18c, d), with bioclastic dolowackestone to dolopackstone. It commonly shows oil stains along the stylolite (Figure 3.18e, f). The general microfacies are bioclastic packstone to wackestone, miliolid-peloidal packstone to grainstone, and fine to medium planer s-e dolomite mosaic.

This subunit has a good porosity ranging between 0.12 and 0.18 (Table 3-5), while the core measured porosity give an average porosity of 0.12. The subunit shows the medium pore throat size (0.87 μm) which is classified as meso pore. Relatively medium porosity and permeability indicate the fine interparticles porosity with the matrix effect. This unit is combined with underlying Subunit (A4) in well Kz-14.

3.7.1.4 Reservoir Subunit (A4)

The Subunit (A4) has the average thickness of more than 10m, and it is combined with underlying Subunit (A5) in most wells except the wells Kz-1, Kz-3 and Kz-16.

The N-D charts (Figures 3.4A4, 3.5A4, 3.6A4, 3.7A4, 3.8A4, and 3.9A4) show the dolomitic limestone to dolomite lithology of this subunit, with the domination of dolomite in most well sections especially wells Kz-5, Kz-11, Kz-14 and Kz-16. The rock fabric classes of this subunit falls on Φ/k cross plot with the class 2, and class 3 (Figure 3.14), then the rock type is represented by fine to medium crystalline mud dominated dolostone or mud dominated limestone.

The thin sections of this subunit show medium crystalline planar-a dolomite mosaic (Figure 3.18 g, h), with bioclastic wackestone to packstone microfacies (Figure 3.19a, b). Medium crystalline planer-e-s dolomitic mosaic facies, with oil stained especially is also common (Figure 3.19c, d). Another type of microfacies also exists and characterizes by bioclastic dolomustone to dolowackestone, oil stained especially within the fossils ghost. (Figure 3.19e).

The well log derived porosity of this subunit ranging from 0.14 to 0.22 (Table 3.4), with an average of 0.17 from core measured porosity. This subunit has a permeability ranged from 0.03 to 49 md (Table 3.5), with an average of 9.03 md. Pore throat size is higher than subunit A3, but its average (1.3 μm) yet classified as meso pore. The matching of permeability with porosity indicates the well sorted interparticles porosity.

3.7.1.5 Reservoir Subunit (A5)

This subunit is also combined with overlain subunit (A4) or underlain one (subunit A6), or with both all over the wells, except in well Kz-16, its average thickness estimated to be 12.5m and the well Kz-3 doesn't reach this subunit.

The N-D charts (Figures 3.4A5, 3.5A5, 3.6A5, 3.7A5, 3.8A5, and 3.9A5) show the dominated of dolomite all over the well sections with dolomitic limestone in few wells. The rock fabric classes of this unit falls on Φ/k cross plot with the class 2, 3 (Figure 3.14), which indicated fine to medium crystalline dolostone fabric. Thin sections examination shows that dolomudstone facies which includes very fine crystalline dolomite (Figure 3.20 a), medium crystalline planer-e-s dolomitic mosaic, highly oil stained (Figure 3.20 b), bioclastic wackestone to packstone facies, with oil stained (Figure 3.20 c), bioclastic dolowackestone to dolopackstone (Figure 3.20 d), and the most potential medium crystalline planer-e-s dolomitic mosaic with oil stained (Figure 3.20 e, f, g, h).

The porosity of this unit ranged between 0.14 and 0.20 (Table 3.5) and with an average permeability of 44.54 md. The average pore throat size is 2.27 μm , so it is classified as macro pores. A5 forms a good reservoir unit, the pores are well sorted and connections between cores are good. This subunit allows high hydrocarbon production.

3.7.1.6 Reservoir Subunit (A6)

This subunit also is not penetrated by well Kz-3, and it is combined with overlain unit (A5) in wells Kz-1, Kz-2, and Kz-4, its thickness in other wells ranging from 6 to 12 m.

The well log derived porosity (Table 3.4) of this subunit ranged between 0.10 and 0.19 with an average of 0.15; while the core porosity is higher and its average is 0.20 (Table 3.5). Also this subunit has large pore throat size (2.22 μm) which is put him within macro pore throat class, and its permeability ranging between 2 and 58 md with an average of 19.44 md. All these properties represent a good reservoir subunit (Figures 3.11; 3.14).

The N-D charts (Figures 3.4A6, 3.5A6, 3.6A6, 3.7A6, 3.8A6, and 3.9A6) also show the dominated of dolomite allover the well sections with dolomitic limestone within a few wells. The rock fabric classes of this subunit fall on Φ/k cross plot with the class 2, and class 3 (Figure 3.14), which indicated the fine to medium crystalline dolostone fabric. The thin-sections of this subunit show the following microfacies: medium crystalline planer-a dolomite mosaic (Figure 3.21a), dolomudstone microfacies (Figure 3.21b) medium crystalline planer-e-s dolomitic mosaic facies, with oil stained (Figure 3. 21 c, d), bioclastic dolowackestone to dolopackstone with oil staned especially along stylolite and the fossils ghost (Figure 3. 21 e, f), and medium crystalline planer-e-s dolomitic mosaic with oil stained, with calcite cement spots within the dolomitic (Figure 3. 21 g, h).

3.7.1.7 The Non Reservoir Subunits

Table 3.5 shows that the measurements of the laboratory petrophysical properties of the five non-potential reservoir layers (N1, N2, N3, N4, and N5); as they are defined previously, they are non porous layers separating the six reservoir subunits (Figures 3.15 and 3.16).

The table illustrates their average porosities ranging from 0.02 to 0.07 with an average permeability from zero to 0.05 md. The pore throat size of these non reservoir layers ranged between 0.006 and 0.04 micron, hence they are

classified as Nano ports subunit. These petrophysical characteristics make the layers N1, N2, N3, N4, and N5 to play as impermeable barriers between the reservoir subunits and make them the isolated pay zones. With an exception of the case of fractures and other secondary channel pathways that may be conduit the reservoir subunits.

Table 3.4: The reservoir subunits of the unit (A), their intervals, thickness, and average porosity from neutron- density combination logs.

Litho. Unit	Reserv. Subunits	Their	Kz-1	Kz-2	Kz-4	Kz-5	Kz-3	Kz-11	Kz-13	Kz-14	Kz-16
Unit (A)	A1	Intervals (m)	2752.4- 2754.9	3025.9 – 3027.4	2979 - 2985	2832- 2834.7	3202.5 – 3206.7	2885.3 - 2890	2806- - 2810.5	2811.6 – 2815.6	2905.7 – 2907.3
		Thickness (m)	2.5	1.5	6.0	2.7	4.2	4.7	4.5	4.0	1.6
		porosity	0.20	0.18	0.22	0.21	0.19	0.26	0.25	0.14	0.10
	A2	Intervals (m)	2756.8- 2765.4	3032 – 3037.8	2985 – 2995.4	2838.4 – 2844.3	3208.3- 3219.2	2894 – 2899.7	2814.2 – 2820.7	2817.9 – 2824.5	2911.3 – 2917.6
		Thickness(m)	8.6	5.8	10.4	5.9	10.9	5.7	6.5	6.6	6.3
		porosity	0.19	0.27	0.16	0.18	0.17	0.21	0.13	0.24	0.20
	A3	Intervals (m)	2772- 2779.9	3044.2 – 3052.9	3000 - 3004	2849.6 – 2857.6	3219.2 - 3228.4	2906.1 – 2908.4	2826.7 – 2835.8	2826.3 - 2828	2923.8 – 2932.1
		Thickness(m)	7.9	8.7	4.0	8.0	9.2	2.3	9.1	1.7	8.3
		porosity	0.15	0.17	0.12	0.16	0.18	0.15	0.13	0.18	0.11
	A4	Intervals (m)	2787 – 2798.8	3059 – 3069.2	3014.2 – 3028.4	2863 – 2873.5	3235.4 – 3244.9	2919.8 – 2931.6	2842 – 2854	2829.2 – 2850.4	2939.1 – 2948.3
		Thickness(m)	11.8	10.2	14.2	10.5	9.5	11.8	12.0	21.2	9.2
		porosity	0.17	0.14	0.19	0.16	0.14	0.22	0.22	0.20	0.12
	A5	Intervals (m)	2799.2 – 2810.5	3069.4 – 3081.9	3028.4 – 3037.2	2873.5 – 2885.5		2931.6 – 2940.1	2854 – 2866.7	2850.9 – 2862.8	2949.3 – 2959.8
		Thickness	11.3	12.5	8.8	13.0		8.5	12.7	11.9	10.5
		porosity	0.17	0.17	0.14	0.16		0.19	0.20	0.15	0.15
	A6	Intervals (m)	2810.5 – 2622.7	3082 – 3091.2	3038.2 – 3064.3	2887.5 – 2896.1		2944.6 – 2951.5	2866.9 – 2876.4	2867.4 – 2873.2	2962 – 2968.1
		Thickness(m)	12.2	9.2	26.1	8.6		6.9	9.5	5.8	6.1
		porosity	0.18	0.13	0.11	0.19		0.17	0.14	0.10	0.17

Table 3.5: Pore throat, porosity, and permeability of reservoir and non-reservoir subunits of unit (A) in well Kz-16. Porosity and permeability data are laboratory core analysis measured.

Sub-Units	R-35 Ranges	R-35 Average microns	Φ ranges	Φ average	K range (md)	K average (md)	Pore Type
A1	0.01—9.95	2.08	0.01-- 0.30	0.17	0.01-304.7	70.79	Macro Pore
A2	0.26-2.55	1.5	0.19-0.32	0.28	5.16-42.12	18.25	Meso Pore
A3	0.003-4.12	0.67	0.02-0.22	0.12	0.01-30.7	4.43	Meso Pore
A4	0.07-3.7	1.3	0.07-0.25	0.17	0.03-48.79	9.03	Meso Pore
A5	0.002-9.67	2.27	0.02-0.37	0.19	0.01-532	44.54	Macro Pore
A6	0.71	2.22	0.03-0.25	0.20	2-58	19.44	Macro Pore
N ₁	0.007-0.18	0.04	0.03-0.08	0.03	0-0.60	0.04	Nano Pore
N ₂	0.006-0.17	0.04	0.01-0.08	0.03	0-0.73	0.05	Nano Pore
N ₃	0.009-0.15	0.03	0.01-0.03	0.02	0	0	Nano Pore
N ₄	0.006-0.009	0.008	0.03-0.05	0.04	0	0	Nano Pore
N ₅	0.004-0.009	0.006	0.03-0.1	0.07	0-0.04	0.01	Nano Pore

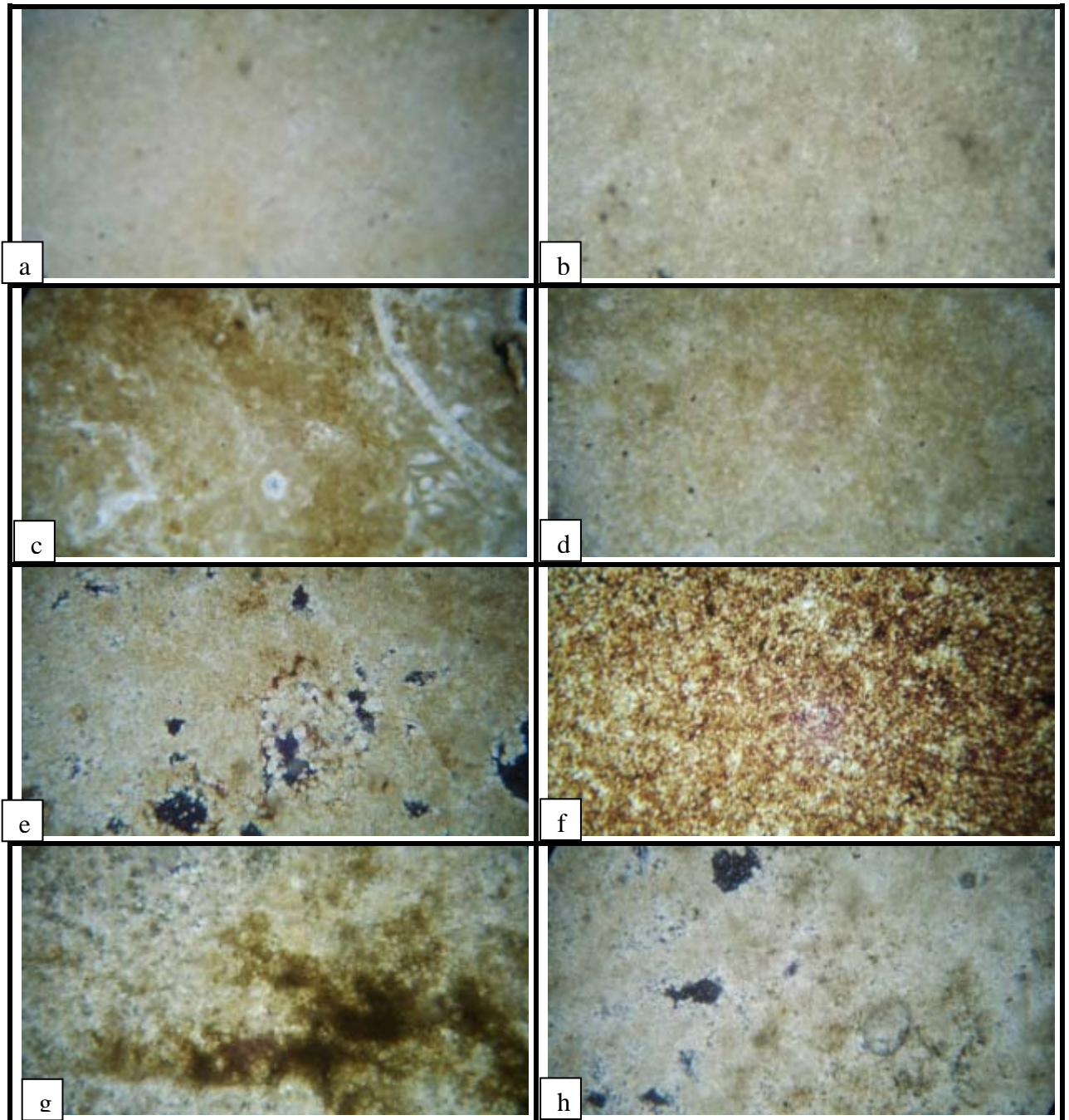


Figure 3.17: Thin-section photomicrographs, **(a)** Kz-11/ 2885-86m, dolomudstone facies very fine crystalline dolomite, this facies belongs to unit A1; all other slides belong to unit A2, **(b)**, Kz-4/ 2989m, is dolomudstone facies. **(c)** Kz-11/ 2893-94m, bioclastic wackestone to packstone oil stained. **(d & e)** Kz-11/ 2893-94 and 2895-96m respectively. **(g & h)** Kz-16/ 2914 & 2917m, these four slides are fine to medium crystalline planar-s-e dolomite mosaic they show oil stained. **(f)** Kz-16/ 2912m is medium crystalline planar-s-e dolomitic mosaic highly oil stained, (all photo's width is around 2mm and cross nickoled).

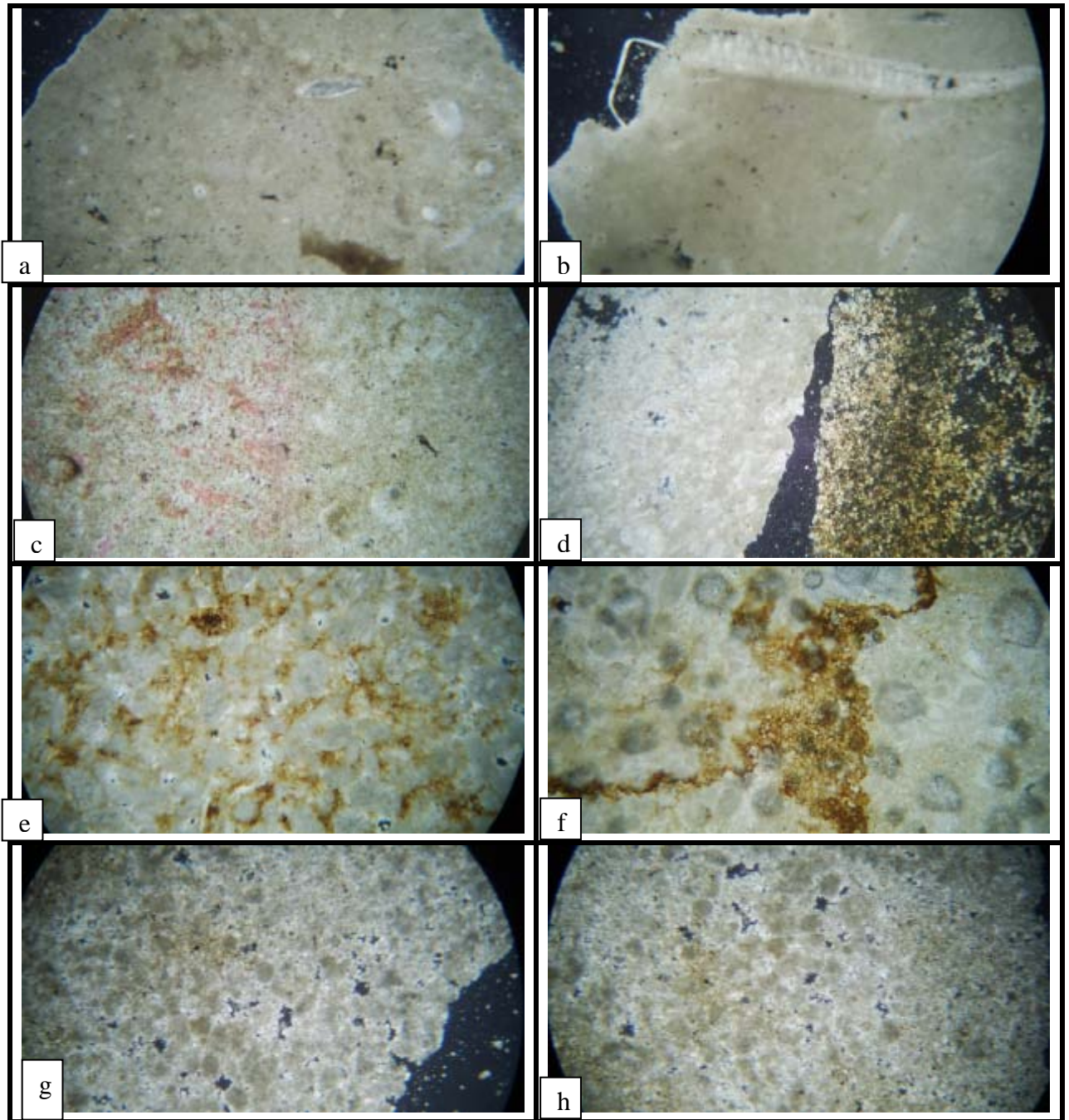


Figure 3.18: Thin-section photomicrographs **(a & b)** Kz-13/ 2827 & 2831m respectively are bioclastic mudstone to wackestone belonging to unit A3. **(c)** Kz-16/ 2924m, and **(d)** Kz-4/3014m are unit A3, they are medium crystalline planar-dolomitic mosaic partly oil stained. **(e & f)** Kz-16/2930 & 2927m respectively are unit A3 bioclastic dolowackestone to dolopackstone oil stained along the stylolite and fossils ghost which show the growth of medium crystalline dolomite. **(g & h)** Kz-14/2842 & 2846m respectively are unit A4 medium crystalline planar-dolomite mosaic. (all photo's width is around 2mm and cross nickoled).

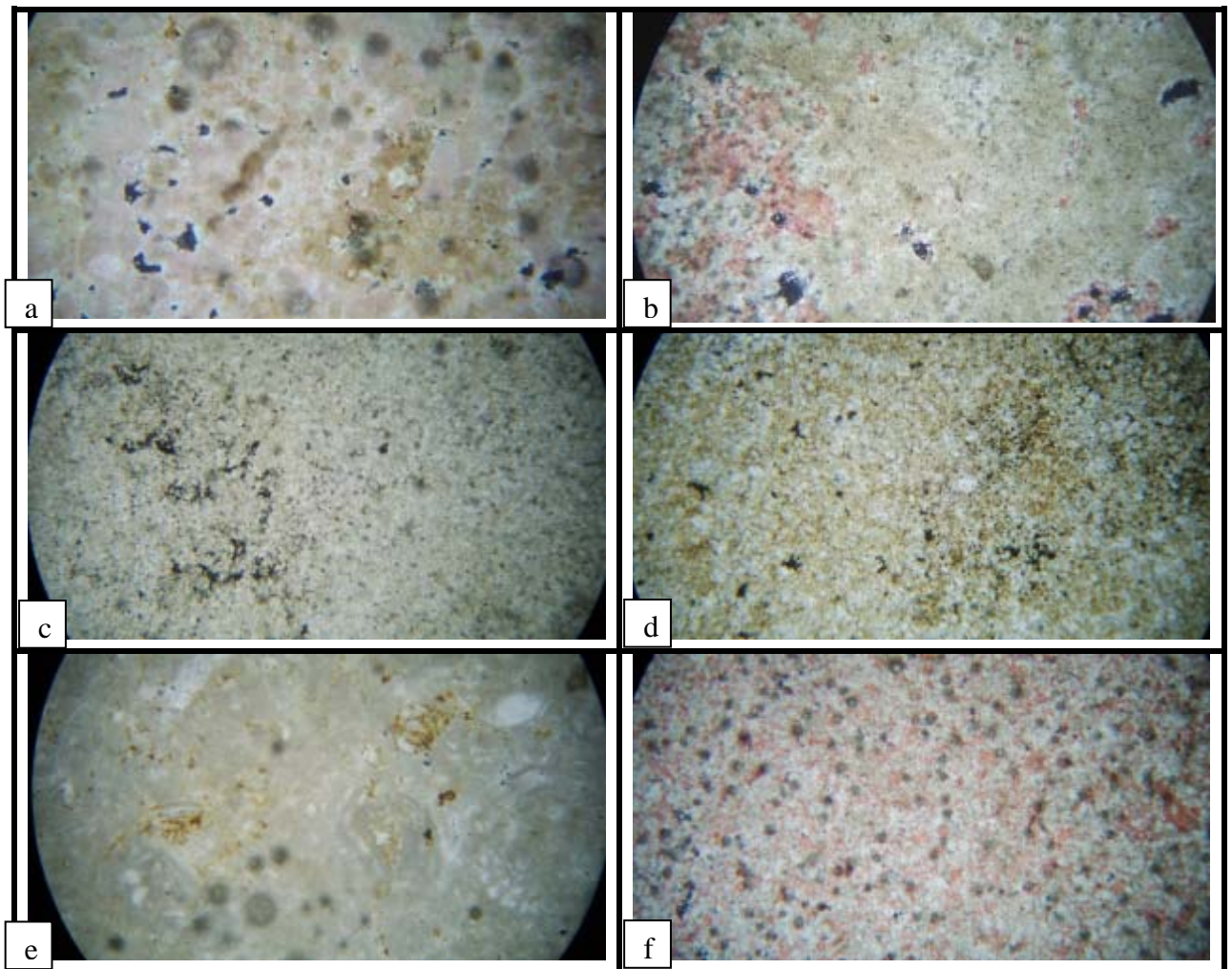


Figure 3.19: Thin-section photomicrographs, (a & b) Kz-16/ 2939 & 2940m respectively, bioclastic wackestone to packstone micro facies belong to unit A4, (c & d) Kz-16/ 2943 & 2944m respectively belong to unit A4, they are medium crystalline planer-e-s dolomitic mosaic facies, oil stained especially slid c. (e) Kz-16/ 2946m, unit A4 bioclastic to dolomudstone dolowackestone oil stained along the fossils ghost. (f) Kz-16/ 2947m is unit A4 medium crystalline dolopackstones. (all photo's width is around 2mm and cross nickoled).

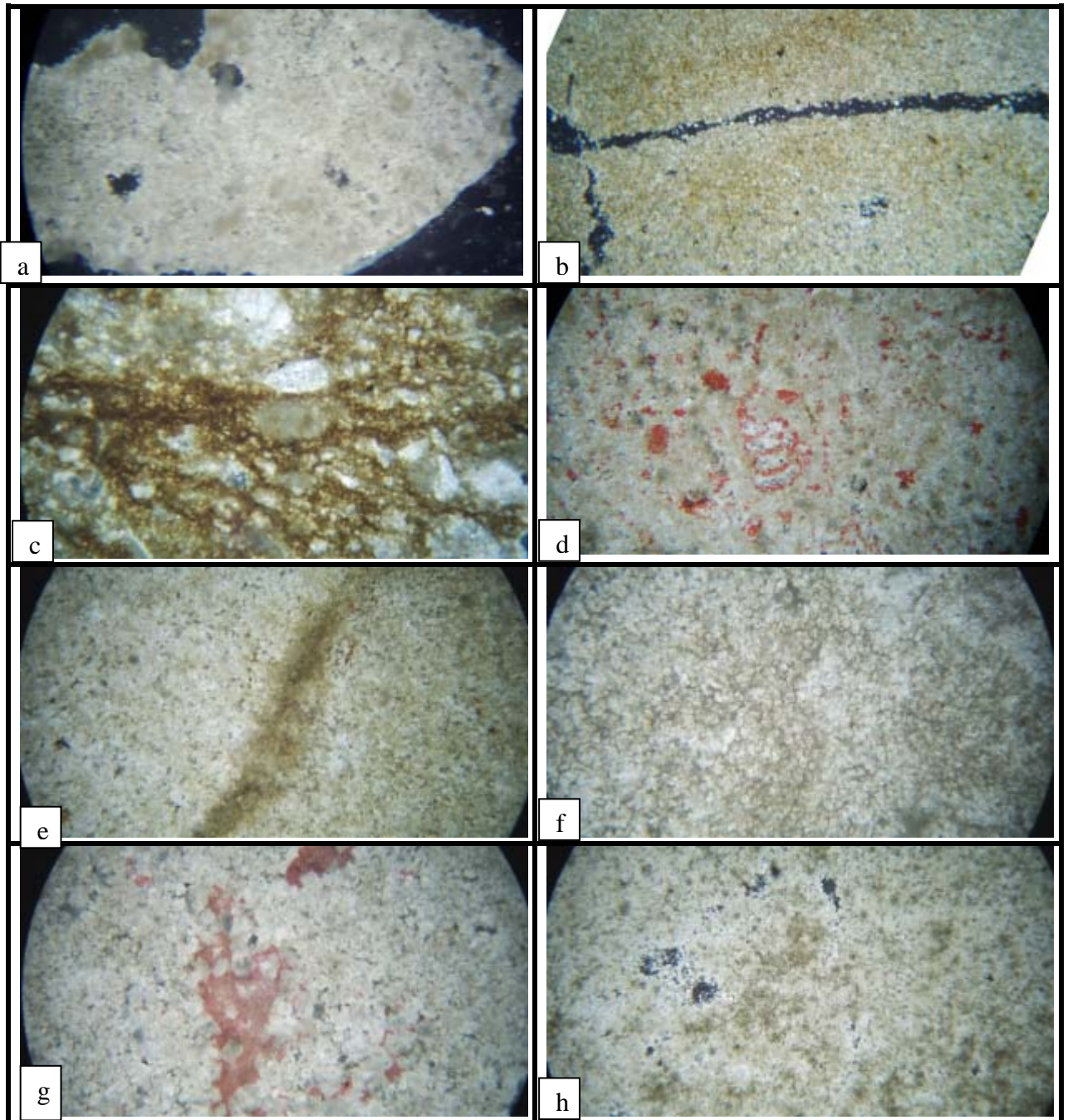


Figure 3.20: Thin-section photomicrographs of unit A5, (all photos width is 2mm and cross nickoled). (a) Kz-13, 2865m dolomudstone facies very fine crystalline dolomite, this facies belongs to unit A5. (b) Kz-14, 2854m is medium crystalline planer-e-s dolomitic mosaic highly oil stained. (c) Kz-14, 2861m bioclastic wackestone to packstone oil stained. (d) Kz-16, 2951m bioclastic dolowackestone to dolopackstone pinked area related to no-dolomitized along the ghost of fossils. (e, f, g & h) Kz-16, 2952, 2958, 2958 and 2959m respectively, they are medium crystalline planer-e-s dolomitic mosaic oil stained, with some spots of non dolomitized limestone area. . (all photo's width is around 2mm and cross nickoled).

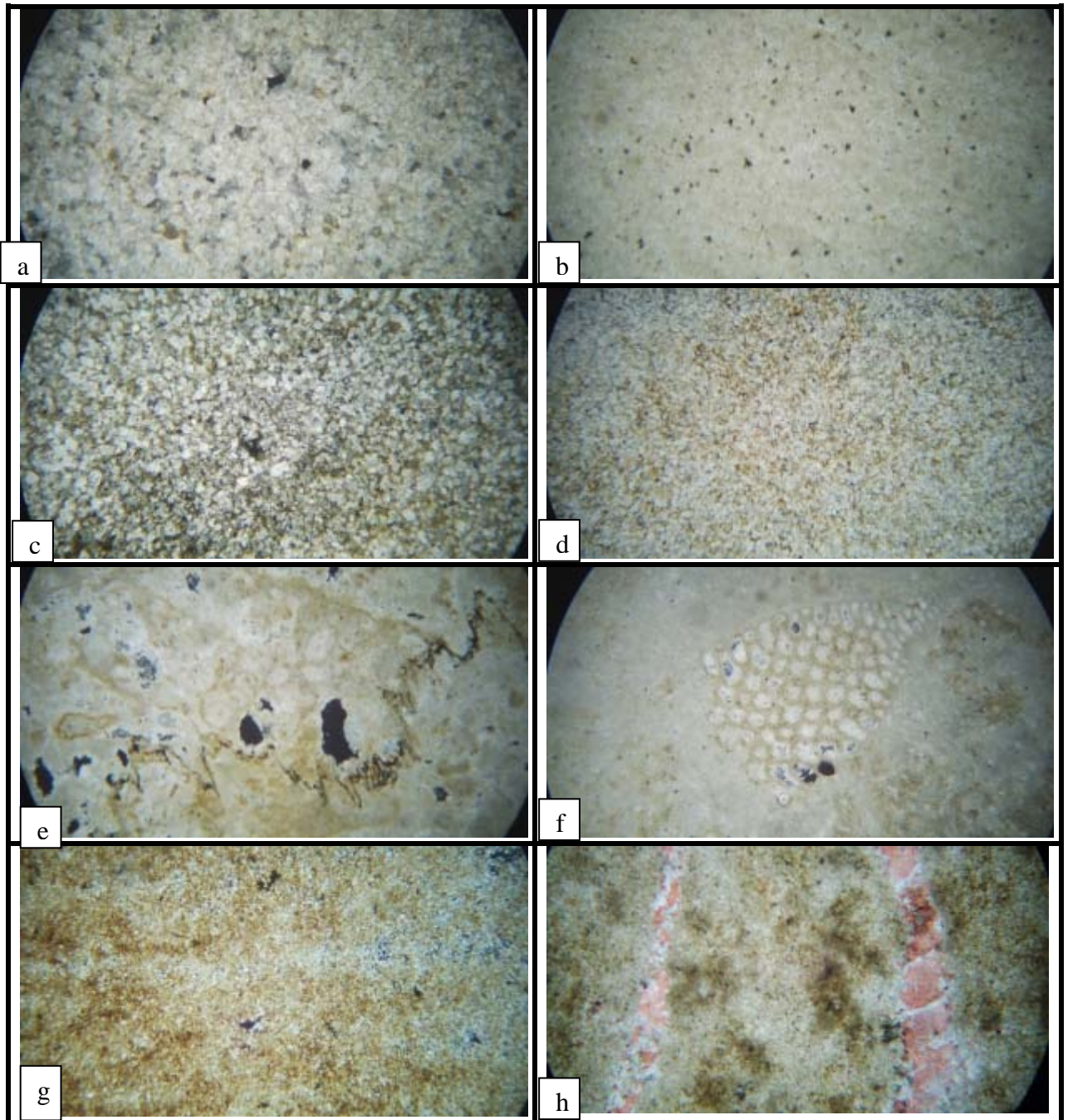


Figure 3.21: Thin-section photomicrographs of unit A6, **(a)** Kz-11/2944m medium crystalline planer-a dolomite mosaic. **(b)** Kz-11 depth 2945m dolomudstone microfacies; **(c & d)** Kz-11/2945.76 & 2949m respectively, they are medium crystalline planer-e-s dolomitic mosaic oil stained, with some spots of non dolomitized limestone area **(e & f)** Kz-11/2950 & 2951m respectively, they are bioclastic dolowackestone to dolopackstone, the latter show *Orbitolina* ghost, oil stained especially along stylolite and the fossils ghost. **(g & h)** Kz-16 /2964 and 2966.85m respectively, they are medium crystalline planer-e-s dolomitic mosaic oil stained, with some pinked spots of non dolomitized limestone area. (all photo's width is around 2mm and cross nickoled).

3.7.2 Unit (B and C).

In general the reservoir characteristics of the Upper Qamchuqa Formation decreased downward. The two lower lithologic units of this formation (B and C) are considered margin or non reservoir units if they are compared with the upper lithologic Unit (A), which the latter includes the main continuous reservoir zones all over the Khabbaz field. The downward decreasing of porosity and permeability are illustrated in appendices A1-A9 and C1-C3. Although there are some discontinuous porous intervals within both units B and C (Figures 3.22 and 3.23). It is possible to represent them as marginal or second order reservoir subunits, and if they are compared with the main reservoir subunits, they are considered insignificant reservoir subunits. Three of these intervals were counted in the unit B, named as B1, B2 and B3; and the fourth one named C1 belonging to the lithologic unit C. These subunits are pinch out shape and have changeable pattern from well to other with uneven thickness and petrophysical characteristics. Below are short descriptions of these margin reservoir subunits:

3.7.2.1 Reservoir Subunit (B1)

This subunit as summarized in table 3.6 has a variable thickness from well to well, ranging from 2 meters in well Kz-2 to 17meters in well Kz-13 (Figures 3.22 and 3.23). The porosity of this zone ranging between less than 0.07 and 0.15, with an average of 0.09. As it was made clear previously, and illustrated in Table 3.6 that there is no lateral depth correlation of this unit from well to well.

3.7.2.2 Reservoir Subunit (B2)

The subunit B2 has varied thickness from well to well, its minimum thickness 2 meters in Kz-14 and maximum (22 meters) in well Kz-1 (Figures 3.22 and 3.23). The porosity of this unit is also variable, for example in well Kz-13 its average porosity reaches around 0.15, in wells

Kz-1, Kz-2, Kz-7, Kz-11 and Kz-16 their porosities come close to 0.10; while in some others decline to around 0.06 (Table 3.6).

3.7.2.3 Reservoir Subunit (B3)

The subunit B3 lies near to the base of the lithologic unit B, its thickness varies from well to well, which ranges between 1m to more than 20ms. The average porosity of subunit B3 varies also from 0.07 to 0.15 (Table 3.6). This subunit is combined with another underlain subunit (C1), this case seemed in some wells such as Kz-5 and Kz-11 (Figures 3.22 and 3.23) which make their importance to increase as a single unit.

3.7.2.4 Reservoir Subunit C1

A porous zone also is present in the base of lithologic unit C, this subunit named C1, its thickness ranged between 1m to around 18m (Figures 3.22 and 3.23). The porosity of this subunit also varied from 0.03 to 0.12 (Table 3.6). The importance of this subunit can be neglected because it lies at the base of Upper Qamchuqa Formation, and grades into the Upper Sarmord Formation. The dominant of shale and marl fractions on this zone reduce its reservoir characteristics.

Table 3.6: The depth intervals, thicknesses, and average porosity, of the porous zones (B1, B2, B3, and C1) of the lower part of the Upper Qamchuqa Formation.

Litho. Units	Reservoir Sub-Unit		Kz-1	Kz-2	Kz-4	Kz-5	Kz-7	Kz-11	Kz-13	Kz-14	Kz16
Unit (B)	B1	Intervals (m)	2831-2838	3110-3112	3047-3064	2916.2-2926.7	2964.4-2975.9	2885.8-2902.9	2881.9-2887.2	2987.7-3002
		Thickness(m)	7.0	2.0	17	10.5	11.5	17.1	5.3	14.3
		porosity	0.11	0.10	0.07	0.10	0.08	0.07	0.15	0.11
	B2	Intervals (m)	2840.6-2863	3127.7-3131.1	3070 -3084	2930.1-2937.5	2931.9-2934.2	2977.9-2983.4	2906.5-2911.3	2893.1-2895.2	3014.9-3018.5
		Thickness(m)	22.4	3.4	14	7.4	2.3	5.5	4.8	2.1	3.6
		porosity	0.10	0.11	0.06	0.07	0.11	0.11	0.15	0.08	0.10
	B3	Intervals (m)	2867.3-2873.2	3149.4-3151.3	3095.6-3119.2	2951-2969	2964.8-2968.9	3009.5-3028.5	2931.4-2946.3	2930.9-2943.3	3026.3-3034.1
		Thickness(m)	5.9	1.9	23.6	18	4.1	19.0	14.9	12.4	7.8
		porosity	0.12	0.15	0.10	0.12	0.07	0.10	0.11	0.08	0.08
Unit (C)	C1	Intervals (m)	2888.7-2894.9	3188.2-3196.8	3120.4-3138.6	2971.4-2973.6	2983.6-2989.4	3029.6-3037.5	2951-2954	2957.3-2959.3	3044.3-3046.1
		Thickness(m)	6.2	8.6	18.2	2.2	5.8	7.9	3.0	2.0	1.8
		porosity	0.12	0.10	0.08	0.12	0.03	0.09	0.08	0.11	0.10

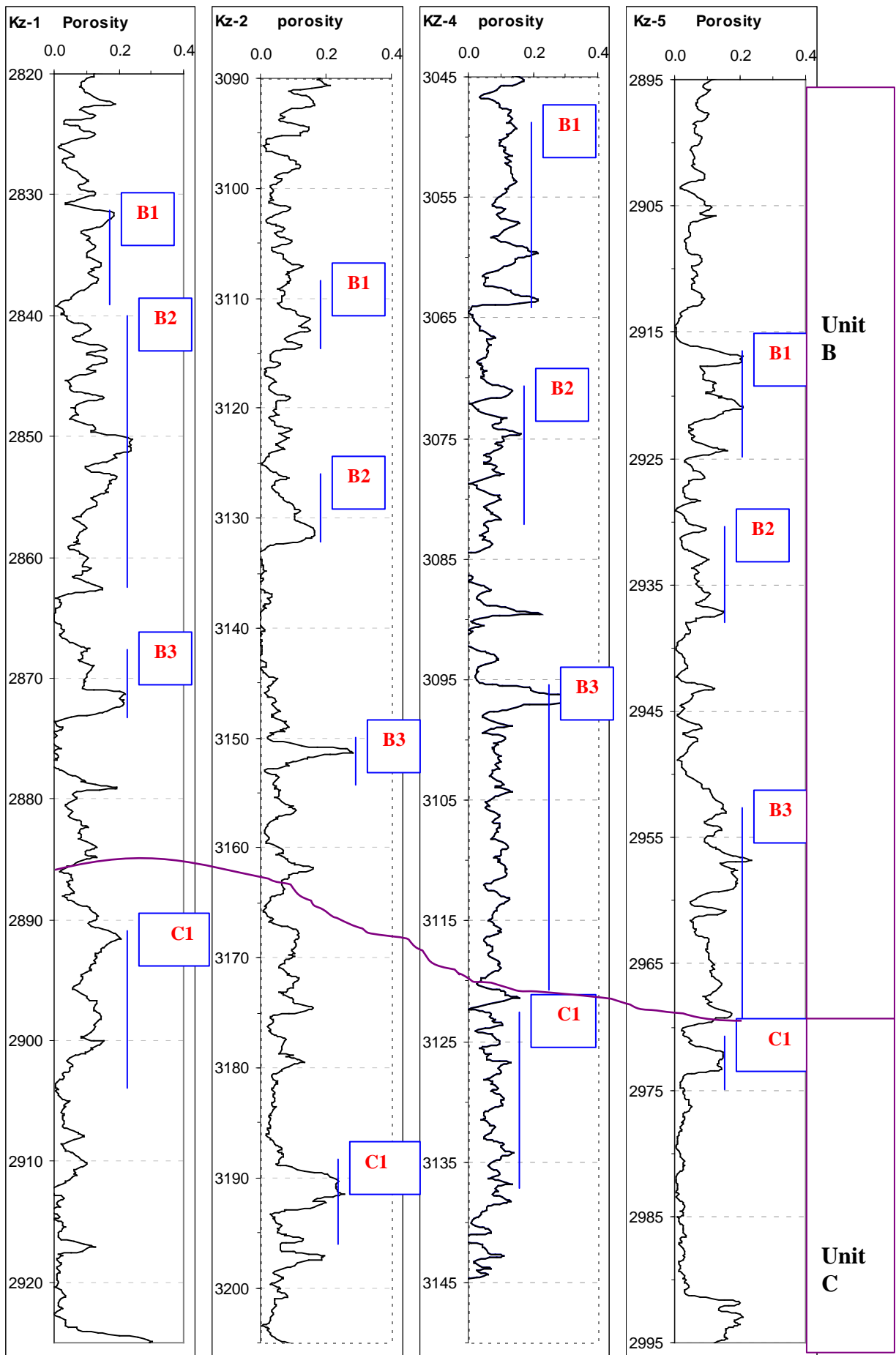


Figure 3.22: Lithologic units (B and C) at wells Kz-1, Kz-2, Kz-4, and Kz-5 showing some irregular porous subunits, using N-D porosity logs.

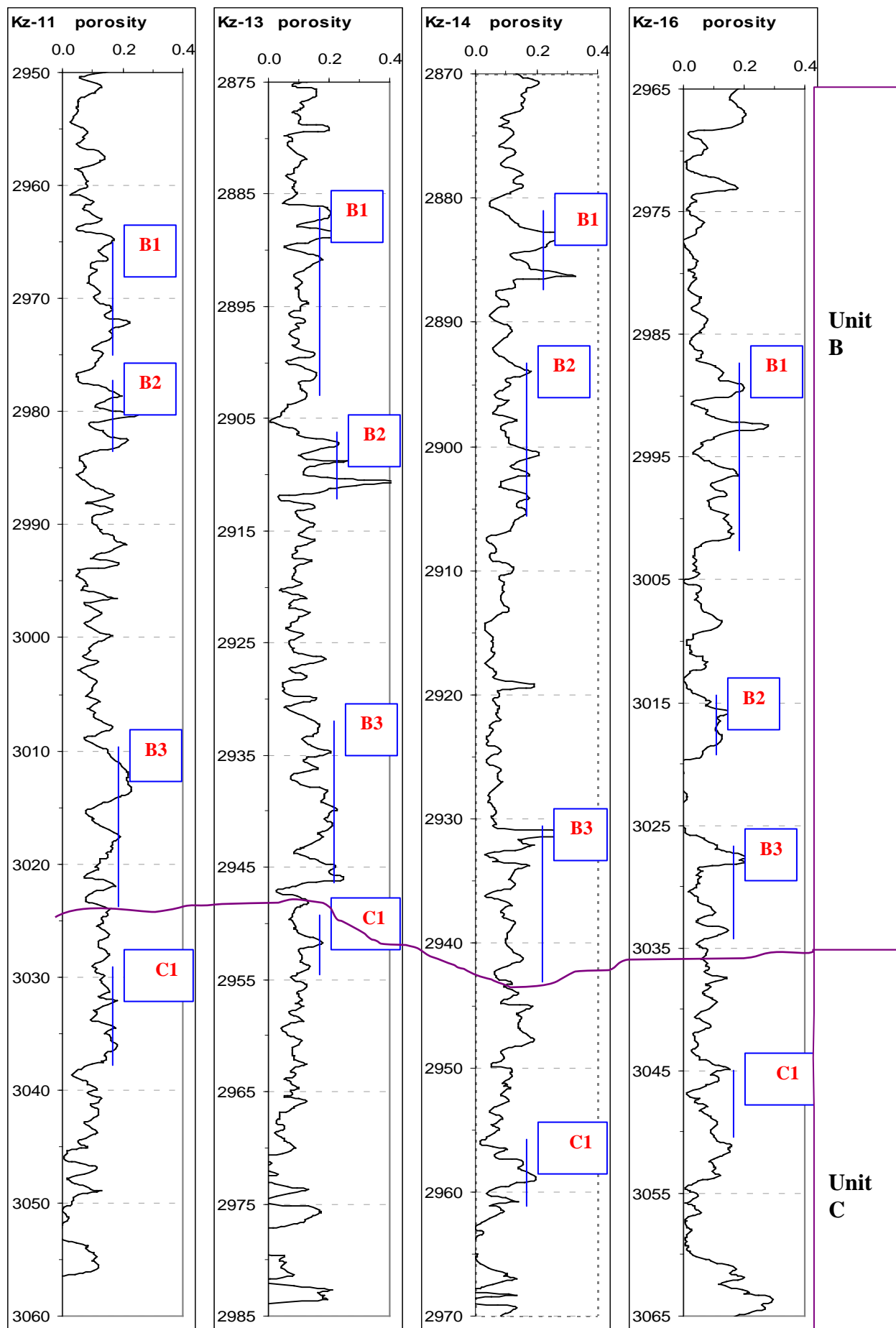


Figure 3.23: Lithologic units (B and C) at wells Kz-11, Kz-13, Kz-14, and Kz-16 showing some irregular porous subunits, using N-D porosity logs.

Chapter Four

Reservoir Fluids

4.1 Introduction

One of the most important functions of the reservoir geology is the periodic calculation of the reservoir oil and gas in place and recovery anticipated under the prevailing reservoir mechanism and condition. Oil recovery is a reflection of the mobility of hydrocarbons through porous media. This mobility is controlled by reservoir rocks, fluid properties, and pressure gradient. Oil in place is calculated either by the volumetric method or by material balance equation. This chapter is an attempt to focus on the reservoir fluids including water saturations (moveable and irreducible waters) and hydrocarbon saturations (movable and residual hydrocarbons), depending on the resistivity log measurements, particularly the resistivity of flushed zone and un-invaded zone.

Also another well log, especially porosity logs (Neutron-Density porosities) application was incorporated in this chapter to support reservoir fluid evaluation of the studied field, in addition to the geological data and laboratory measurements.

4.2 Resistivity Logs

The principal use of resistivity well logs is to detect the existence oil and gas, and to quantify them. The resistivity parameter which is of greatest interest is true formation resistivity (R_t), because it is related to the hydrocarbon saturation. Determination of R_t , is therefore of paramount importance. Resistivity of flushed zone (R_{xo}) is also parameter of interest because a comparison of R_{xo} and R_t can indicate hydrocarbon moveability (Asquith and Krygowski, 2004, and Hamada, 2004).

Resistivity data are normally used to evaluate water saturation, using porosity values derived from porosity logs (neutron-density combination as it is done in this study). Determination of initial hydrocarbons (either oil or gas) in place is based on porosity, hydrocarbon saturation, and thickness

obtained from openhole logging (see chapter 3). In this study deep (R_t), and shallow (R_{xo}) resistivity data obtained from Dual laterolog deep (LLD) and Micro spherical focused log (μ SFL) respectively, and in some of the studied wells they had been replaced by Induction electrical log (Short Normal and Induction). Also with resistivity log data other petrophysical parameters also must be known, including tortuosity factor (a), cementation exponent (m) and saturation exponent (n). These parameters could be used with log resistivity data to calculate the fluids saturation (Asquith and Krygowski, 2004).

4.3 Estimation of Cementation Factor (m)

Archie 1942 (in Serra, 1986) was the first to put forward an empirical equation relating the formation factor. For Archie $a = 1$ and m varies as a function of grain size and distribution or as a function of the channels linking the pores. The estimation of cementation factor (m) depends on the laboratory measurements, where the plug samples are taken from the reservoir core rocks; they must be cleaned to eliminate all traces of hydrocarbon and then impregnated them of water with known resistivity.

In this study, the laboratory measurement data were carried out by N. O. C, and the measured data (porosity and the formation resistivity factor) from plug samples of wells Kz-2, Kz-11 and Kz-16 (Appendix D) used to derive m . The logarithmic of data are plotted against each other (Adisoemarta et al 2000). Each as a function of the other, horizontal axis is the porosity and vertical is the formation resistivity factor (Figure 4.1); m is the slope of the average trendline ($m = \frac{y}{x}$), and the trendline equation on top of the figure

gives the relation: $y = -0.9188x + 2.5709$ 5.1

By assumption of $x=1$, it will be $y = 1.65$, as well as the slope of average trendline ($m = \frac{1.65}{1}$) which is equal to 1.65.

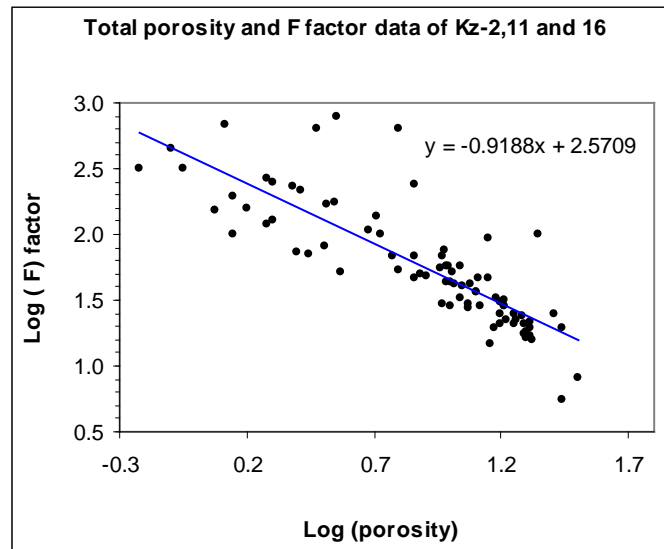


Figure 4.1: The cementation factor (m) from the porosity-formation resistivity factor plotting equal to the slope of the line (m) =1.65; the data belong to wells Kz-2, Kz-11, and Kz-16

4.4 Fluids Resistivity Correction

In general the borehole environment is electrochemically influenced by the drilling mud, which makes its resistivity graded from the drilling mud resistivity (R_m) in the borehole, mud filtrate resistivity (R_{mf}) of flushed zone, and uninvaded formation water resistivity (R_w). These resistivities are greatly affected by temperature changes from depth to depth (Schlumberger, 1972). After the temperature of a formation is determined either by chart or by calculation, the resistivity of the different fluids (R_m , R_{mf} , or R_w) must be corrected to formation temperature before they are being used in any calculations. The resistivity is corrected by a specific chart; the chart is closely approximated by the Arp's formula (Asquith and Krygowski, 2004):

$$R_{TF} = \left[\frac{R_{temp}(Temp + 6.77)}{(Tf + 6.77)} \right], \text{ for depth in feet] 5.2}$$

$$\text{or } R_{TF} = \left[\frac{R_{temp}(Temp + 21.0)}{(Tf + 21.0)} \right], \text{ for depth in meter] 5.3}$$

Where:

R_{TF} = Resistivity at formation temperature

R_{temp} = Resistivity at a temperature other than formation temperature

Temp = temperature at which Resistivity was measured (usually Fahrenheit for depth in feet F°/ft , Celsius for depth in meters C°/m)

Tf = formation temperature (F°/ft , or C°/m).

The average formation temperature of Upper Qamchuqa reservoir is 207 F° (97.2 C°) measured at depth of 2685m with the temperature gradient of 1.55 $F^{\circ}/100ft$ or around 2.87 $C^{\circ}/100m$, and the reservoir pressure of 4364 psi (Reports of Petroleum Engineering Department, 1976-1982). Table (4.1) illustrates the resistivity of the mud filtrate (R_{mf}), measured at the temperature denoted against each one and the third column shows their correction to the formation temperature by the Arp's formula. Also the table shows the resistivity of formation water (R_w) measured in three wells (Reports of Petroleum Engineering Department, 1976-1982), so they were corrected to the formation temperature. After these corrections they were used in Archie equation to calculate the fluid saturations.

**Table 4.1: Correction of (R_{mf} , R_w), into formation temperature.
The data reported by Petroleum Engineering Department of N. O.C**

Wells	R_{mf} (Ω . m) at measured temperature	Corrected R_{mf} to the formation temperature	R_w (Ω . m) at measured temperature	Corrected R_w to the formation temperature
Kz-1	0.474 at 112 F ^o	0.26 (Ω .m)		
Kz-2	0.703 at 88 F ^o	0.31 (Ω .m)	$R_w = 0.022$ at 218 F ^o	0.023(Ω .m)
Kz-3			$R_w = 0.024$ at 200 F ^o	0.023(Ω .m)
Kz-4	0.505 at 77 F ^o	0.20 (Ω .m)	$R_w = 0.024$ at 200 F ^o	0.023(Ω .m)
Kz-5	0.108 at 72 F ^o	0.0397 (Ω .m)		
Kz-7	0.527 at 52 F ^o	0.1446 (Ω .m)		
Kz-11	0.461 at 27.7 C ^o	0.19 (Ω .m)		
Kz-13	0.558 at 22.2 C ^o	0.2039 (Ω .m)		
Kz-14	0.341 at 24.4 C ^o	0.1309 (Ω .m)		
Kz-16	0.334 at 61 C ^o	0.2317 (Ω .m)		

4.5 Water Saturation and Oil Saturation

4.5.1 Archie water saturations: S_w and S_{xo} .

Water saturation (S_w) of the reservoir's uninvaded zone is calculated by the Archie (1942) formula (in Asquith and Krygowski, 2004)

$$S_w = [(a \cdot R_w) / (R_t \cdot \Phi^m)]^{1/n} \dots\dots\dots 5.4$$

Where:

S_w = water saturation of the uninvaded zone

R_w = resistivity of formation water at formation temperature (here $R_w = 0.023 \Omega$.m; Table 4.1)

R_t = true formation resistivity (i.e., deep laterolog or deep induction log)

Φ = porosity (here calculated from log).

m = cementation exponent ($m=1.65$ from Figure 4.1).

a = tortuosity factor ($a = 1.0$ for carbonate rocks)

n = saturation exponent (n assumed to be 2.0; Asquith and Krygowski, 2004)

Water saturation of the formation's flushed zone (S_{xo}) is also based on the Archie equation, but two variables are changed: mud filtrate resistivity (R_{mf}) in place of formation water resistivity and flushed zone resistivity (R_{xo}) in place of uninvaded zone resistivity (R_t):

$$S_{xo} = [(a \cdot R_{mf}) / (R_{xo} \cdot \Phi^m)]^{1/n} \dots\dots\dots 5.5$$

S_{xo} = water saturation of the flushed zone

R_{mf} = resistivity of mud filtrate at formation temperature.

R_{xo} = shallow resistivity from a very shallow reading device such as Laterolog-8, Micro-spherically focused log (μ SFL), or short normal logs.

Φ = porosity

a = tortuosity factor ($a = 1.0$ for carbonate rocks)

m = cementation exponent ($m=1.65$ from Figure 4.1))

n = saturation exponent (n assumed to be 2.0)

Since $S_h = (1 - S_w)$, and $S_{hr} = (1 - S_{xo})$, we can find the bulk-volume fraction of the oil displaced by invasion as $\Phi (S_h - S_{hr})$, which equals to $\Phi \cdot (S_{xo} - S_w)$.

4.5.2 Bulk Volume water (BVW)

The bulk volume water calculation depends on two essential parameters; such as water saturation of uninvaded zone (S_w), and porosity as it is illustrated in the following equation: (Asquith and Krygowski, 2004)

$$BVW = S_w \cdot \Phi \dots\dots\dots 5.6$$

If values of bulk volume water calculated at several depths in a formation are constant or very close to constant Figure 4.2, they indicate that the zone is of a single rock type and at irreducible water saturation ($S_{w_{irr}}$). This means that the water in the uninvaded zone (S_w) does not move, because it is held on grains by capillary pressure. Therefore, hydrocarbon production from a zone at irreducible saturation should be water free (Asquith and Krygowski, 2004)

To define the fluid production to be expected, good values of Φ and S_w are not sufficient. An evaluation of irreducible water saturation ($S_{w_{irr}}$) is also needed since water production, with or without hydrocarbons, is to be expected where S_w is larger than ($S_{w_{irr}}$).

It is often possible to derive ($S_{w_{irr}}$) from the representation of **S_w** versus Φ . It has been found that, for a given rock type, the points fall in a fairly coherent pattern on the crossplot diagram, approximating a hyperbolic curve. On a crossplot of log derived values of Φ and **S_w** , the points at irreducible water saturation fall in the leftmost part of the figure and conform roughly to a simple hyperbolic curve (Figure 4.2A). Points which fall to the right of this curve are referring to the transition zone and indicate levels which will exhibit wide variations in bulk volume water and it will produce water with or without hydrocarbons (Figure 4.2B). While if the points have random distributions (Figure 4.2C), they indicate that the formation is not at irreducible water saturation and it will be producing 0% oil (all water). (Schlumberger, 1972; Serra, 1986; Asquith and Krygowski, 2004).

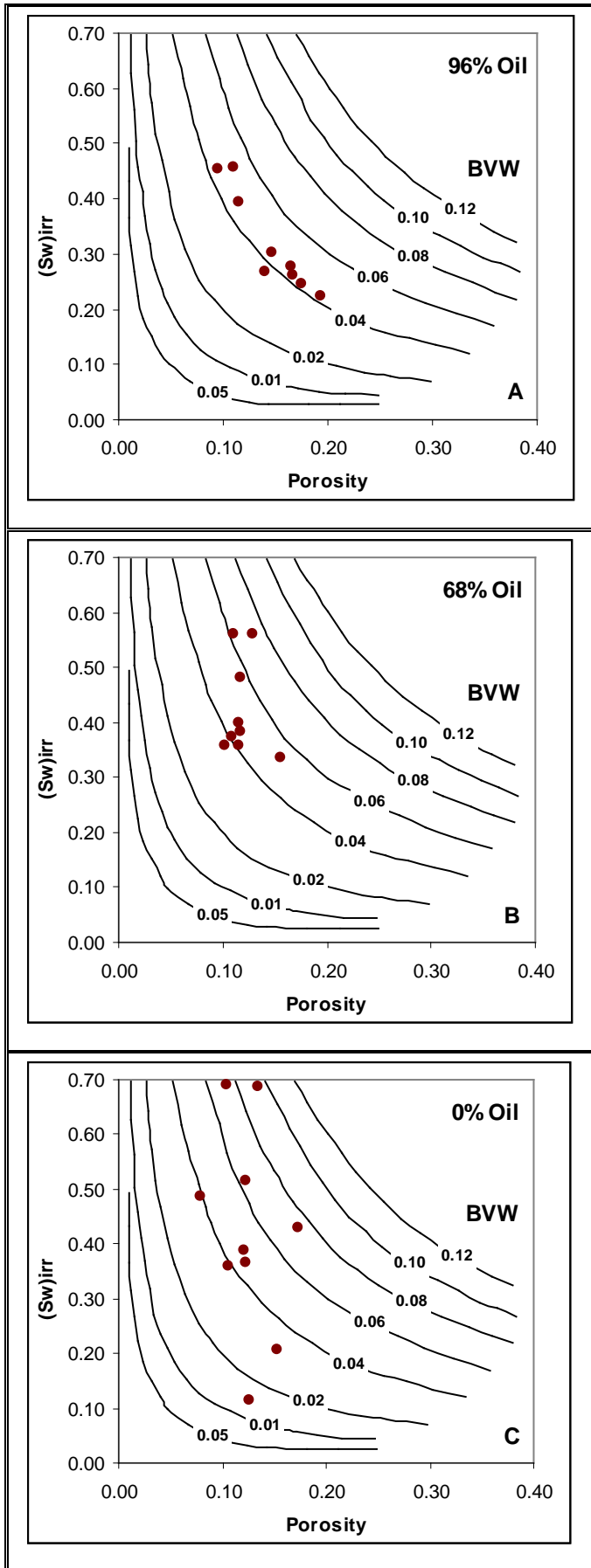


Figure 4.2: porosity vs. water saturation used to determine bulk volume water (BVW). When the values of BVW plot along hyperbolic lines or, in other words are constant or close to constant, the formation is homogeneous and close to irreducible water saturation (S_{wirr}), and a reservoir will not produce water. In figure (A), the BVW values are close to constant (parallel to the 0.04 hyperbolic line) and the formation produces 96% oil. As the amount of formation water increases, the BVW becomes scattered from the hyperbolic lines and the formation has more water than it can hold by capillary pressure, thus more water is produced relative to oil. Figure (B) shows a well producing 68% oil, and Figure (C) shows a well producing 0% oil (all water). Note the scatter of crossplot values from the hyperbolic lines in figures B and C (Asquith and Krygowski, 2004)

The figure (4.3) illustrates the porosity – water saturation (S_w) relations of entire unit "A" represented by its six reservoir subunits (A1, A2, A3, A4, A5 and A6), mixed with their interlayer non reservoir units in six wells (Kz-3, Kz-4, Kz-5, Kz-11, Kz-13 and Kz-14), except in well Kz-3, in which they were plotted separately. The selection of these wells is based on the availability of the resistivity log data, the following are the discussions of the relations in each well:

Well Kz-3 (Figure 4.3A) shows that the points of non-reservoir layers (open circles) fall to the most left side of the diagram on the curve; it represents the irreducible water saturation ($S_{w_{irr}}$), the water held on grains and in micro pores by capillary pressure, because these layers are already characterized by neglected porosity and permeability, while the solid points represent the water saturation (S_w) of porous units A1, A2, A3 and A4 in Kz-3 (the total depth of the well did not reach lower part of the section). The figure illustrates that most of these points fall to the right side of the diagram, the field of high water saturation against high porosity, which indicates the movable water and therefore the well is water producer. This result is reasonable because the well Kz-3 is located at the southeastern nose of the field, and it is beyond the hydrocarbon zone (see figure 1.2).

Well Kz-4, (Figure 4.3B) shows that most of the points conform a simple hyperbolic curve, indicating irreducible water of un-invaded zone and refer to water free hydrocarbon producing well. The figure also shows a small group of points fall at the rightmost part of the figure. These points indicate a movable water, because this well is located nearby the north-west end of the field and possible that it is affected by the oil-water transition zone (Figure 1.2).

Well Kz-5, (Figure 4.3C) shows that the points fall in a fairly coherent pattern on the crossplot diagram, approximating a hyperbolic curve which belongs

to the irreducible water saturation, also the distribution of the points refer to the water free hydrocarbon producing. The few points shifted from the coherent pattern and fall at the rightmost part of the figure, these points represent a movable water saturation, but these points are considered a small fraction if compared with the others.

Well Kz-11, (Figure 4.3D) shows that the points fall in a good coherent pattern on the hyperbolic curve, which indicate that the formation water saturations are at the irreducible (S_{wirr}) condition, and this mean that the water held on grains and in micro pores by capillary pressure, and the well will produce water free hydrocarbons.

Well Kz-13, (Figure 4.3E), the points of this figure belongs to the two lower reservoir subunits (A5 and A6), due to lack of some log data of other subunits. These two subunits in well Kz-13, as in most other wells are combined into single thick unit with good reservoir properties, and their in-between non-reservoir layer is reduced, though most of the data fall on high porosity field and low formation water saturation. Also this phenomenon indicates irreducible formation water, and water free hydrocarbon productions.

Well Kz-14, (Figure 4.3F) shows that points fall in a good concentric pattern on the hyperbolic curve, which indicate that the formation waters saturation are at the irreducible (S_{wirr}) condition. The water held on grains and in micro pores by capillary pressure, this mean that the well will produce water free hydrocarbons in a good manner.

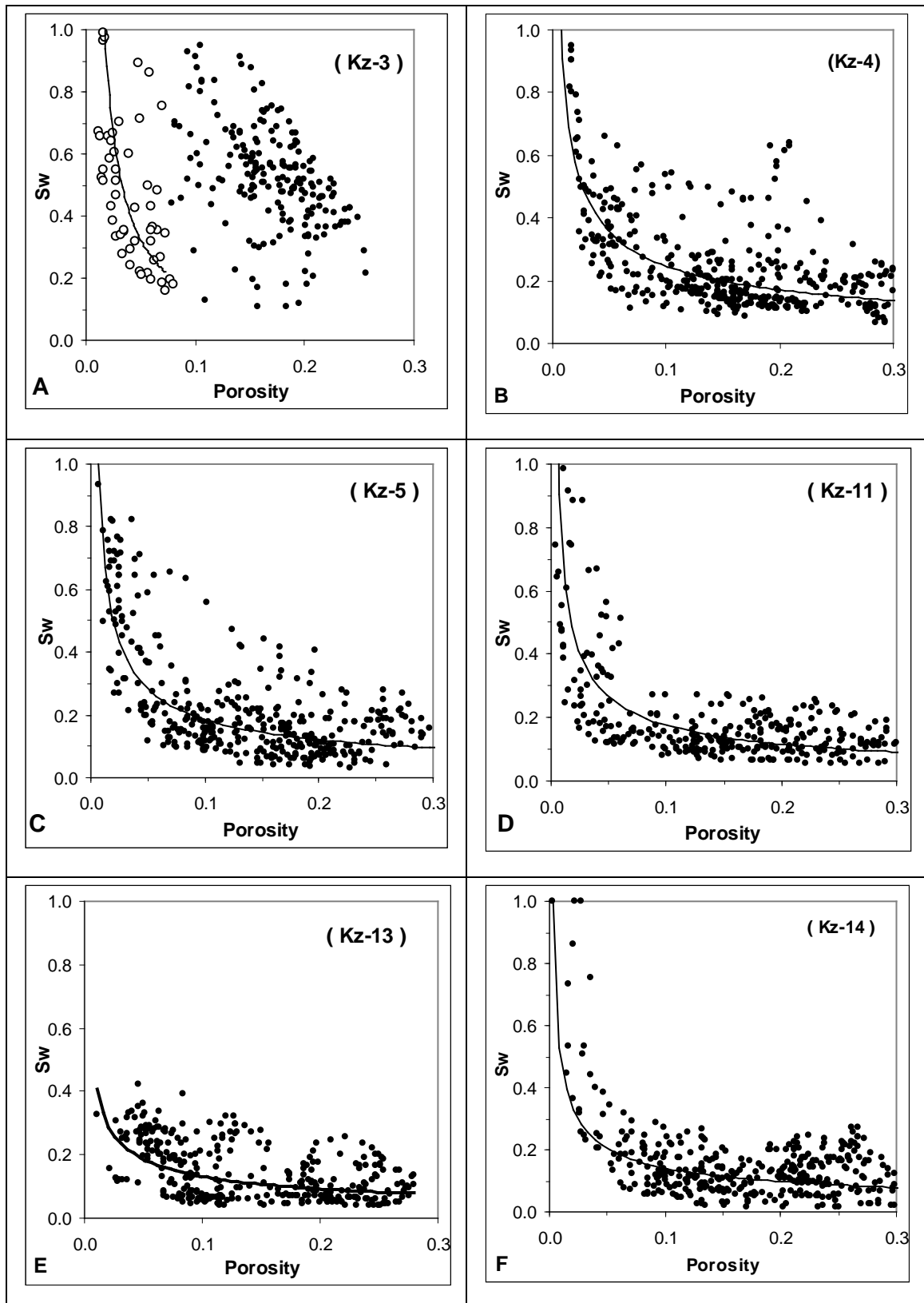


Figure 4.3: Porosity versus water saturation plotting in some of the studied wells, all figures showing the constant or close to constant hyperbolic pattern, which indicate that the formation is at irreducible water saturation. Except (A) well Kz-3, shows scatter pattern which indicate water producing, open circles are non-reservoir subunits and the solid dots are reservoir subunits.

4.5.3 Residual and Movable Hydrocarbons

Residual hydrocarbon saturation (S_{hr}) is equal to $(1 - S_{xo})$. The equation gives the saturation in unmoved or residual hydrocarbons of the invaded zone after it is filtrated by the drilling mud. This term (S_{hr}) gives good information related to the production. Also comparison of S_w and S_{xo} in a hydrocarbon zone is considered to give movable hydrocarbons, so the difference between the water saturation of flushed zone (S_{xo}) and the original uninvaded formation water saturation (S_w) is equal to the fraction of movable hydrocarbons in the formation. The percentage volume in terms of the reservoir is given by multiplying the term by the porosity, i.e. % volume of reservoir with movable hydrocarbons = $(S_{xo} - S_w) \cdot \Phi$, (Rider, 1996).

In this study, the porosity is estimated from two well logs; neutron and density tools by means of averaged values of the two measurements (see chapter three). Also shallow and deep resistivity (R_{xo} and R_t) were obtained from LLD and μ SFL respectively, and in some wells they had been replaced by Induction resistivity log. As it was discussed previously, the two groups of data (porosity and resistivity) in addition to other formation parameters (**a**, **n**, and **m**) were used to calculate the formation water saturations (S_w and S_{xo}) in addition to BVW.

The total hydrocarbon saturation S_h estimated from the general relation:

$$S_h = 1.0 - S_w \quad \dots\dots\dots 5.7$$

The hydrocarbon saturation S_h of formation include both of movable hydrocarbons and residual hydrocarbon, the former is recoverable hydrocarbons which can be produced and the latter left in reservoir and can not be produced (depending on the production technique) (Bates and Jacksonl, 1980).

The three terms; water saturation, movable hydrocarbons and residual hydrocarbon were multiplied by the porosity to represent them as volume fractions occupying the porosity:

Bulk Volume of water = $S_w \cdot \Phi$ 5.8

Bulk Volume of hydrocarbons = $(1 - S_w) \cdot \Phi$ 5.9

Bulk Volume of movable hydrocarbons = $(S_{xo} - S_w) \cdot \Phi$ 5.10

Bulk Volume of residual hydrocarbons = $(1 - S_{xo}) \cdot \Phi$ 5.11

The summation results of the above three terms were shown in figures (4.4 and 4.5), the outer curves represent the porosity, and the blue color area represents the bulk volume of water saturation ($S_w \cdot \Phi$) occupied the fraction of porosity, the rest part of porosity area represents the fraction of porosity occupied by hydrocarbon saturations. The movable fraction illustrated by light brown color, while the dark grey areas are residual or irreducible hydrocarbons. The following are the discussions of the figure from the point of view of reservoir subunit correlations along the well sections.

4.5-3.1: Unit (A)

As it was discussed in chapter three, the unit (A) of Upper Qamchuqa Formation represents the main reservoir zone all over the Khabbaz oil field. Figure 4.4 illustrates the porosity curve, bulk water saturation, residual and movable hydrocarbon saturations of the unit (A) within the reservoir which was divided into subunits (A1, A2, A3, A4, A5 and A6) through a group of wells. In the following, the case of distribution and properties of the unit A within the studied wells are made clear. The location of the selected wells shown in figure 1.2, have approximately northwest to southeast trend.

Well Kz-4 is located to the most northwest plunge of the structure (see figure 1.2), the (Figure 4.4a) shows that this well is characterized by high bulk volume of hydrocarbon saturation, but most of them are the residual oil

(dark grey color) and only a small fraction of them is the movable hydrocarbon (light brown color). This result well agrees with the location of the well, which is located to the northwest end of the field and it is a site of interfacing of the lateral oil-water contact or transition zone. The affecting of the oil by the marginal water is possible. The alteration of oil by the formation water sometimes leads to removing the lighter fractions of the oil and increasing of heavier portions. Also this well have some other production problems that come into sighted after some years of productions, the chemical analysis of the crude oil was deduced to interpret this phenomenon, also for more detail (see chapter 5).

The two wells Kz-11 and Kz-5 are located to the southwest limb of the structure, the reservoir sections through these two wells (Figure 4.4b,c) are characterized by good movable hydrocarbon (light brown color), particularly the lower part of them including subunits A4, A5 and A6, which have good thickness and low water saturation. Also the upper part of well Kz-11 represent by two subunits A1 and A2, both are relatively high movable hydrocarbon.

The reservoir section of the well Kz-2 (Figure 4.4d) illustrate moderate movable oil particularly its two subunits A2 and A3. The section shows that the residual hydrocarbon is highly dominated over the section, also water saturation relatively somewhat high, these belong to the situation of the well, where it is located to the northeast limb of the structure close to the lateral oil-water interface.

Well Kz-14 is located between the southeast plunge and the central part of the field, to the west of the fault (see figure 1.2). The section of this well entirely represents good reservoir (Figure 4.4e), especially subunits of A3, A4 and A5, except for the lower subunit A6, which has low porosity. Also the section of this well relatively shows rather high water saturation.

Well Kz-3, is located to the most southeast plunge of the structure (see figure 1.2), only four units (A1, A2, A3 and A4) were penetrated by this well, although these subunits have high porosity, they are occupied by water, only small fractions of them saturated by oil. Figure 4.3A shows that this water is movable and it makes the well produce high amount of water with low oil due to the location of this well, sited to the most end of the southeast plunge and may be out of the hydrocarbon pool.

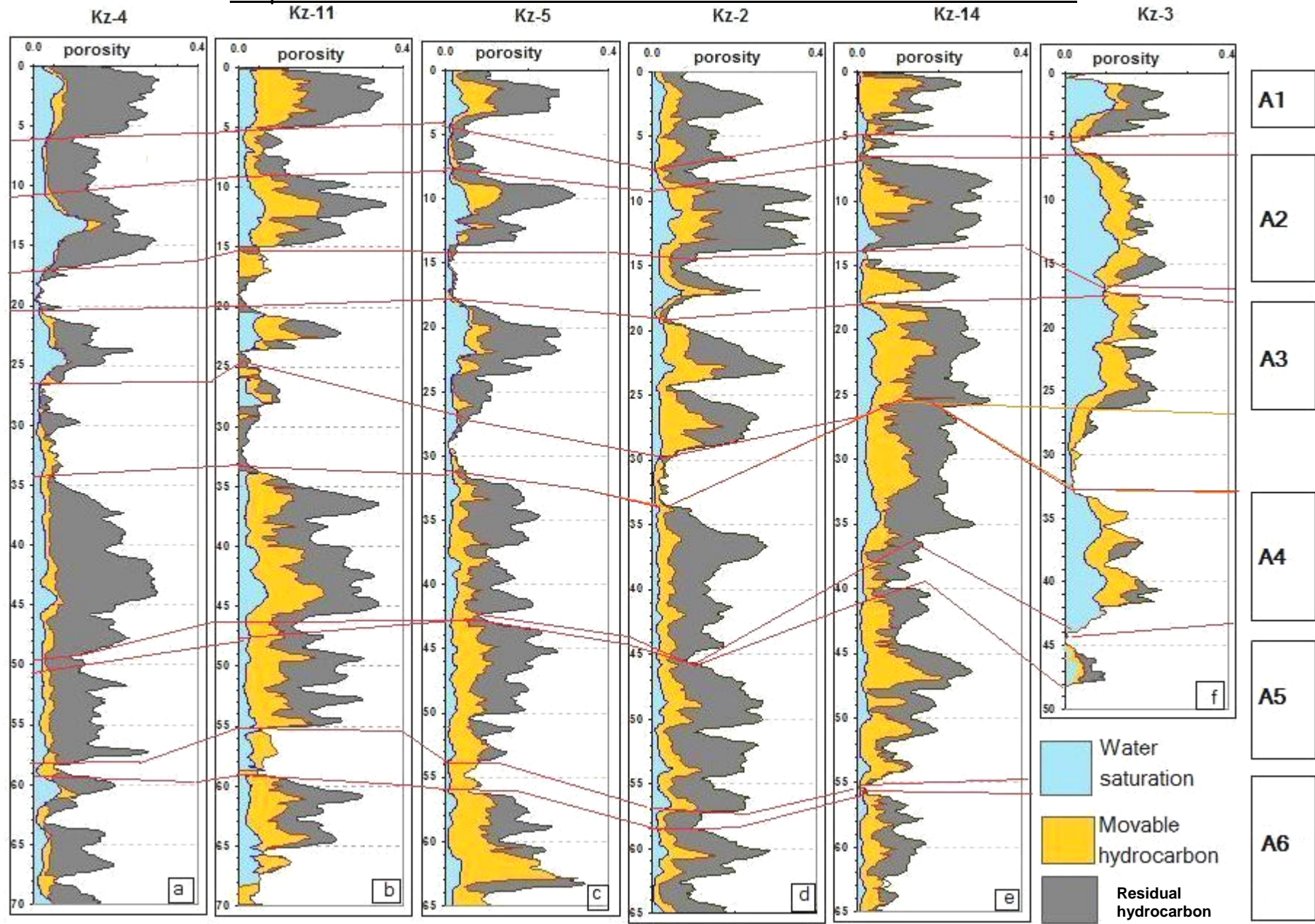


Figure 4.4: Water saturation, oil saturations (residual and moveable) of unit A, represented by its subunits

4.5-3.2: Unit (B and C)

In the previous chapter it was cleared that these two units B and C are compared with the unit A. They represent very weak (marginal) or non reservoir unit. Figure 4.5, shows the porosity curve and its occupation fractions with water saturation (blue color), movable and residual hydrocarbon saturations (brown and black color respectively).

The figure shows that the two units (B and C) of well Kz-4 are characterized by very rare movable oil and could be neglected, while most of the porosities are occupied by residual oil (dark grey color) and water (blue color). This case in both units B and C are similar to that of unit A in this well.

Well Kz-11 has some movable hydrocarbons, especially at the zone of the lower part of unit B with combination of upper part of unit C. Most of their porosities are filled with movable oil (brown color), and the water saturation of this zone is comparatively not small.

Well Kz-5, the two units B and C are show vary rare movable hydrocarbon, while the two zones of high porosity, one of them to the middle part of unit A, and the second one to the lower part of it, extending to the upper part of unit C. These two zones are occupied by residual hydrocarbons (black color).

For well Kz-2, the two units B and C are characterized by low porosity and also low movable oil except for some peaks at the lower part of unit B, and proximately the whole section of unit C show moderate movable oil.

For well Kz-14, the two units within this well are characterized by somewhat moderate to good movable hydrocarbons, with consideration to their low porosity in comparing to unit A.

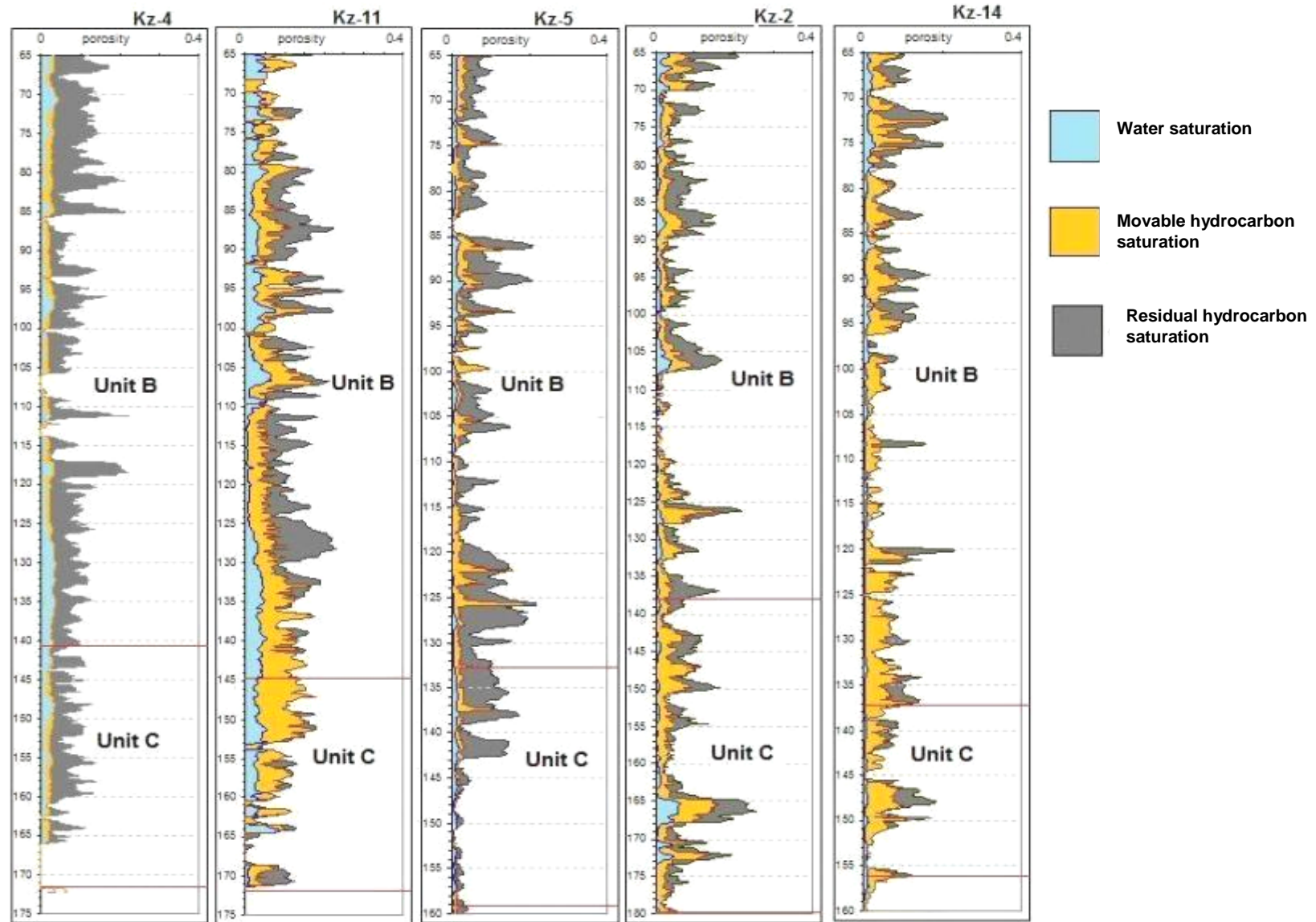


Figure 4.5: Water saturation, residual and movable oil saturation of the unit B and C

4.6 Permeability Estimation from Φ and S_w

In some cases there may exist rough relationships between the porosity and permeability, but such correlations usually are derived for given formation in a given area.

These relationships show that it is highly preferable to base an empirical relationship between porosity and permeability on the type of rock or even better on the type of facies and environment furthermore since as we have seen, irreducible water saturation is a function of grain size, and hence permeability. Several equations have been proposed in order to estimate permeability from measurements of porosity and irreducible water saturation. For example Willey and Rose equation (1950) (in Schlumberger, 1962) proposed the following relation to calculate the permeability (K) with md :

$$K^{1/2} = C\Phi^3/S_{w_{irr}} \quad \dots\dots\dots 5.12$$

$$\text{And } K = [C\Phi^3/S_{w_{irr}}]^2 \text{ which } K \text{ is in md}$$

Where the factor C depends on the density of the Hydrocarbons, C=250 for oils of average density $\rho_h = 0.8 \text{ g/cm}^3$ and 79 for gas. The value of $S_{w_{irr}}$ (irreducible water saturation) is taken from log calculation above the transition zone.

Also the Chart relationship proposed by Schlumberger (1962), (Serra, 1986) to estimate permeability from porosity and irreducible water saturation. The permeability of the zone at each point on the irreducible saturation line can be determined from permeability lines are sketched on the crossplot (Schlumberger 1972).

Chapter Five

Reservoir Geochemical Analysis

Part I. Formation Water Evaluation

5.1 Introduction

The basic mechanisms governing the hydrodynamic pattern in sedimentary basins are ultimately related to the pressure, reservoirs, water salinity and chemical composition, and the regional geological environment, all of which are interdependent (AL-Mashadani, 1986). The hydrodynamic framework influences the petroleum prospects of a sedimentary basin, since the processes of generation, migration, accumulation and alteration of hydrocarbons take place in direct association with the formation water.

According to Selley(1998), four types of subsurface water can be defined according to their genesis:

Meteoric waters...occur near the earth's surface and are caused by the infiltration of rain water. Their salinity, naturally, is negligible, and they tend to be oxidizing. Meteoric waters are often acidic because of dissolved humic carbonic and nitrous acid, although they may quickly become neutralized in the subsurface, especially when they flow through carbonate rocks.

Connate waters...are harder to define. They were originally thought of as residual seawater that was trapped during sedimentation. Current definitions proposed for connate waters include "interstitial water existing in the reservoir rock prior to disturbance by drilling" and "waters which have been buried in a closed hydraulic system and have not formed part of the hydraulic cycle for long time" connate waters differ markedly from seawater both in concentration and chemistry.

Juvenile waters... are primary magmatic origin. It may be difficult to prove that such hydrothermal waters are indeed primary and have received no contamination whatsoever from connate waters.

Mixed water... The mixed waters may be caused by the confluence of juvenile, connate, or meteoric waters. In most basins a transition zone exists between the surface aquifer and the deeper connate zone.

5.2 Classification of Oil Field Waters

The concentrations of solids present in oil field brines are reported in several different ways. Among these are part per million, milligrams per liter, and weight percent solid. Another set of units is milliequivalents per liter. Milligram per liter can be converted to milliequivalents per liter by dividing it by the equivalent weight (McCain, 1990).

Subsurface waters are classified according to the dominant mineral ions present in solution. A widely used classification is that proposed by the Russian geochemist i.e. V. Sulin, 1946 (in Collins, 1975). He had classified the system based upon various combinations of dissolved salts in the waters. He found four basic chemical types of water (Table 5.1) belonging to the four environments of natural water distribution:

- 1- Continental (terrestrial) conditions which promote the formation of sulfate waters; the genetic type of such waters is "sulfate-sodium".
- 2- Continental conditions which promote the formation of sodium bicarbonate waters. The genetic type is "bicarbonate-sodium".
- 3- Marine conditions and formation of "chloride-magnesium" type of water.
- 4- Deep subsurface conditions within the earth's crust and the formation of a "chloride-calcium" type of water.

The first two types are characteristic of meteoric and/or artesian waters, the third of marine environments and evaporate sequences, and the fourth of deep stagnant conditions.

Table 5.1: Coefficients characterizing the genetic type of water (Sulin, 1946)

Type of water	$\text{Na}^+ / \text{Cl}^-$	$(\text{Na}^+ - \text{Cl}^-) / \text{SO}_4^{2-}$	$(\text{Cl}^- - \text{Na}^+) / \text{Mg}^{+2}$
chloride – calcium	< 1	< 0	> 1
chloride - magnesium	< 1	< 0	< 1
bicarbonate – sodium	> 1	> 1	< 0
sulfate – sodium	> 1	< 1	< 0

Bojarski, 1970 (in Collins, 1975), had modified Sulin's system. He distinguished subsurface water types as following:

- 1- Water of the bicarbonate-sodium type. Such waters occur in the upper zone of a sedimentation basin, with "intense water exchange" (hydrodynamic), which promotes unfavorable conditions for the preservation of petroleum and natural gas deposits.
- 2- Water of the sulfate – sodium type, indicating that all of the sodium will react with chloride or sulfate.
- 3- Waters of the chloride – magnesium type, such water is characteristic of the transition zone between hydrodynamic areas which is becoming more hydrostatic in the deeper part of the basin.
- 4- Water of the chloride – calcium type, occurs in deeper zones which are isolated from the influence of infiltration waters and are hydrostatic. Bojariski 1970 (in Collins, 1975) observed a large variation in the chemical composition in the chloride – calcium type and subdivided this type as following:

a- The first class, "chloride – calcium I" with $\text{Na/Cl} > 0.85$ characterizes an active hydrodynamic zone with considerable water movement. It is considered as a zone of little prospect for the preservation of the hydrocarbon deposits.

b- The second class, "chloride – calcium II" with $\text{Na/Cl} = 0.85 - 0.75$, characterizes the transition zone between an active hydrodynamic zone and a more stable hydrostatic zone, which is generally considered a poor zone for hydrocarbon preservation.

c- The third class, "chloride – calcium III" with $\text{Na/Cl} = 0.75 - 0.65$, characterizes favorable condition for the preservation of hydrocarbon deposits. It is designated as a fairly favorable environment for the preservation of hydrocarbon.

d- The fourth class, "chloride – calcium IV" with $\text{Na/Cl} = 0.65 - 0.50$, is characterized by complete isolation of the hydrocarbon accumulation as well as by the presence of residual water. It is considered a good zone for the preservation of hydrocarbon.

e- The fifth class, "chloride – calcium V" with $\text{Na/Cl} < 0.50$, is characterized by the presence of ancient residual sea water which has been highly altered. This type is one of the most likely areas of hydrocarbon accumulation.

Table 5.2: Converting the ions in Khabbaz Formation water from ppm (upper part) into epm (lower part).

Wells No.	TDS ppm	Ca ⁺² ppm	Mg ⁺² ppm	Na ⁺¹ ppm	SO ₄ ⁻² ppm	Cl ⁻¹ ppm	HCO ₃ ⁻¹ ppm	NaCl ppm
Kz-3	130137	6006	1091	43008	1239	77823	1832	109317
Kz-4	151310	4830	1840	46998	1059	84909	1220	119461
Kz-7	27580	662	458	6302	1654	10295	1220	16018
Kz-23	127937	26588	13220	811	641	86380	Nil	2061
<p>Milligram per liter (ppm) converted to milliequivalents per liter (epm) by dividing by the equivalent weight. Equivalent weight is obtained by dividing the atomic weight of ion by its valence. Not: the lower table is the converting result of upper table from ppm of N.O.C into epm in this study.</p>								
Wells No.	TDS ppm	Ca ⁺² epm	Mg ⁺² epm	Na ⁺¹ epm	SO ₄ ⁻² epm	Cl ⁻¹ epm	HCO ₃ ⁻¹ epm	NaCl ppm
Kz-3	130137	300	91	1870	26	2192	30	109317
Kz-4	151310	242	153	2043	22	2392	20	119461
Kz-7	27580	33	38	274	34	290	20	16018
Kz-23	127937	1329	1102	35	13	2433	Nil	2061

5.3 Classification of the Formation Water in the Studied Wells

The chemical analysis of the formation water in Khabbaz oil field was carried out by N.O.C during the time of drilling the wells (Reports of Petroleum Engineering Department, 1976-1982). The data were available for four wells of Upper Qamchuqa reservoir, including the concentrations of dissolved salts (cations and anions) present in brines in different ratios as shown in (Table 5.2). The data had been converted from part per million (ppm) into milliequivalents per liter (Lower part of table 5.2) to be used in water classification. The classification system of Bojarski and Sulin's (in Collins, 1975) for formation water type is applied to the analytical data and the result is shown in Table 5.3.

The ratios Na/Cl , $(\text{Na-Cl})/\text{SO}_4$ and $(\text{Cl-Na})/\text{Mg}^2$ of the chemical composition of the formation water analysis of the four wells are illustrated in (Table 5.3), and they indicated that all of these waters are belong to the chloride calcium type, because the ratio $(\text{Cl-Na})/\text{Mg}^2$ is greater than the one within the three samples. This type of water characterizes hydrostatic deeper zones which are isolated from the influence of infiltration waters according to Bojarski, 1970.

Although the waters of all the wells belong to the same stagnant isolated type (Chloride calcium) except Kz-7, which is an indicator of the hydrostatic condition. There are some variations in their Na/Cl ratios, which make them to be classified under the deferent subdivisions classes:

Table 5.3: The formation water classes of Khabbaz oil field according to Bojarski and Sulin's classification.

Wells No.	Na/Cl	(Na-Cl)/SO ₄	(Cl-Na)/Mg	Water type	Class
Kz-3	0.85	-12.49	3.69	Chloride calcium	II
Kz-4	0.85	-15.79	2.37	Chloride calcium	II
Kz-7	0.94	-0.46	0.44	Chloride magnesium	---
Kz-23	0.01	-179.57	2.27	Chloride calcium	V

The ratio Na/Cl of two wells (Kz-3 and Kz-4) is equal to 0.85; this value belongs to the second class subdivision (chloride-calcium II) of formation water near to the contact with the first class (chloride-calcium I). This ratio (0.85) is characteristic of the transition zone between hydrodynamic zone and a stable hydrostatic zone, which is generally considered a poor zone for hydrocarbon preservation, such result may be related to the locations of the wells, because these two wells (Kz-3 and Kz-4) are located to the most end southeastern and northwestern part of the field respectively (see Figure 1.2), and their affect by the marginal waters is possible.

The Na/Cl ratio in well Kz-7 equals 0.94. This belongs to the first class of formation water (chloride-calcium I), near to the contact with the third genetic type (chloride – magnesium) of formation water. Such water is characteristic of the transition zone between hydrodynamic areas which is becoming more hydrostatic in the deeper part of the basin. This result belongs to the location of the well, which is passes through the fault (see Figure 1.2) and may be influenced by some turbulent of water along the fault plane.

The ratio of Na/Cl ions in the well Kz-23 is 0.01. This value is classified as fifth class (chloride-calcium V), which is considered a good zone for the preservation of hydrocarbon.

This well is located near to the central part of the field and it is possible to represent the actual condition of the formation water in Khabbaz oil field, which is one of the deep reservoirs and its age belongs to the middle cretaceous. The formation water of such conditions is expected to be chloride-calcium type of deep stagnant conditions and it is characterized by the presence of ancient residual sea water which has been highly altered and most likely areas of hydrocarbon accumulation Bojarski1970 (in Collins, 1975).

Although the Khabbaz oil field is located to the Foothill zone, this area is the domain of intense hydrodynamism by gravity, which is imposed by

the Zagros outcrops. The invasion by surface water as well as contamination of formation water is expected. While enrichment of its overlain geological column with multi layers of clay and anhydrite successions offer greater resistance to this invasion and remain the site of hydrodynamism by compaction, connate water and closed system (AL-Mashadani. 1986). Also the formation conditions of Upper Qamchuqa reservoir is characterized by high pressure which reached 4364 psi/ft, measured at depth of 2685m (Reports of Petroleum Engineering Department, 1976-1982). This pressure clearly indicates the anomaly hydrodynamic condition because if it is compared with theoretical estimated hydrostatic pressure or interstitial fluid pressure which has the pressure gradient of around 0.48 psi/ft or 1.50 psi/m(Serra, 1986), the pressure will be 4028 psi at the same depth (2685m). These results suggest the highly pressure, closed, and isolated system to Upper Qamchuqa reservoir in Khabbaz oil field.

Part II. Crude oil Geochemical Analyses

5.4 Crude Oil Composition

Petroleum is a complex mixture of liquid and gaseous compounds, whose proportions depend in particular on the reservoir properties such as pressure-temperature condition, and this may be reflected on the hydrocarbon characteristics (gross properties) like API gravity, Sulfur% content, gas-oil ratio (GOR), and Viscosity (Balance and Connan, 1993 A). The chemical gross composition of pooled oils, is expressed as a percentage of Saturates, Aromatic, Resins and Asphaltenes. However significant fraction changes are recorded during expulsion, migration, and other processes likely to affect oil composition in pools.

Aliphatic (saturation) hydrocarbons make up between 40 and 97% (w/w) of the crude oil and include n-alkanes, branched alkanes and

cycloalkanes. Between 20 and 45% (w/w) of crude oil are aromatic hydrocarbons. Resins and asphaltenes include high molecular weight substances and constituents with high contents of heteroatoms, together they make up 0-40% (w/w) of the crude oil (Skaare, 2007).

5.5 Oils Alteration Through Secondary Processes in the Reservoir.

Before the illustration of the geochemical properties of the crude oil in Upper Qamchuqa reservoir, and probability of its exposing to any later geological process, it is necessary to discuss theoretically the importance of oil alteration through secondary process in the reservoir.

Once trapped, petroleum mixture can undergo significant compositional changes due to various chemical and physical processes. Among them, biodegradation, generally associated with water washing, is a widespread phenomenon which chemically results in the oxidation of hydrocarbons by bacteria. Other events can be quoted, such as gravity segregation, dysmigration of oil through cap rock, faulting, or natural deasphalting induced by influx of gaseous hydrocarbons (Connan, 1993; Balance and Connan, 1993A).

When the petroleum mixture has been generated, expelled, migrated and trapped, it has to cope with numerous chemical and physical secondary processes which alter its composition within the reservoir.

5.5.1 Biodegradation and Water Washing

Biodegradation is a microbial alteration of crude oil in reservoir usually taking place whenever the oil pools in contact with the water sources especially in shallow reservoirs (Balance and Connan, 1993A; Connan, 1993). The primary zone for biodegradation in the reservoir is the oil-water contact (Skaare, 2007). Aerobic degradation of hydrocarbons at the surface is well documented, flow of oxygen and nutrient-bearing meteoric water into reservoirs was necessary for in-reservoir petroleum biodegradation (Aitken et al, 2004). The upper limit in temperature for

biodegradation to persist is less than 75 °C. (Mason et al, 1995), the rates of biodegradation decrease with increasing temperature approaching zero at about 80 °C (Skaare, 2007).

The process of water washing based on solubilities of hydrocarbons, simulation experiments and field example, water washing has been shown to be particularly effective in the low-boiling range of hydrocarbons, hence involving a decrease of API gravity: aromatics (especially benzene and toluene) are the most soluble compounds, then light alkanes and then naphthenes (Balance and Connan, 1993A; Connan and Coulome, 1993). Molecular indications have been tentatively proposed to assess a water washing phase without a biodegradation process: decrease in the amount of aromatics and n-alkanes while naphthenes are unaltered; partial removal of C₁₅₊ aromatics while C₁₅₊ alkanes are unaffected; decrease in sulfur bearing aromatics (especially dibenzothiophene) while the C₁₅-C₂₀ saturate fractions remains unchanged. Recently, Phenols (13) have been proposed as sensitive indicators for water washing (Balance and Connan, 1993A).

5.5.2 Infilling of Reservoir by Gases. Natural Deasphalting

Oils and condensates in traps are usually associated with gas. This gas can originate from the thermal maturity of a source rock as well as from secondary alteration processes affecting oil already in the reservoir rock. Gas content depends on numerous parameters such as kerogen type, hydrocarbon availability (oil or gas) at the time of pool formation, reservoir pressure, reservoir temperature, trap efficiency, and secondary alteration processes.

The post accumulation introduction of gas into the oil field can lead to chemical changes because the influx of gaseous hydrocarbons decreases the average of the molecular weight of the pool mixture. Hence, what the chemist does in the laboratory when precipitating

asphaltenes from oil by adjunction of n-heptane for instance. It is also naturally undertaken in the oil field when gas moves up through the oil column. This natural deasphalting can be triggered by external gas injection as a result of secondary migration, or by oil cracking within the reservoir rock. This process therefore leads to the formation of light oil on the one hand and a solid residue containing asphaltenes on the other (Connan, 1993; Balance and Connan, 1993B).

The process of deasphalting by natural gas liberation is the reasonable interpretation to the Kz-4 problem, in view of the fact that the Upper Qamchuqa reservoir in Khabbaz field is a high pressure oil reservoir (4380 psi), with associated gas (gas dissolved in oil), (Petroleum Engineering Department reports). Any technical error such as the extreme oil production from a well, more than its potentiality leads to intense drop in pressure around the well and causes gas dissolved in the oil to come out of the solution (Selley, 1998). These new gases move through the oil and lead to precipitation of residual oil around the well and make an annual zone of heavy oil or asphaltene, locally isolated the well from the original normal oil pool. This asphaltenes can also participate in the closing of the pipelines. Also the rapid excess gas injections to the well could have the same effects.

It has to be noted that during the last years, some of the decision of oil production in Iraq was governed by administration rather than technician decision, which can severely influence the normal field production.

5.6 Oil Characterization of Khabbaz field

The Upper Qamchuqa Cretaceous-reservoir of Khabbaz oil field is relatively a small oil reservoir (considering its dimension) with high associated gas. The oil of this field shows a narrow range in gross composition and properties particularly in the well Kz-4, its oil differs from others in its API gravity, resins and asphaltene compounds, also Ni, V content, and it makes some problems to the production process.

Although the Qamchuqa pay zones are considered as deep reservoir (around 2700m), and its temperature reach 100 °C and pressure of 4380 psi (Petroleum Engineering Department reports), such as these conditions are usually not suitable for biodegradation, due to some anomalous properties of the produced oil in this well, and exposing the Khabbaz structure to some fault systems which make the occurrence of some alteration processes possible, the crude oil was analyzed by gas chromatography – mass spectrometry (GC –MS), and other chemical analyses. The results were examined to possibility if the oil exposed to biodegradation or not?. Also to indicate the type of source rock which generates these oils and degrees of maturation of the oil.

In this study crude oil samples are collected from six wells; five of them in the Upper Qamchuqa reservoir including; Kz-4, Kz-12, Kz-21, Kz-23 and Kz-24 in addition to a sample of Lower Qamchuqa reservoir from well Kz-1, the latter sample was taken for the comparison purpose. The samples were geochemically analyzed to their compositional parameters including:

- Compositional fractions of the samples (saturated, aromatic, resins and asphaltenes) compounds.
- API gravity.
- % Sulfur and some trace elements (Ni and V)
- GC - MS analysis.

The above geochemical analyses were carried out by TOTAL Oil Company in their Fluid and Organic Geochemistry department in France. The original geochemical data utilized in this study, were carried out by the North Oil Company during the date of the drilling of these wells. Some further new analyses were added to the crude oils during my work, including API gravity, water content, and hydrogen sulphide, and the latter analyses carried out by Research and Quality Control Department of N. O. C.

Table 5.4 illustrated the crude oil fractions ratio, and other heterogeneous compounds in addition to API gravity of the oil samples. Saturation compounds ranged between 30.5–50.2%, aromatic 41.1–53.9% and polar compounds 4.1 – 15.6%.

Table 5.4: Crude oil fraction ratios, heterogeneous compounds and oil API density of the studied crude oil samples, Qamchuqa Reservoir, Khabbaz oilfield.

Well	Density	Sulfur	Ni	V	Distillate	Residue	Asphaltenes	Saturated HC	Aromatic HC	Polar compounds
No.	API	% weight	ppm-wt	ppm - wt	% weight	% weight	% weight	% weight	% weight	% weight
Kz-1	32.304	1.63	<5	<5	29.5	70.5	1.2	50.2	45.7	4.1
Kz-12	24.422	2.4	13	33	28.7	71.3	6.2	45	41.1	13.9
Kz-21	23.259	3.21	7	30	21.7	78.3	6.6	34.5	52.5	13
Kz-23	23.27	3.22	6	26	21.4	78.6	4.5	34.3	53.6	12.2
Kz-24	23.27	3.33	6	27	19.3	80.7	4.6	36.3	54.2	9.4
Kz-4	22.403	3.85	17	61	20.3	79.7	11.2	30.5	53.9	15.6

The ternary plot (saturated-aromatic-polar) figure 5.1 shows that all of the oil samples fall in the area of the high saturated - aromatic compounds and low ratio of polar compounds, the two samples of Kz-1 and Kz-12 wells have relatively higher saturated compounds. The Kz-1 oil sample belongs to the Lower Qamchuqa reservoir which contains the lowest ratio of polar compounds. The plot illustrates that almost all samples fall close to each other with a small range of compositional fractions variety, this indicate that all examined belong to the same family of oil and same source rock.

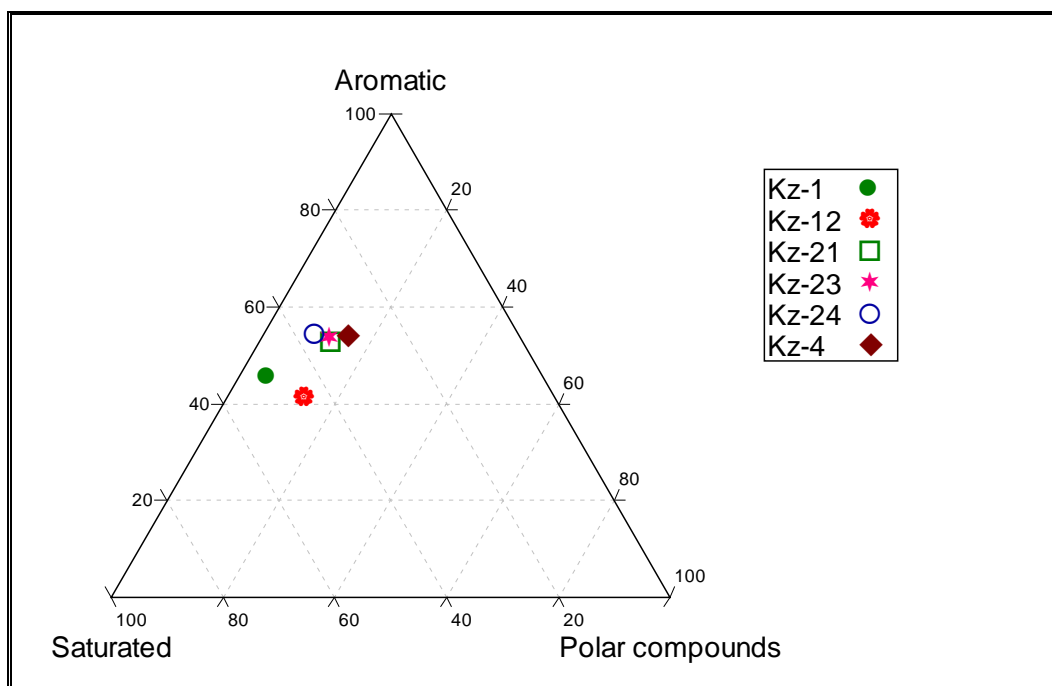


Figure 5.1: Ternary plot of oil compositional fractions of the crude oils.

5.6.1 Compositional Relationship

Petroleum is a complex mixture of oil and gas that is difficult to preserve. Easily degradable and it undergoes compositional changes during migration and accumulation. The secondary alteration after oil entrapment can lead to considerable changes in both composition, quality of the oil, and some fractions of oil destroyed or lost which leads to the change of its properties. The oil samples of Khabbaz field analyzed to their content of some trace elements and estimation of their specific gravity, Figure 5.2.A shows an increase of API gravity versus sulfur content (S %wt), the sample from well K-4 has a high value of S% within low API, while the oil sample from Kz-1 belonging to the Lower Qamchuqa reservoir is characterized by lowest S% and highest API gravity. At the same time Figure 5.2.B&C illustrates the API gravity versus Nickel (Ni) and Vanadium (V) contents respectively. The figure shows the inverse relations between API gravity and both of Ni and V. Finally Figure 5.2.D, can clearly reflect the relations between asphaltenes with both of Ni (solid circles) and V (triangles), the figure illustrated that the two elements have normal linear relations with asphaltenes. They increased as a normal trend with increasing of asphaltenes content. These results were expected due to the genetic relationship between the asphaltenes and API in one hand and the asphaltenes with both Ni and V on the other hand, a decrease of API gravity is usually thought to correlate negatively with an increase of asphaltene content and both Ni and V, as in Kz-4 sample, and the Ni, V have the positive correlate with asphaltenes because precipitation of asphalt enriched the residual contents like Ni and V. (Balance and Connan, 1993A).

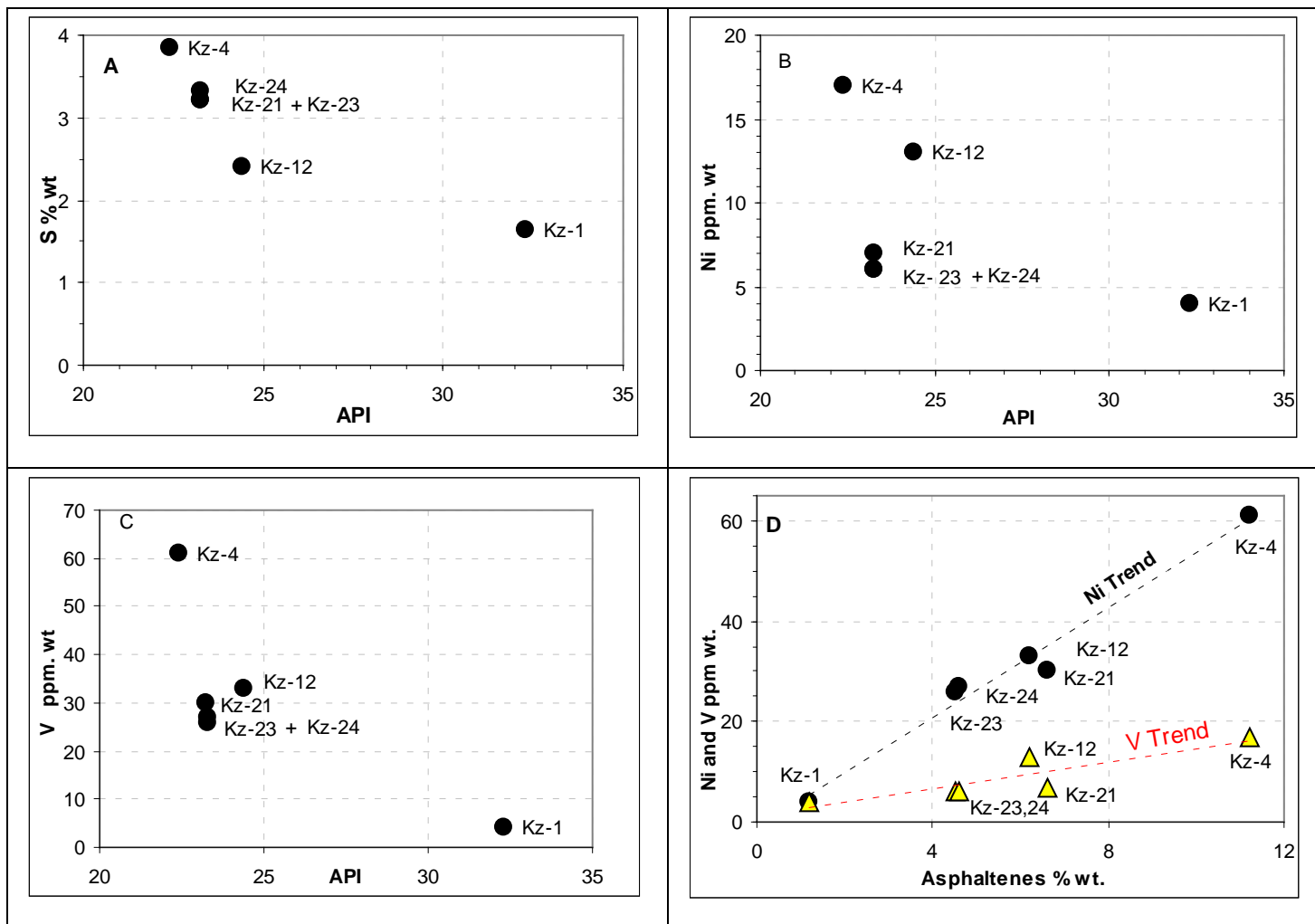


Figure 5.2: (A) API gravity vs. S% the inverse relation between them, (B and C) API gravity vs. Ni and V, ppm the inverse relation between them,(D) Asphaltenes% vs. Ni and V ppm, the linear relation between them.

5.6.2 Bacteriological Examination

To insure the possibility of exposing the oil in Kz-4 to any biodegradations, due to its low API with the high amount of asphaltene and resins comparatively with other wells, two samples of crude oil were selected to bacteriological test. One of them from Kz-4 and the second from Kz-1. The latter well produces from Lower Qamchuqa, and it was chosen for comparison purpose. The crud oil samples were taken to the microbiology laboratory of biology department of Sulaimani University and they submitted to bacteriological studies as follows:

From both samples by using sterile loops two small drops were taken aseptically and inoculated on two different bacteriological plates (nutrient agar) for each sample two replicates were taken. The first was incubated at 37°C for 48 hours aerobically, while the latter was incubated under anaerobic state under the same conditions.

All the inoculated plates from aerobic and anaerobic conditions did not show any bacterial growth after 24, and 48 hours. The bacteriological results indicate that there are no any traces of bacterial species in the crude oil; the results are demonstrated by the table (5-5).

Table 5-5. The bacteriological tests of the crude oil samples.

Sample no.	Aerobic condition on nutrient agar		Anaerobic conditions on nutrient agar	
	After 24hr. at 37°C	After 48hr. at 37°C	After 24hr. at 37°C	After 48hr. at 37°C
Kz-1	No growth	No growth	No growth	No growth
Kz-4	No growth	No growth	No growth	No growth

5.6.3 Origin of the Oils

Generally, oils in reservoir rocks and their source rock have many similarities as far as their composition is concerned. In general, the original biological marker fingerprint of source rock is preserved sufficiently in migrated oils to allow its use as a tool to assess oil-source rock (Balance and Connan, 1993A). GC-MS analyses of the saturation fraction of the oils show low Pr/Ph ratios (0.60-0.73) and relatively high Ph/n-C₁₈ (0.23-0.33) ratios (see table 5.6). These characteristics may be attributed to low oxygenated marine conditions present during source deposition (Yessalina et al, 2006).

Sterane biomarkers are used to correlate oils and assess the source of the oil. Oils derived from terrestrial environment are enriched in C₂₉ steranes determination from a saturate fraction GS-MS analysis results from (217 or 218 m/z ion chromatogram). Oils derived from algal source have higher amounts of C₂₇ and C₂₈ steranes. Marine vs. lacustrine determinations are made from the presence or absence of 24-n-propylcholestane.

The nature of the original source rock, the depositional environments, the maturation and the biodegradation are further elucidated from a plot of the isoprenoid ratio Pr/C₁₇ versus Ph/C₁₈ (Figure 5.3). All of the oil samples fall in the marine source rocks region under reducing conditions, Type II organic matter, which is denoted by letter D, also the samples site in the maturation zone. The carbon isotope composition of $\delta^{13}\text{C}$ saturation ranging from -26.6 to -27.5‰ to the all samples (Table 5.8) indicating the generation from marine source rock at relatively moderate levels of thermal maturity (Younes and Philp, 2005; Rabbani and Kamali, 2005; Akinlua et al, 2007; Petersen et al, 2007; Alsharhan and Abd El-Gawad, 2008).

Table 5.6: The molecular ratios of Pr/Ph, Pr/C17 and Ph/C18

Wells No.	Molecular ratios		
	$\frac{\text{Pr}}{\text{Ph}}$	$\frac{\text{Pr}}{\text{C17}}$	$\frac{\text{Ph}}{\text{C18}}$
Kz-1	0.60	0.13	0.23
Kz-12	0.73	0.23	0.33
Kz-21	0.68	0.17	0.28
Kz-23	0.71	0.17	0.26
Kz-24	0.65	0.17	0.28
Kz-4	0.65	0.16	0.27

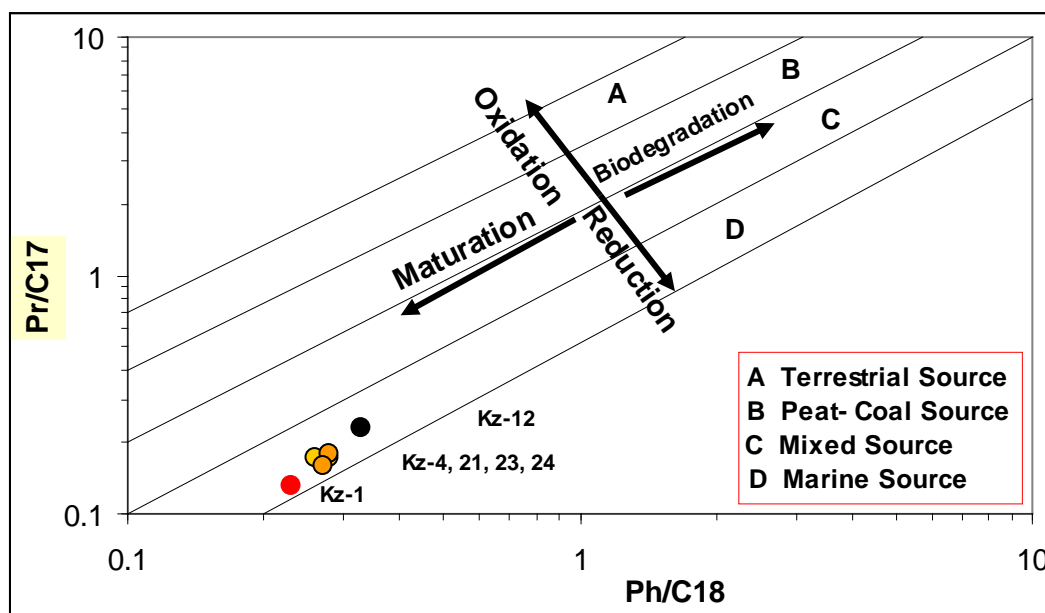


Figure 5.3: Crossplot between Ph/C_{18} and Pr/C_{17} of crude oil samples from selected well in the Khabbaz oil field, all samples fall in the reducing marine environment and mature area. (after Younes and Philp, 2005).

The sterane fraction distribution in the analyzed crude oil samples table 5.7 were used frequently to clear the origin of organic matter source rock of Khabbaz oil field, and to determine the genetic relationship between oils and source rock (Lirong et al, 2004).

Table 5.7: Normalized ratio of C27, C28 and C29%.

Steranes		
% C27	% C28	% C29
27	28	45
29	30	41
30	28	42
30	29	42
29	28	43
29	28	43

The trianary diagram of C27, C28, and C29 for regular sterans analyzed crude oil samples is used (Table 5.7). The figure 5.4 shows that all points are close to each other. This indicates that all samples belong to the same oil family. In addition it suggests that the family similarity between the oils of Upper Qamchuqa and Lower Qamchuqa reservoirs, the latter represented by Kz-1 oil sample. Also the plot used for the classification of organic matter type and depositional environment, shows that the oils are derived from source rocks deposited in nearest to mix to marine environments (Grantham and Wakefield, 1988; in Rabbani and Kamali, 2005).

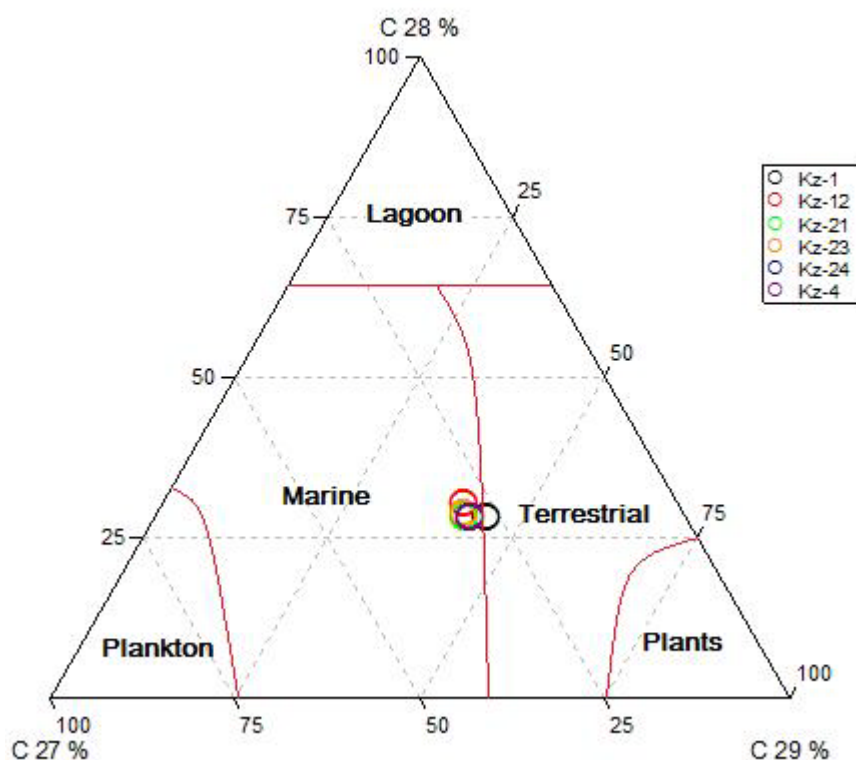


Figure 5.4: The trianary diagram of regular sterane C27, C28, and C29, from selected wells within Khabbaz oil field, all sample fall to the area of marine source rock near to the boundary of terrestrial area this indicate to the mixed source.

5.6.4 Stable Carbon Isotopic Compositions

Isotopes are atoms whose nuclei have the same number of protons but different number of neutrons. There are two fundamental classes of isotope; stable and radioactive isotopes. Carbon is available in two stable isotopes, ^{12}C and ^{13}C . The carbon isotope composition is usually reported using δ -notation (Skaare, 2007). The use of stable isotopes has become an important tool in oil-oil and source rock correlations and in assessing biodegradation of crude oil. The isotope fraction during biodegradation leads to the enrichment of heavier isotopes in the residual fraction as a result of ^{12}C - ^{12}C bonds requiring less energy to be broken than ^{12}C - ^{13}C bonds (Vieth and Wilkes, 2006; in Skaare, 2007).

The stable carbon isotopic composition of organic matter is an important tool which differentiates algal and land plant source input materials and marine from continental depositional environments (Mason et al, 1995; Younes and Philp, 2005). Coaly sample shows the heaviest ratio values of carbon isotopic while shaly and sandy samples are generally lighter. This can be interpreted in terms of kerogen type (Justwan et al, 2005).

Table 5.8: Stable carbon isotopes in saturated and aromatic fractions of oil samples.

Well No.	$\delta^{13}\text{C}$ (‰ PDB) Saturated HC	$\delta^{13}\text{C}$ (‰ PDB) Aromatic
Kz-1	-27.5	-27.3
Kz-12	-26.6	-26.5
Kz-21	-26.9	-26.9
Kz-23	-26.9	-27.0
Kz-24	-26.9	-26.9
Kz-4	-27.0	-27.0

Stable carbon isotopes data for the saturate and aromatic hydrocarbons are given in Table 5.8, and plotted in Figure 5.5. The stable carbon isotope compositions of the saturate fraction range between -26.6‰ and -27.5‰, while the aromatic fraction ranges from -26.5‰ and -27.3‰. The results point to the almost marine near to mixed origins of the Qamchuqa reservoir oils in Khabbaz oil field (Younes and Philp, 2005). This result also agrees with the Pr/C₁₇- Ph/C₁₈ relation Figure 5.3. Also the results of the two figures of all Upper Qamchuqa samples show well matching, in addition to their matching with a sample from the well Kz-1 which is producing from Lower Qamchuqa reservoir, these results

indicate that the oils of the two reservoirs belong to the same source rock and they belong to the same oil family.

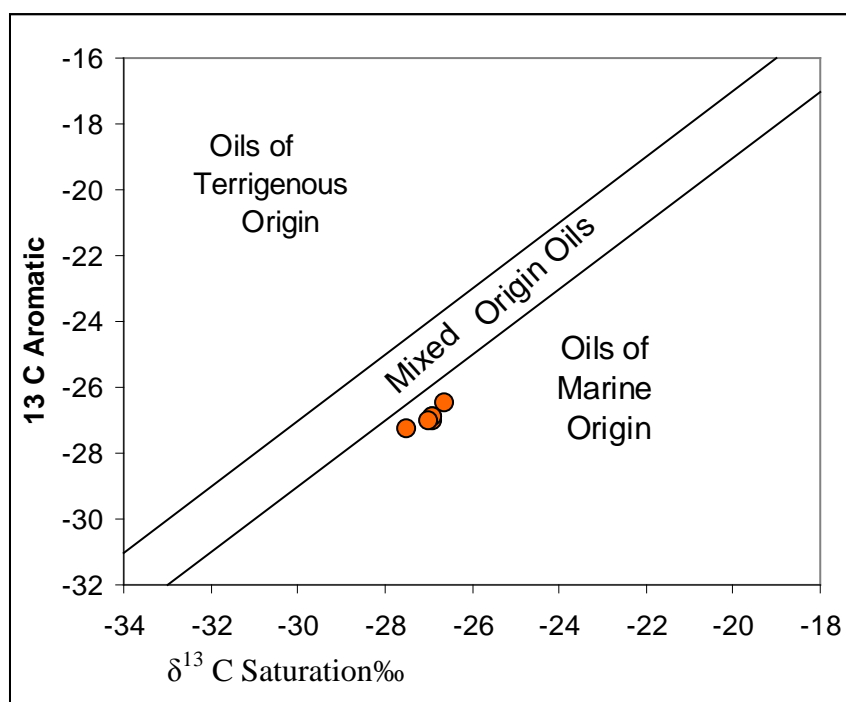


Figure 5.5. Relationship between the carbon stable isotopic of the saturate and aromatic fractions (after Younes and Philp, 2005).

5-6.5 Maturity Levels

The maturity levels of the oils were assessed by maturity parameters based on aromatic components of GC-MS analysis molecular ratios results, such as the methylphenanthrene ratio (MPR), the methylphenanthrene index 1 (MPI-1), the methylphenanthrene distribution fraction (MPDF), the methynaphthalene ratio (MNR), also the trimethylnaphthalene ratio 2 (TNR-2) (Yessalina et al, 2006). All of these maturity parameters indicate that the oils are of high maturity level (Table 5.9), the maturity estimates suggest that expulsion of

hydrocarbons from source rocks took place during the peak oil window, corresponding to vitrinite reflectance values (R_o) (Lirong et al, 2004) of between 0.90 and 0.96 % (Table 5.9).

Also Pr/C17- Ph/C18 relations (Figure 5.3) suggest high maturity degree of the oil samples (Younes and Philp, 2005).

Table 5.9: Aromatic hydrocarbon molecular ratios

	<i>Phenanthrene</i>					<i>Naphthalene</i>	
	MPI3	MPI1	R0	MPI2	MPR	DNR2	IN1
Kz-1	0.86	0.91	0.95	1.05	1.61	2.32	0.79
Kz-12	1.01	0.94	0.96	1.12	1.53	2.56	0.93
Kz-21	0.85	0.85	0.91	1.02	1.41	2.68	0.88
Kz-23	0.84	0.85	0.91	1.02	1.42	2.58	0.84
Kz-24	0.84	0.86	0.92	1.02	1.37	2.52	0.85
Kz-4	0.82	0.84	0.90	1.00	1.40	2.05	0.78

$$\%R_o = 0.6 \text{ MPI1} + 0.4 \text{ (Lirong et al, 2004)}$$

Gas chromatogram C_{15+} performed on saturate fractions shows that normal alkanes predominantly range from C_{15} to C_{35} . The range of the most oils show a marine origin (Table 5.10, Figure 5.6). Relatively high concentrations of light n -alkanes together with carbon preference index (CPI) values less than 1 suggest that most oils are mature. The presence of appreciable concentration of light n -alkanes suggests that these oils have not been affected by secondary alteration such as water wash and biodegradation (Rabbani and Kamali, 2005).

Table 5.10: Analytical data for oil samples from the selected wells of Khabbaz oil field.

<i>n</i> -C %	Kz-1	Kz-12	Kz-21	Kz-23	Kz-24	Kz-4
C15	10.2	8.5	9.7	12	9	10.3
C16	10.5	9.4	10.4	1.4	9.6	10.5
C17		9.4	10.2	1.4	9.5	10.1
C18	9.5	9	9.5	1.4	9.1	9.4
C19	8.4	8	8.4	1.2	8.2	8.3
C20	7.8	7.6	7.7	11.5	7.6	7.7
C21	6.9	7	6.8	10.5	6.9	6.9
C22	6.1	6.4	6.1	9.5	6.2	6.3
C23	5.3	5.6	5.3	8.3	5.5	5.5
C24	4.8	5.2	4.8	7.6	5	5
C25	4.1	4.4	4.1	6.5	4.3	4.3
C26	3.6	3.9	3.6	5.7	3.8	3.7
C27	3	3.3	3	4.9	3.3	3.1
C28	2.4	2.7	2.4	4	2.7	2.4
C29	2	2.2	2	3.3	2.2	1.8
C30	1.6	2	1.7	2.8	1.9	1.4
C31	1.3	1.6	1.3	2.3	1.5	1.1
C32	1	1.2	1	1.8	1.2	0.8
C33	0.7	1	0.8	1.4	1	0.6
C34	0.5	0.8	0.6	1.1	0.8	0.4
C35	0.5	0.7	0.6	1.1	0.7	0.4
Even	47.8	48.2	46.8	46.8	47.6	47.3
Odd	52.3	51.7	52.2	52.9	52.1	52.4
CPI	0.91	0.93	0.90	0.89	0.91	0.9

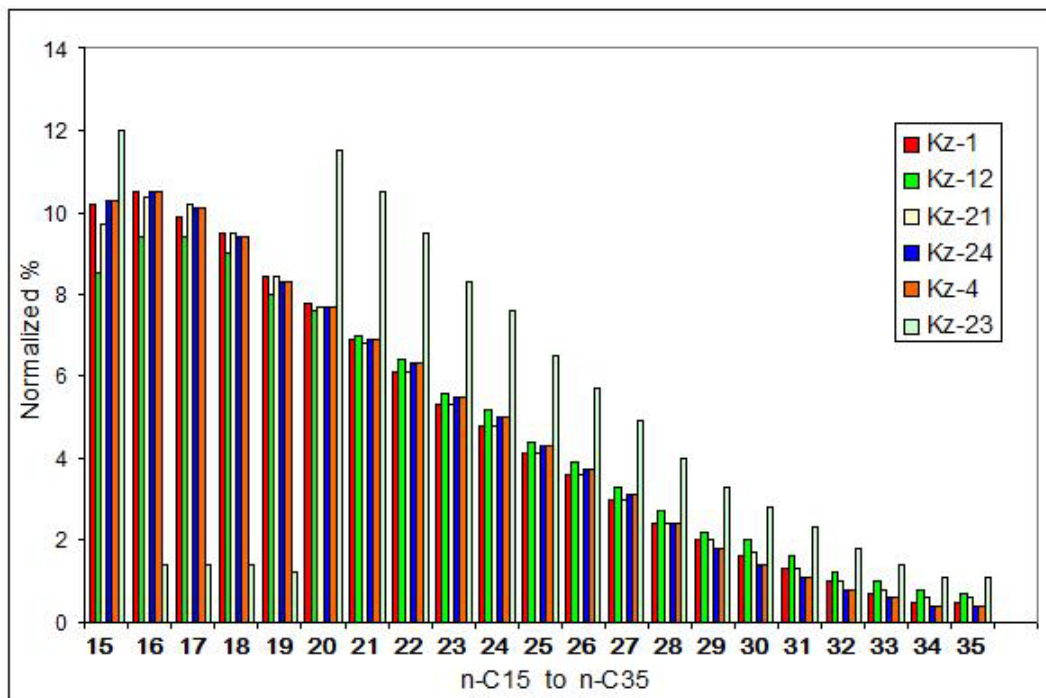


Figure 5.6: Gas chromatographic analyses of whole oil samples, showing the regular decreasing of *n*-alkanes from the C₁₅ to C₃₅.

Chapter Six

Summary and Conclusions

- 1- The Khabbaz oil field represents asymmetrical subsurface anticline, with around 20 Km length and 4 Km width at the top of Upper Qamchuqa. Its northeastern limb dipper than the southwestern limb, the structure located between Jambour and Bai Hassan oil fields. The Upper Qamchuqa Carbonate Formation is one of the most prolific Khabbaz reservoirs with 156 to 180 m thickness.
- 2- Using core, thin-section examination and well log interpretation, the Upper Qamchuqa Formation of the Khabbaz oil field is subdivided into three lithological units, named from the top to bottom: Unit (A) with an average of 66m, Unit (B) with an average of 73m, and Unit (C) with an average of 34m.
- 3- The dolomitization is pervasive and affects most of the formation section especially the middle and lower part of unit (A), the upper part of unit (B), and some intervals of unit (C). The rest of the formation consists of inter-bedded limestone with dolomitic limestone, and the dominance of marly limestone, marl and shale over unit (C) is due to gradational change to the underlain Upper Sarmord Formation
- 4- The best reservoir characters are associated with unit (A). It is classified into six continuous reservoir subunits, from the top (A1, A2, A3, A4, A5, and A6). These reservoir subunits have good correlation, laterally and vertically, which make them easily followed by mean of well logs especially porosity logs.
- 5- The other porous subunits are associated with lithologic unit (B). They are named B1, B2, and B3, and lithologic unit (C) including subunit C1. These subunits are less uniform, poorly laterally correlated and with poorer reservoir characters.

- 6- Porosity is better developed in the fine to medium crystalline planer-e-s dolomite, especially in the three reservoir subunits (A4, A5 and A6), which are represented by single thick unit in some wells and are considered to be the main prolific reservoir interval allover the field. Thus dolomitization is the main factor responsible for the enhanced intercrystalline porosity of the reservoir.
- 7- According to the chemical analysis of the formation water, the formation water of the Upper Qamchuqa Formation belongs to the chloride calcium type, which indicates association with a closed system reservoir, isolated from influence of infiltration waters and considered as a good zone for preservation of hydrocarbons.
- 8- The formation water of the Khabbaz oil field is non-mobile type, which makes most of field wells produces water free hydrocarbons.
- 9- The geochemical analysis of the crude oils suggested the marine to the mix origin of the source rock, also the correlation between the oil chemistry of the Upper Qamchuqa reservoir and the Lower Qamchuqa Reservoir suggest that the two reservoirs have the same origin source rock and they belongs to the same reservoir condition system.
- 10- This study suggests that the heavy oil problem of the well Kz-4 belongs to some misconduct and unusual production technique. It is related to the extreme production or gas injection to the well, which leads to the precipitation of the residual fraction of the oil (deasphalting) around the well section and isolate the well from the lighter oil in the rest of the reservoir.

References

- Adisoemarta, P. S., Anderson, G. A., Frailey, S. M., Asquith G. B. 2000. **Historical Use of *m* and *a* in Well Log Interpretation: Is Conventional Wisdom Backwards.** Society of Petroleum Engineering (SPE 59699).
- Aguilera, R., 2004. **Integration of geology, petrophysics and reservoir engineering for characterization of carbonate reservoirs through Picket plots.** AAPG Bulletin V.88, No.4 PP 433-446.
- Aitken, M. Carolyn, D. M. Jones and Larter, S. R., 2004. **Anaerobic hydrocarbon biodegradation in deep subsurface oil reservoir.** NATURE V.431/16 September. PP291-394. Nature publishing group.
- Akinlua, A., Torto N. and Ajayi, T.R., 2007. **Oils in the NW Niger Delta: Aromatic Hydrocarbons Content and Infrared Spectroscopic Characterization.** Journal of Petroleum geology, V.30 (1), PP91-100.
- AL-Karadaghi, A. I. F., 2001. **Sedimentological Study of the Maaddud Formation in selected borehole from several oilfields Central Iraq.** Ph.D. Theses unpublished, University of Bghdad.
- AL-Mashadani, A., 1986. **Hydrodynamic Framework of the Petroleum Reservoir and Cap Rocks of the Mesopotamian**

- Basin of Iraq.** Journal of Petroleum Geology, Vol. 9(1), PP 89-110.
- Allah-Werdi, N., 2001, **Sequence Stratigraphy of the Lower Cretaceous Formations in Bai Hassan, Khabbaz and Jambour fields, North Iraq.** Unpublished Ph.D Thesis University of Baghdad.
 - AL-Sadooni, F. N., 1978. **Sedimentology and Petroleum prospects of the Qamchuqa group – Northern Iraq.** Ph.D. Thesis (unpublished), University of Bristol. 367 Pages.
 - Alshrhan, A. S. and Abd El-Gawad, E. A., 2008. **Geochemical Characterization of Potential Jurassic/Cretaceous Source Rocks in the Shushan Basin, Northern Western Desert, Egypt.** Journal of Petroleum Geology, Vol. 31(2), PP 191-212.
 - Al-Peryadi K. H. K., 2002. **Sedimentological Study and Reservoir Characterizations for Upper Qamchuqa and Jawan Formations to Determine the Effective Porosity in Bai-Hassan Field.** M. Sc. Thesis (in Arabic), University of Bagdad.178 pages.
 - Al-Shakiry, A.J., 1977. **The Petrology of part of the Upper Qamchuqa Formation in Jambur Oil Field Iraq.** M. Sc. Thesis, University of *Bagdad*.158 Pages..
 - Al Shdidi, S., Thomas G. and Delfaud, J., 1995. **Sedimentology, Diagenesis and Oil Habit of Lower Cretaceous Qamchuqa Group, Northern Iraq.** AAPG Bulletin, V.79, No.5, PP.763-779.

- Ameen, B. M., 2008. **Sedimentology and Lithostratigraphy of Qamchuqa Formation from Kurdistan Region, NE-Iraq.** Unpublished Ph.D. Thesis, University of Sulaimani. PP127.
- Andrew, H. and Al-Sadooni, F. N., 2006. **Northern Iraq study, by Cambridge Carbonate Ltd.**
- Asquith, G. and Krygowski, D., 2004. **Basic Well Log Analysis.** 244 Pages. AAPG Method in Exploration Method, No.16.
- Balance, Ph. and Connan, J., 1993A. **Crude Oils in Reservoirs: the Factors Influencing Their Composition** (Chapter 1.6 in Applied Petroleum Geochemistry, 1993 Ed. By M. L. Bordenave. Elf Aquitaine) PP 149-174.
- Balance, Ph. and Connan, J., 1993B. **Preservation, Degradation, and Destruction of Trapped Oil.** (Magoon, L. B. and Dow W. G. The Petroleum System-From Source to Trap. AAPG Memoir).
- Bates, R. L., and Jackson, J. A., 1980, **Glossary of Geology.** Second edition (by American Geological Institute, Falls Church, Virginia 1980) 749 Pages.
- Bellen, R.C. Van, Dunnington, H. V., Wetzel, R. and Morton, D. 1959. **Lexique Stratigraphique International.** ASIE, Fascicule 10 a, Iraq, Paris, 333 Pages.
- Buday, T., 1980. **The Regional Geology of Iraq, Volume I; Stratigraphy and Paleogeography.** Dar AL-Kutib publishing house, University of Mosul. Iraq. 445 Pages.

- Buday, T. and Jasim, S. Z., 1987. **The Regional Geology of Iraq, Volume II; Tectonism, Magmatism and Metamorphism.** Dar AL-Kutib publishing house, University of Mosul. Iraq. 352 Pages.
- Choquette, P. W. and Pray, L.C., 1970. **Geologic Nomenclature and Classification of Porosity in Sedimentary Carbonates.** AAPG. V.54, No.2; PP 207-250.
- Collins, A. Gene, 1975. **Geochemistry of oil field waters,** Elsevier Scientific Publishing, 496 Pages.
- Connan, J., 1993. **Molecular Geochemistry in Oil Exploration.** (Chapter 1.7 in Applied Petroleum Geochemistry, 1993 Ed. By M. L. Bordenave. Elf Aquitaine) PP 175-2004.
- Connan, j. and Lacrampe-Coulome, G., 1993. **The Origin of the Lacq Superieur Heavy Oil Accumulation and of the Giant Lacq Inferieur Gas Field (Aquitaine Basin, SW France).** (Chapter III.2 in Applied Petroleum Geochemistry, 1993 Ed. By M. L. Bordenave. Elf Aquitaine) PP 465-488.
- Cuddy, S. J. and Glover, P. W. J., **The Application of Fuzzy Logic and Genetic Algorithms to Reservoir Characterization and Modeling.** (Unpublished research).
- Dickson, J. A. 1966. **Carbonate Identification and Genesis as reveled by staining.** Journal of Sedimentary Petrology, V.36, PP 491-505.

References

- Dovton, J. H. 1944. **Log Analysis Subsurface Geology**. Copyright 1986 by Jhon Wiley & Sons, Inc. 273 Pages.
- Dunham R. J., 1962. **Classification of Carbonate Rocks According to Depositional Texture**: in Ham W. E. (ed), Classification of Rocks; a symposium , AAPG, No.1, PP 108-121.
- Final well reports, (Kz-1, Kz-2, Kz-3, and Kz-4), 1977, and (Kz-11, Kz-13, Kz-14) 1982. North Oil Company, Department of Geology.
- Flugel, E., 1982. **Microfacies Analysis of Limestones**. Springer Varlag, Berline, 633Pages
- Hamada, G. M., 2004. **Hydrocarbon Moveability Factor (HCM): New Approach to Identify Hydrocarbon Moveability and Type from Resistivity Logs**. Emirate Journal for Engineering Research, V.9 No.1 2004. PP 1-7.
- Holtz, M. H., John, A., Katherine, G. and Major, R. P., 2002. **Petrophysical Characterization of Permian Shallow-Water Dolostone**. Society of Petroleum Engineers SPE 75214.
- Jassim, S. Z. and Goff, J. C., 2006. **Geology of Iraq**. Published by Dolin, Prague and Moravian Museum, Brno. 341 Pages.
- Jennings, J. W. and Lucia, F. J., 2003. **Predicting Permeability From Well Logs in Carbonates With a Link to Geology for Interwell Permeability Mapping**. SPE Reservoir Evaluation & Engineering, August 2003. PP. 215-225.

References

- Jodry, R. L., 1972. **Pore Geometry of Carbonate Rocks (Basic Geologic Concepts)**, Chapter 2 in Book (Oil and Gas Production from Carbonate Rocks) Edited by Chalinger G. V., R. W. Mannon and H. H. Rieke. PP.35-82.
- Justwan, H., Dahl, B., Iskasen, G. H., and Meisingset, I., 2005. **Late to Middle Jurassic Source Facies and Quality Variations, South Viking Graben, North Sea.** Journal of Petroleum Geology, V.28(3).July 2005, PP 241-268.
- Levorsen, A. I., 1967. **Geology of Petroleum**, by Freeman and Company. 724 Pages.
- Lirong, D., Dingsheng, Ch., Jianjun, W., Rubondo, E. N. T., Kasande, R., Byakagaba, A. and Mugish, F., 2004. **Geochemical Significance of Seepage Oils and Bituminous Sandstones in the Albertine Graben, Uganda.** Journal of Petroleum Geology, V.27(3).July 2004, PP 299-312.
- Lucia, F. J., 1999. **Characterization of Petrophysical Flow Units in Carbonate reservoirs:** Discussion. AAPG Bulletin V.83. No.7 (July 1999), PP.1161-1163.
- Lucia, F. J., Jennings, J.W., Rahnis, M and Meyer, F.O., 2001. **Permeability and Rock Fabric from Wireline Logs. Arab-D Reservoir, Ghawar Field, Saudi Arabia.** Geo Arabia V.6, No.4 (2001). PP619-646.

References

- Martin, A. J. (Jeff)., Solomon, S. T., and Hartmann D. J., 1997. **Characterization of Petrophysical Flow Units in Carbonate Reservoir:** AAPG Bulletin, V. 81, No. 5(May 1997), PP.734-759.
- Martin, A. J. (Jeff)., Solomon, S. T., and Hartmann D. J., 1999. **Characterization of Petrophysical Flow Units in Carbonate Reservoir,** Reply: AAPG Bulletin, V. 83, No. 7(July 1999), PP.1164-1173.
- Mason, P. C., Burwood, R. and Mycke, B., 1995. **The reservoir geochemistry and petroleum charging histories of Paleogene-reservoired fields in the Outer Witch Ground Graben. From the Geochemistry of Reservoirs,** 1995, Geological Society Special publication No. 83, PP 281-301.
- McCain, W. D. Jr., 1990. **The properties of Petroleum Fluids** (Second edition), PennWell Publishing Company, 548 Pages.
- North, F. K., 1985. **Petroleum Geology.** Allen & Unwin Inc. 607 Pages.
- Petersen, H. I., Nytoft, H. P., Ratanasthien, B., and Foopatthanakamol, A., 2007. **Oils from Cenozoic Rift-Basins in Central and Northern Thailand: Source and Thermal maturity.** Journal of Petroleum Geology, V.30 (1).January 2007, PP 59-78.
- Pittman, F. D., 1992. **Relationship of Porosity and Permeability to Various Parameters Derived from Mercury Injection-Capillary Pressure Curve for Sandstone.** AAPG Bulletin, V.76, .No.2 (February 1992) PP 191-198.

- Rabbani, A. R. and Kamali, M. R., 2005. **Source Rock Evaluation and Petroleum Geochemistry, Offshore SW Iran**. Journal of Petroleum geology, V.28 (4), October 2005, PP413-428.
- Reeckmann, A. and Friedman, G. M., 1982. **Exploration for Carbonate Petroleum Reservoirs**. Elf-Aquitaine Center. John Wiley& Sons Publication, 213 Pages.
- **(Reports of Petroleum Engineering Department)** North Oil Company. During the years 1976-1982.
- Rider, M., 2000. **The Geological Interpretation of Well Logs**. Second edition, Whittles Publishing, 280Pages.
- Ruf, M. and Aigner, T., 2004. **Facies and Poroperm Characteristics of a Carbonates Shoal. (Muschelkalak, South German Basin): A Reservoir Analogue Investigation**. Journal of Petroleum Geology, V.27 (3).July 2004, PP 215-239.
- Sadooni, F. N. and Alsharhan, A. S., 2003. **Stratigraphy, microfacies, and petroleum potential of the Mauddud Formation (Albian-Cenomanian) in the Arabian Gulf basin**. AAPG Bulletin, V.87.No.10 (October 2003) PP1653-1680.
- Sahar, A. A., 1987. **Dolomitization of Upper Qamchuqa Formation Northern Iraq**. Unpublished, M.Sc thesis University of Baghdad. 182 Pages.

References

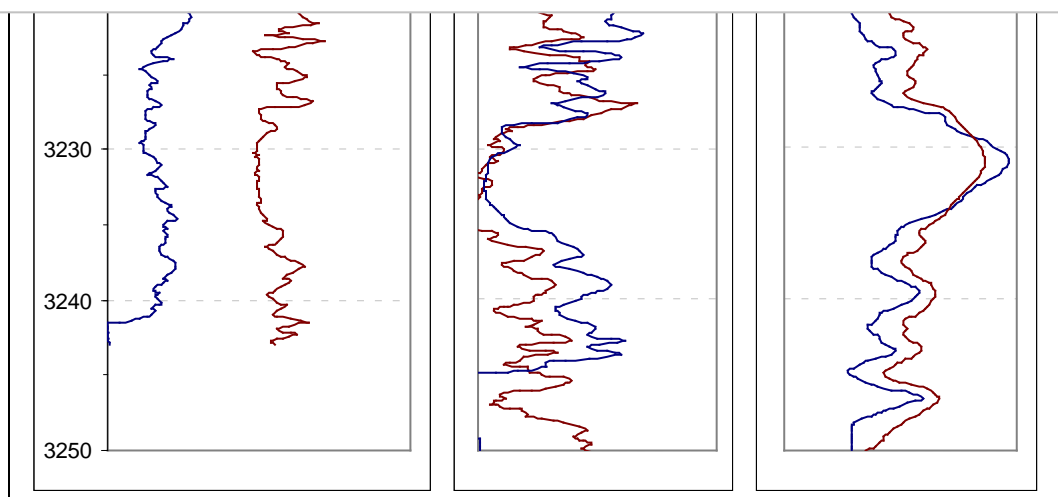
- Selley, R. C., 1998. **Elements of Petroleum Geology** (Second Edition) Academic Press, 470 Pages.
- Serra, O., 1986. **Advanced Interpretation of Wireline Logs.** (Schlumberger book), 295 Pages.
- Schlumberger, 1972. **Log Interpretation Charts**
- Schlumberger, 1979. **Log Interpretation Charts**
- Schlumberger, 1972. **The Essentials of Log Interpretation Practice.**
- Sibley, D. L., and Gregg, 1982. **The origin of Common Dolomite Fabrics, Clues from the Pliocene.** Journal of Sedimentary Petrology, V.52, No.4, PP 1087-1100.
- Skaare, B. B., 2007. **Effect of initial anaerobic biodegradation on crude oil and formation water composition.** (Ph.D. Thesis at the University of Bergen), 51 Pages.
- Spearing, M., Allen, T. and McAulay, G. **Review of the Winland R35 methods for net pay definition and its application in low Permeability sands.** (unpublished study).7 Pages.
- Tagavi, A. A., 2005. **Improved Permeability Estimation Through Use of Fuzzy Logic in a Carbonate Reservoir From Southern Iran.** Society of Petroleum Engineers (SPE) Inc.

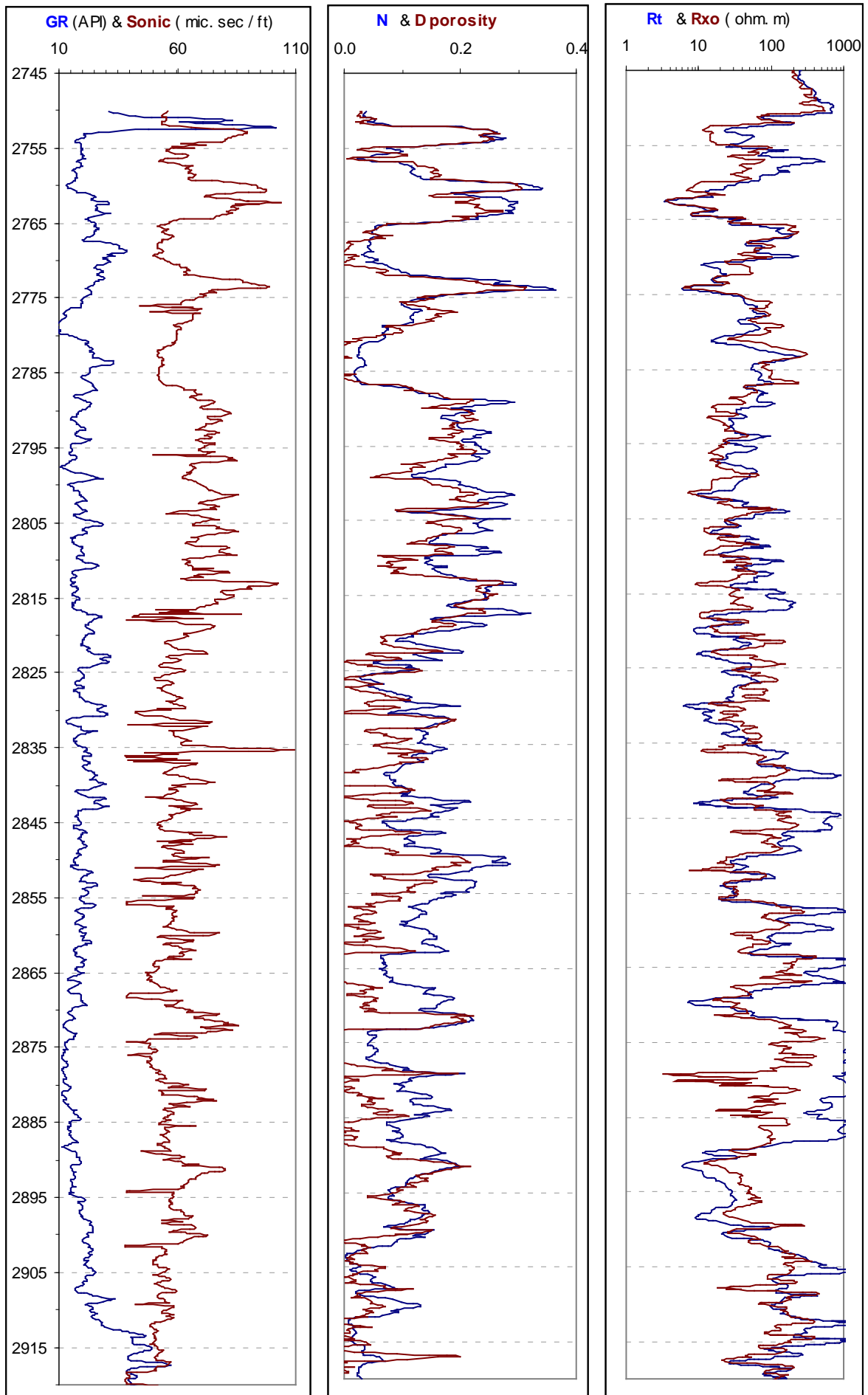
References

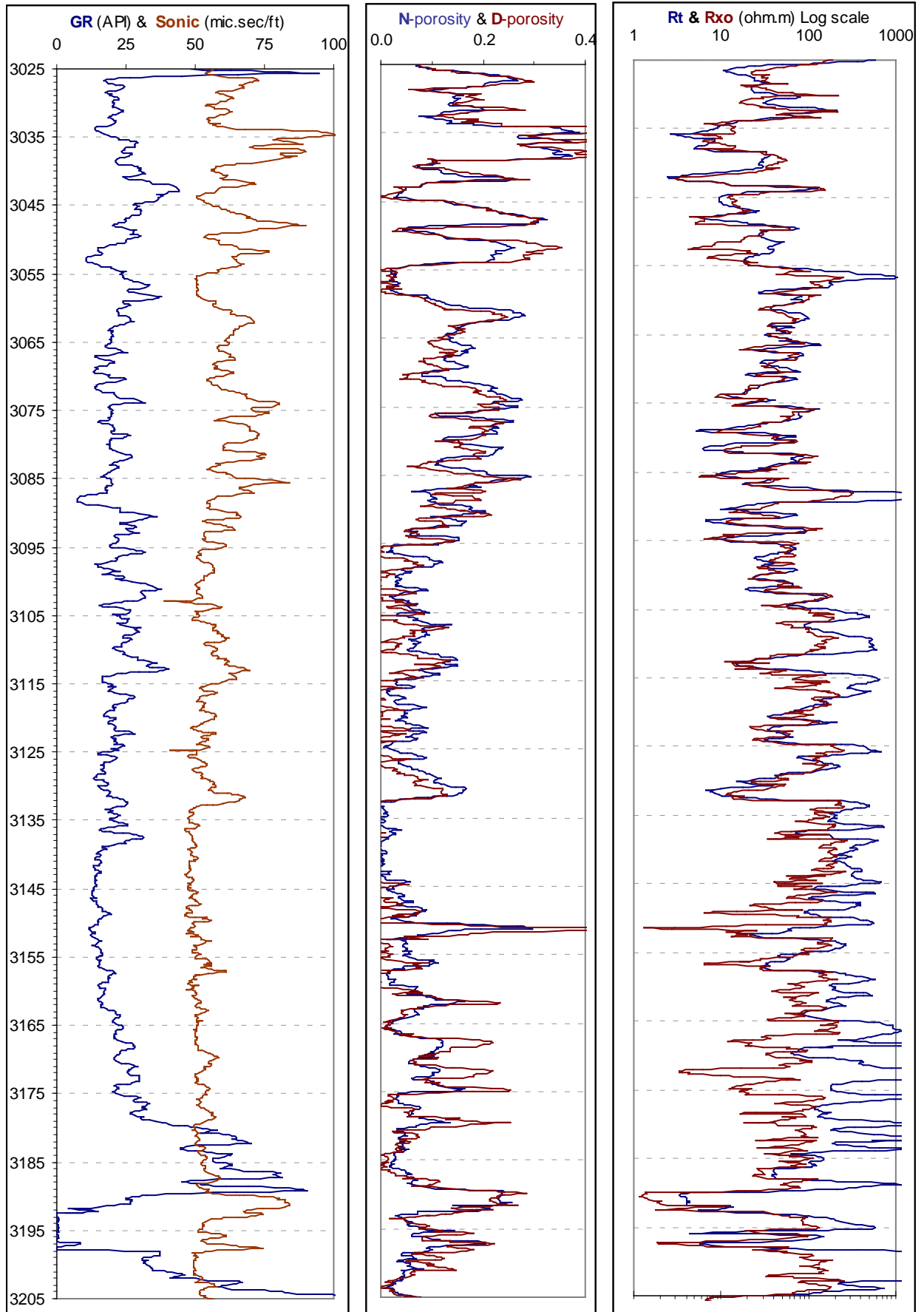
- Tagavi, A. A., Mørk A. and Kazemzadeh E. 2007. **Flow Unit Classification for Geological Modeling of a Heterogeneous Carbonate Reservoir: Cretaceous Sarvak Formation, Dehluran Field, SW Iran.** Journal of Petroleum Geology, Vol.30 (2), April 2007, PP129-146.
- Wilson, J. L., 1975. **Carbonate Facies in Geology History,** Springer-Verlag, New York, 471 Pages.
- Yessalina, S., Suzuki, N., Nishita, H., and Waseda, A., 2006. **Higher Plant Biomarkers in Paleogene Crude Oils from the Yufutsu Oil-and Gas Field and Offshore Wildcats, Japan.** Journal of Petroleum geology, V.29 (4), October 2006, PP327-336.
- Yuones, M. A. and Philp, R. P., 2005. **Source Rock Characterization Based on Biological Marker Distributions of Crude Oil in the Southern Gulf of Suez, Egypt.** Petroleum geology Vol.28 (3) 2005, PP301-317.

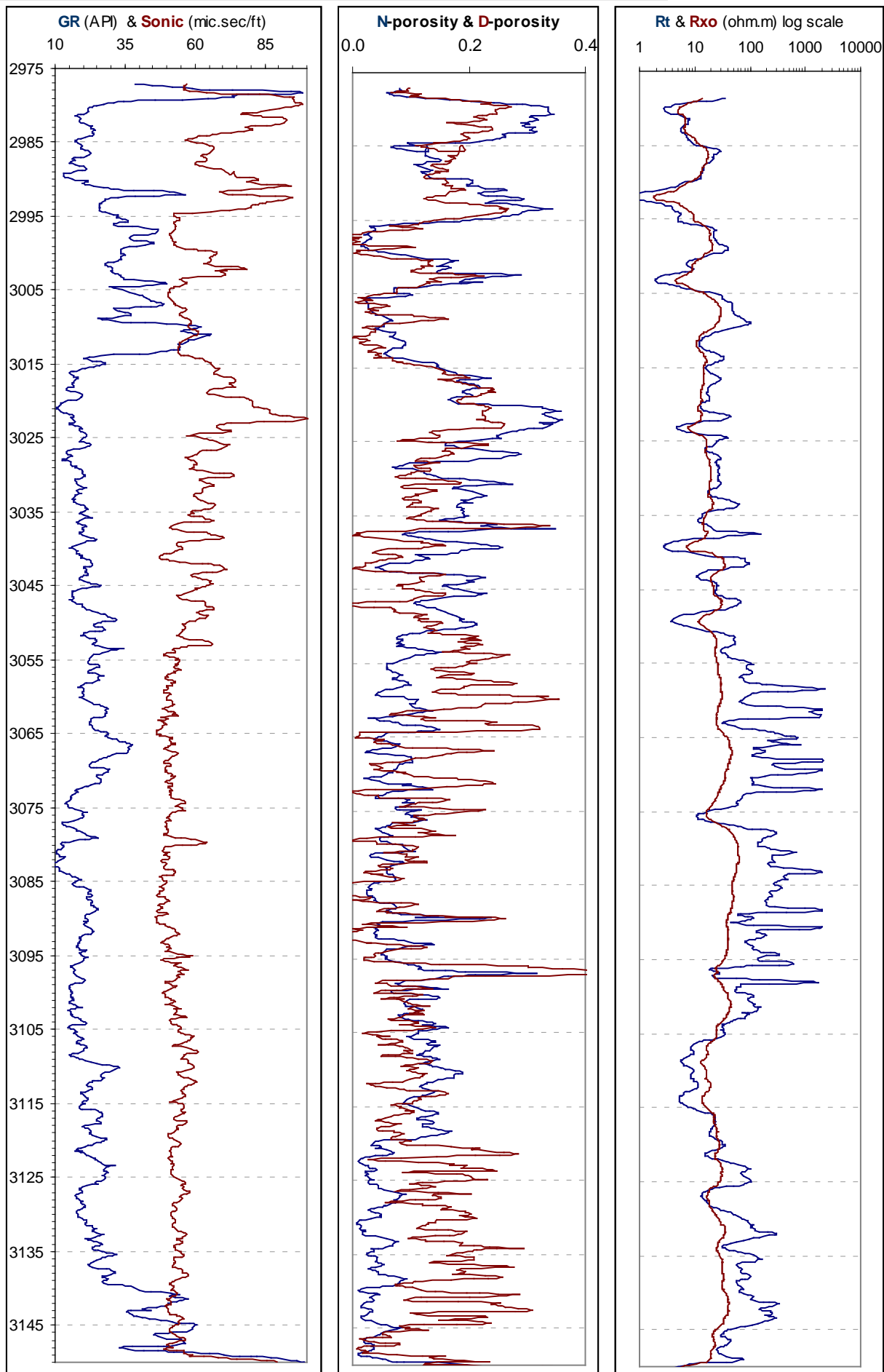
Appendices (A_{ns}):

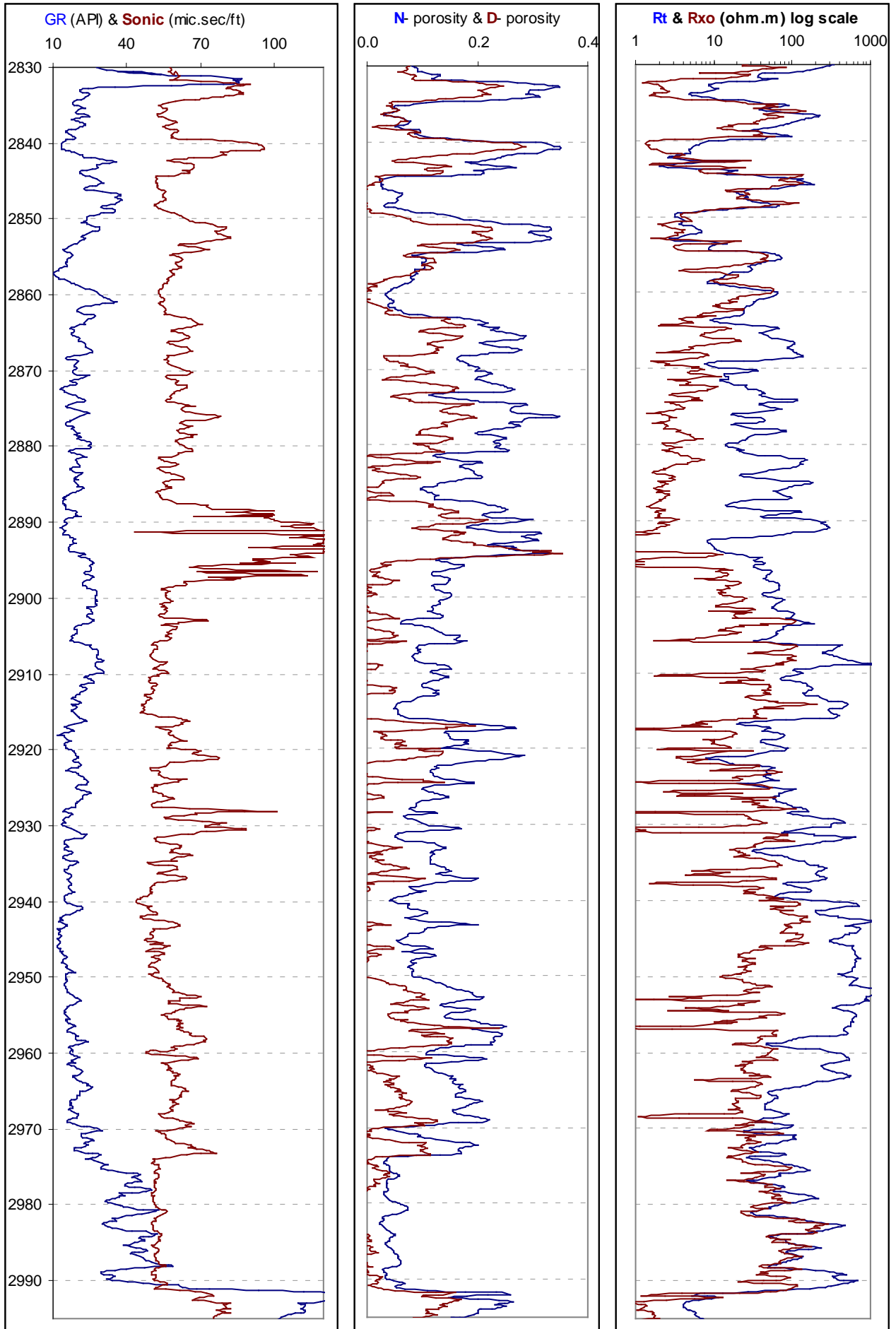
The raw log graphs from nine wells, illustrated with three columns in each well. Left column represents Gamma (GR) and Sonic logs, middle column is Neutron (N) and Density (D) porosities, and the right column is the Resistivity logs for true formation (R_t) and flushed zone (R_{xo}). The colors of the title words are matching with their curve colors.

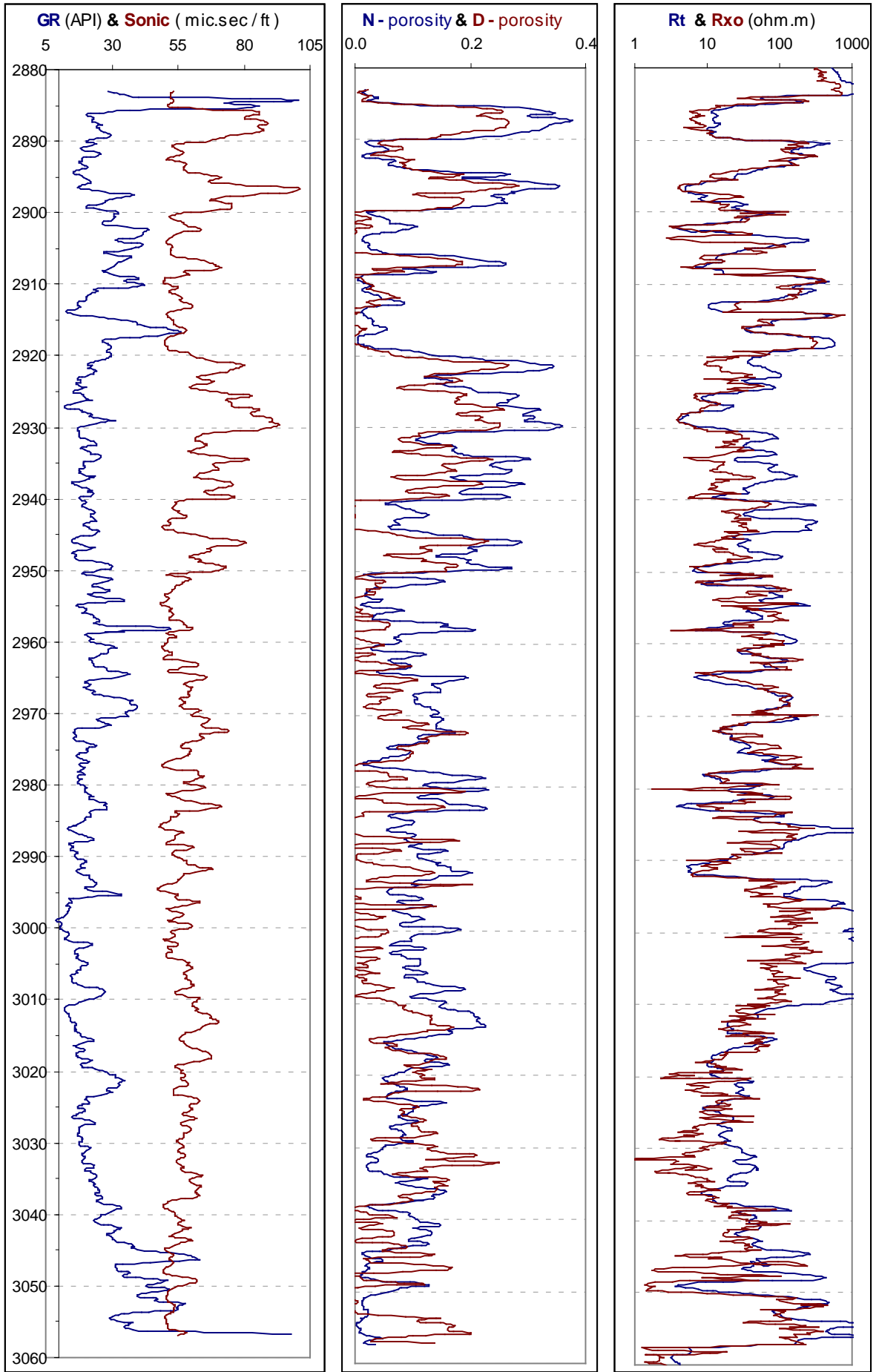


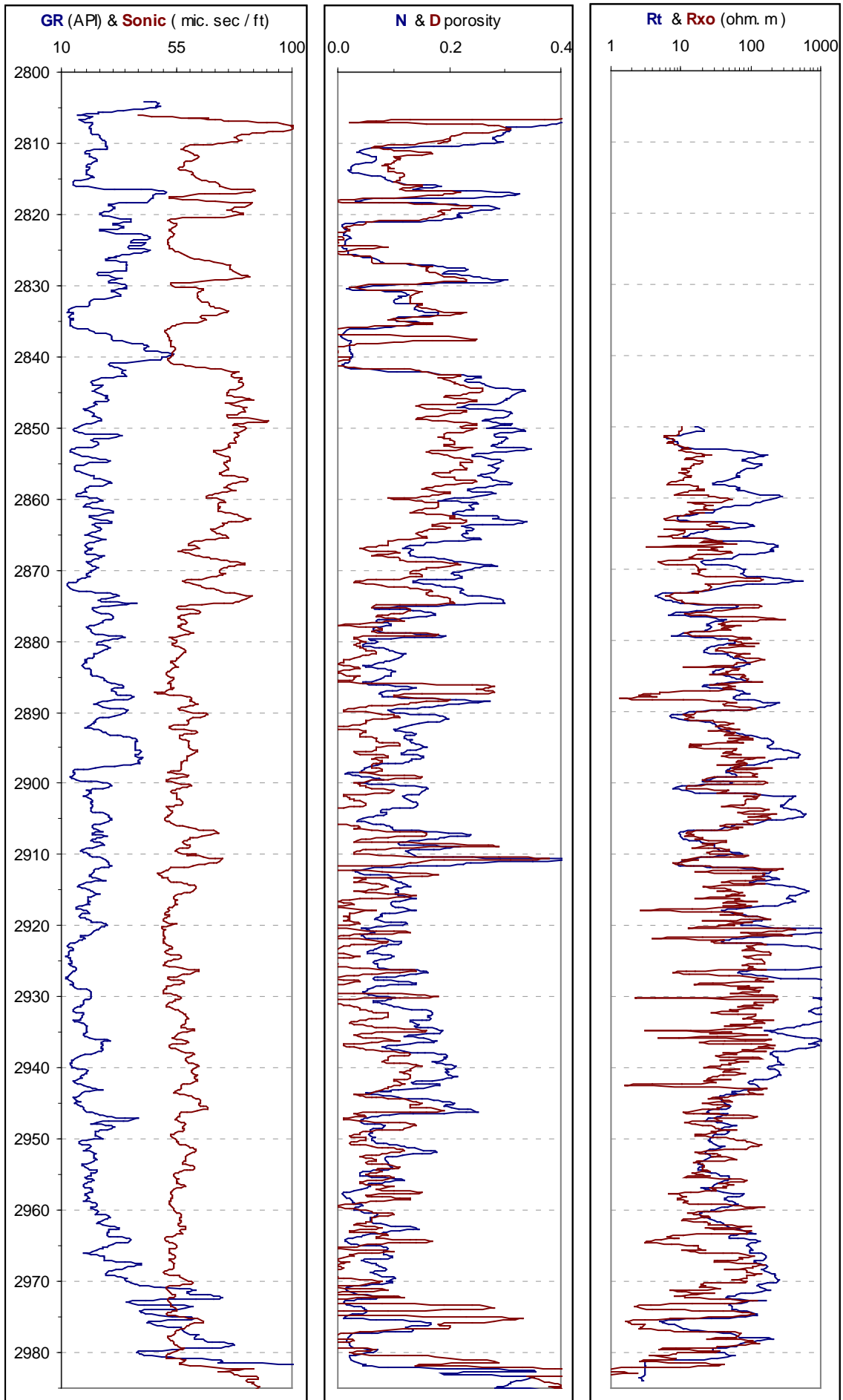


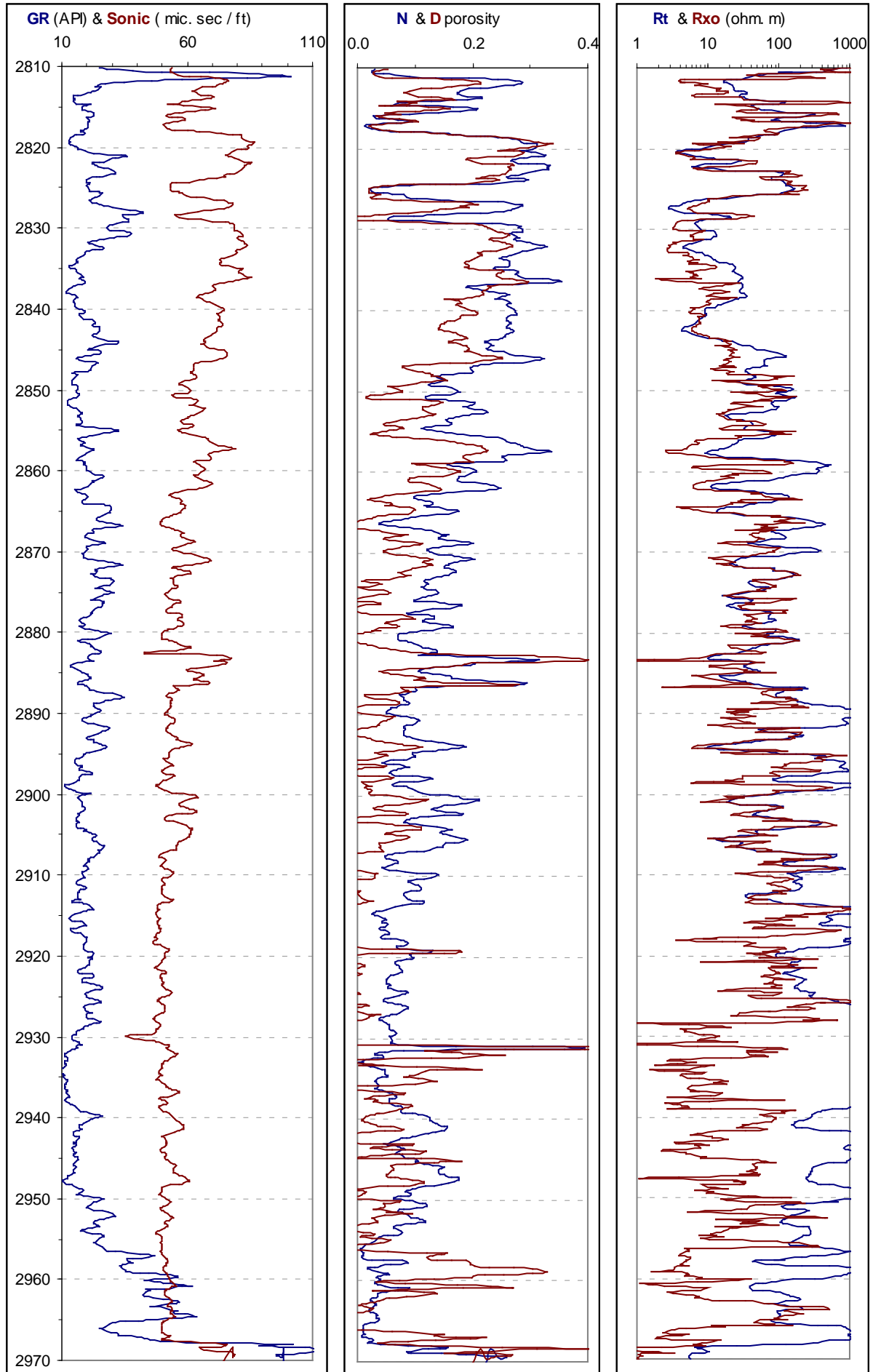


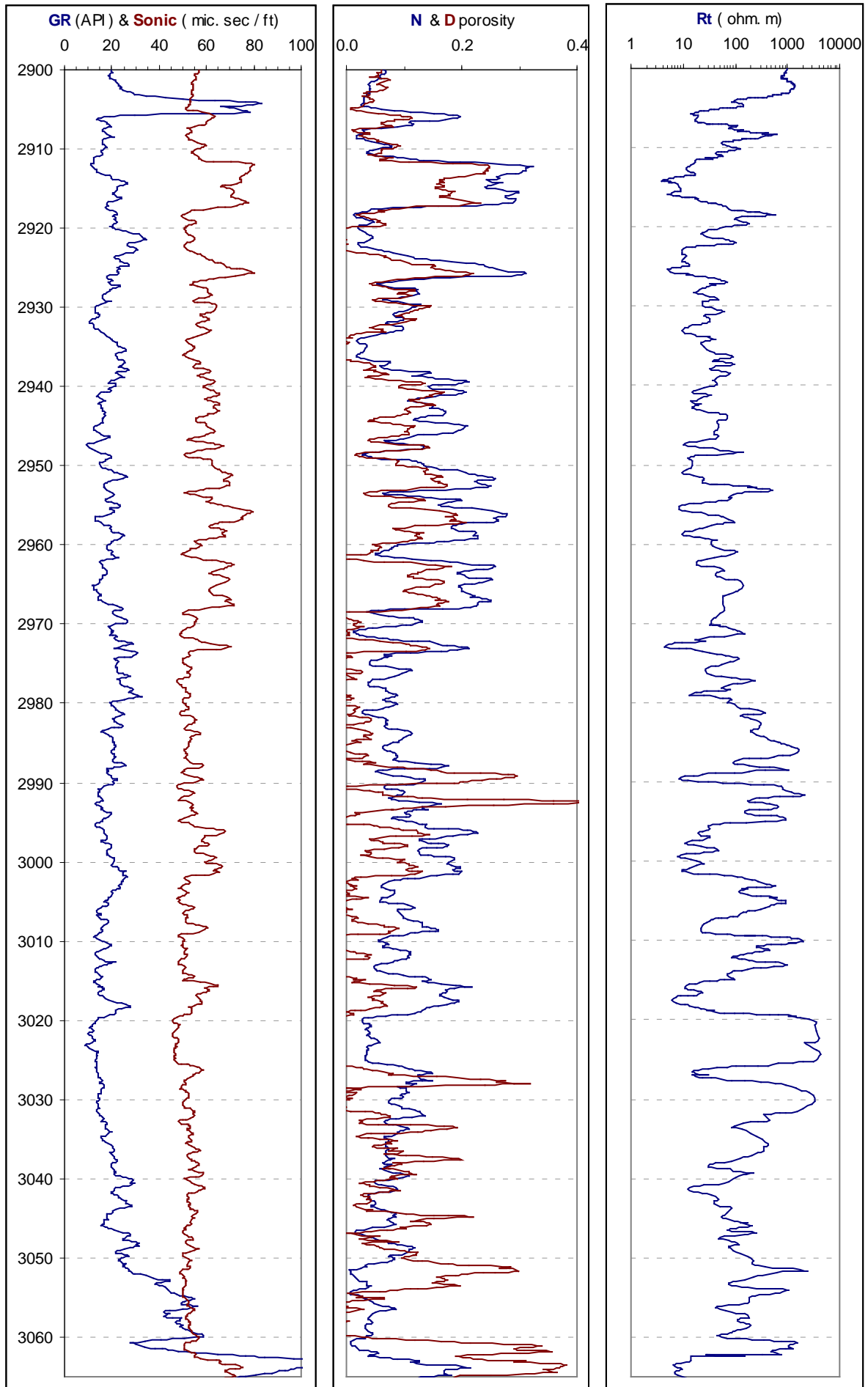












Appendix (B):

Porosity (Φ) and permeability (K), from laboratory core measurements. Kz-16, Upper Qamchuqa

Depth (m).	$\Phi\%$	K(Air) md	Depth (m).	$\Phi\%$	K(Air) md
2910.10	31.80	5.16	2929.30	12.60	26.16
2910.40	30.30	42.12	2929.60	14.30	17.51
2910.70	30.20	33.78	2930.00	7.00	0.73
2911.00	29.40	30.70	2930.30	4.70	0.03
2911.30	30.20	27.84	2930.60	8.10	0.01
2912.40	19.10	0.45	2930.90	12.60	0.05
2913.00	23.50	6.28	2931.20	10.20	0.01
2913.30	27.20	8.65	2931.50	7.20	0.00
2913.90	27.30	28.26	2931.80	6.60	0.05
2914.20	28.70	12.12	2932.10	6.80	0.01
2914.50	24.90	5.44	2932.40	2.90	0.01
2915.10	3.20	0.15	2932.70	3.40	0.01
2915.40	6.80	0.73	2933.00	1.70	0.01
2915.70	3.80	0.01	2933.30	3.10	0.00
2916.10	2.20	0.00	2933.60	2.60	0.00
2916.40	1.70	0.00	2933.90	1.50	0.00
2916.70	2.90	0.01	2934.20	1.20	0.00
2917.00	7.80	0.01	2934.50	1.90	0.00
2917.30	1.40	0.01	2934.80	2.80	0.01
2917.60	1.80	0.00	2935.10	3.20	0.00
2917.90	2.00	3.83	2935.40	6.80	3.44
2918.20	2.70	0.00	2935.80	16.00	4.27
2918.50	2.50	0.00	2936.10	12.00	0.05
2918.80	2.30	0.00	2936.40	14.40	5.56
2919.10	3.10	0.00	2936.80	10.70	0.91
2919.40	2.70	0.00	2937.10	21.40	6.67
2919.70	1.90	0.00	2937.40	25.30	37.70
2920.00	1.70	0.00	2938.00	17.20	1.85
2920.30	2.30	0.01	2938.30	11.30	0.65
2920.60	2.80	0.00	2938.60	21.30	16.66
2920.90	5.00	0.00	2939.20	19.90	4.61
2921.20	7.60	0.01	2939.50	21.20	3.93
2921.50	10.10	0.00	2939.80	19.30	5.60
2921.80	12.40	0.01	2940.10	16.70	2.24
2922.10	21.60	6.63	2940.40	13.30	1.41
2922.40	22.40	10.41	2940.70	21.30	36.03
2922.70	3.90	0.00	2941.00	17.70	4.89
2923.00	6.40	0.00	2941.30	16.30	0.04
2924.50	7.00	0.00	2941.90	16.60	2.19
2924.80	14.50	3.13	2942.30	10.00	0.03
2925.10	12.50	0.94	2942.60	16.20	6.09
2925.50	12.10	1.62	2943.50	17.40	6.35
2925.80	16.50	1.77	2943.80	21.80	48.79
2926.10	16.30	1.21	2844.10	17.40	16.73
2926.40	2.80	0.00	2944.70	3.00	0.00
2926.70	14.20	0.85	2945.00	4.60	0.00
2927.00	15.20	11.85	2945.30	18.40	0.05
2927.30	19.10	30.70	2945.60	17.40	0.05
2928.40	15.60	1.44	2945.90	17.80	0.05
2928.70	3.90	0.00	2946.20	4.50	0.00
2929.00	6.20	0.01	2946.80	12.30	0.01

Continue.....

Depth (m).	Φ%	K(Air) md	Depth (m).	Φ%	K(Air) md
2947.10	14.80	0.05	2968.70	21.90	3.73
2947.40	13.20	0.04	2969.00	20.10	0.05
2947.70	11.80	0.00	2969.40	2.00	0.00
2948.00	22.50	23.00	2970.00	7.00	0.00
2948.70	24.90	5.49	2970.60	4.40	0.00
2949.00	23.30	63.79	2970.90	9.00	20.09
2949.30	21.20	16.56	2971.20	5.10	0.00
2949.60	28.50	13.12	2971.50	7.50	1.78
2949.90	23.60	17.67	2971.80	9.20	0.82
2950.20	25.60	34.13	2972.40	6.70	1.65
2950.90	2.30	0.04	2972.70	7.10	4.11
2951.20	9.40	17.95	2973.00	1.90	0.00
2951.60	22.50	42.15	2973.30	3.80	3.89
2951.90	21.30	7.98	2973.90	6.10	0.71
2952.20	15.20	14.59	2974.50	5.80	2.28
2953.40	23.40	2.93	2975.10	7.90	1.67
2953.70	28.40	162.31	2975.40	9.80	3.74
2954.00	26.70	126.25	2975.70	7.00	1.16
2954.30	16.30	35.28	2976.00	6.40	0.00
2954.60	36.50	532.67	2976.30	5.80	0.04
2954.90	6.90	20.37	2977.20	8.00	0.69
2955.20	16.20	16.33	2977.50	9.10	2.72
2955.50	10.30	5.09	2977.80	4.10	0.06
2955.90	7.80	0.00	2978.10	3.60	0.00
2956.70	10.00	0.03	2978.40	3.10	0.00
2957.00	7.20	3.87	2978.70	4.70	1.02
2957.60	6.50	0.04	2979.00	4.90	0.06
2957.90	3.10	0.00	2979.40	9.00	6.47
2958.20	5.90	0.00	2979.80	6.30	4.47
2959.10	23.90	6.01	2980.10	7.10	8.53
2959.40	24.50	4.87	2980.40	6.10	23.20
2959.70	24.90	10.90	2980.70	4.50	1.81
2960.00	12.90	3.54	2981.00	7.30	0.04
2960.90	24.60	17.63	2982.60	6.10	12.92
2961.40	24.20	12.60	2983.10	5.70	0.00
2961.70	18.50	8.60	2983.40	2.30	0.00
2962.00	19.50	57.93	2983.70	16.30	112.31
2962.30	19.80	47.84	2984.30	11.60	18.33
2962.60	20.40	40.92	2984.90	2.50	0.00
2962.90	17.80	24.93	2985.50	3.30	2.12
2963.20	19.30	40.24	2986.20	9.70	15.88
2963.50	21.90	19.85	2986.50	6.40	0.02
2964.10	23.10	11.43	2986.80	4.80	0.36
2964.40	25.40	3.72	2987.70	9.30	5.03
2964.80	3.00	2.02	2992.20	29.60	44.48
2965.10	1.50	0.00	2992.50	18.90	3.34
2965.70	5.00	0.00	2992.80	13.50	2.73
2966.00	8.30	0.00	2993.70	14.50	3.56
2966.30	4.50	0.00	2994.50	22.80	15.37
2966.60	7.40	0.01	2995.10	23.10	3.29
2966.90	7.30	0.00	2995.80	3.30	0.00
2967.20	2.10	0.00	2996.30	3.40	0.00
2967.50	3.40	0.00	2996.90	5.00	0.00
2967.80	2.30	0.00			

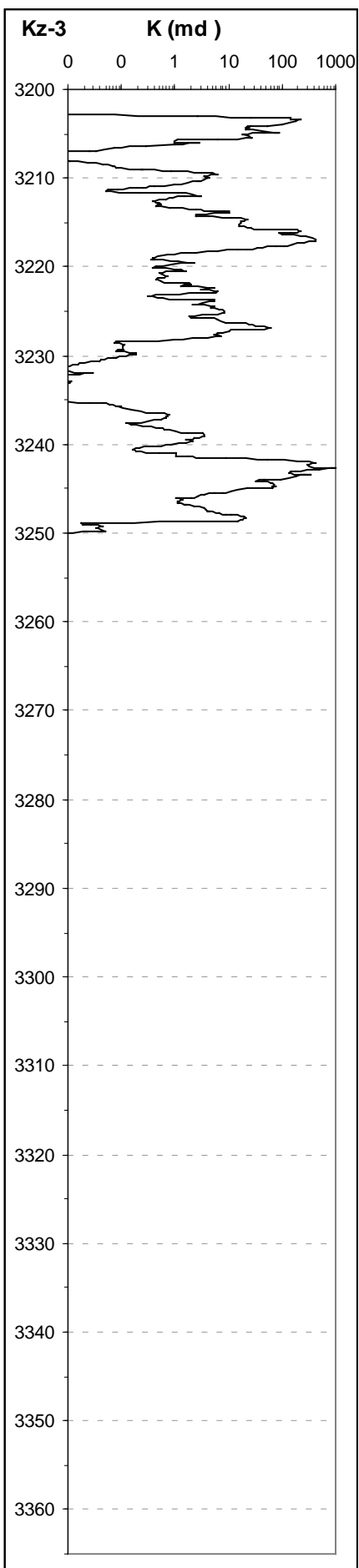
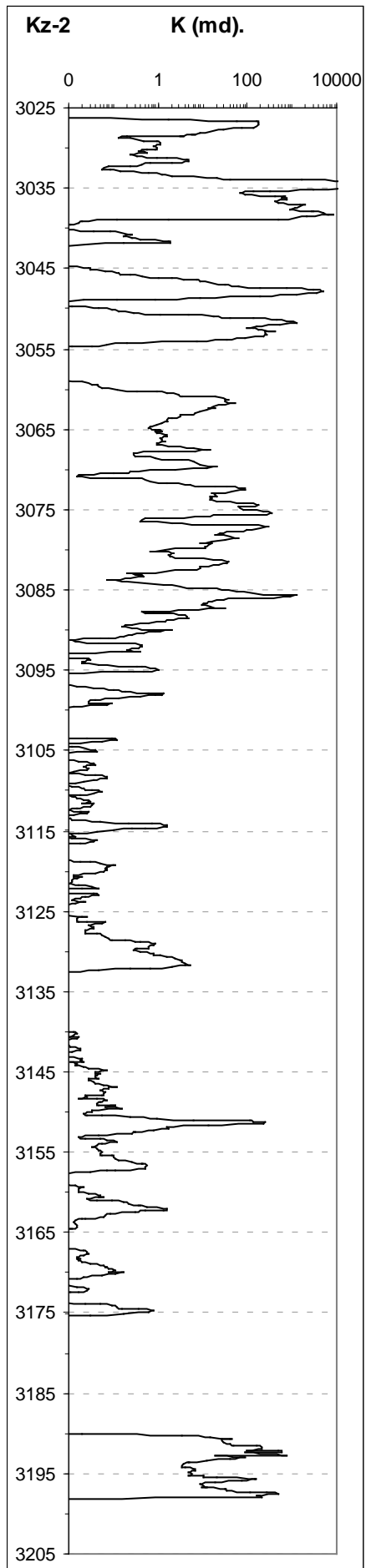
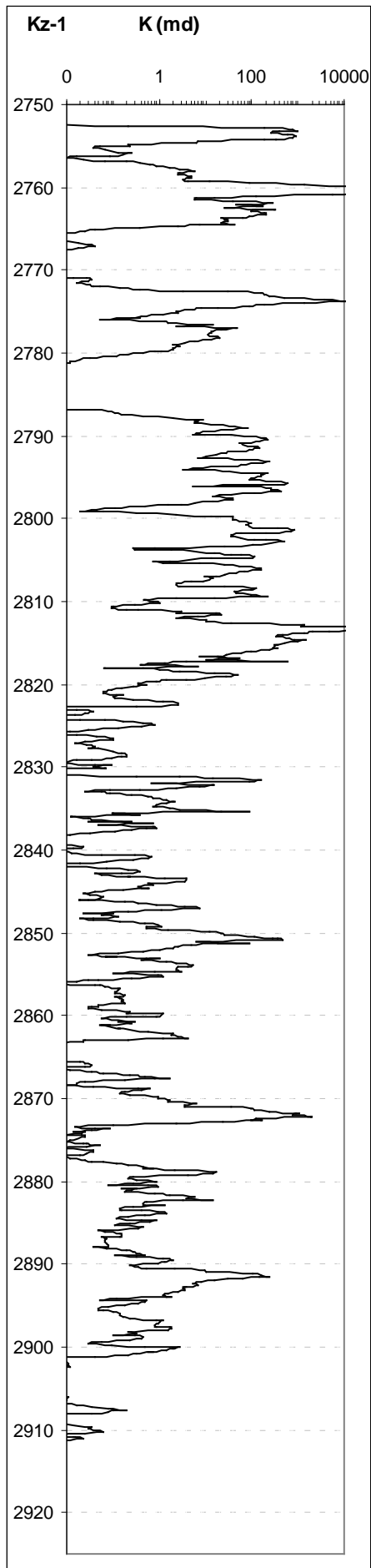
Appendices (C_{ns}):

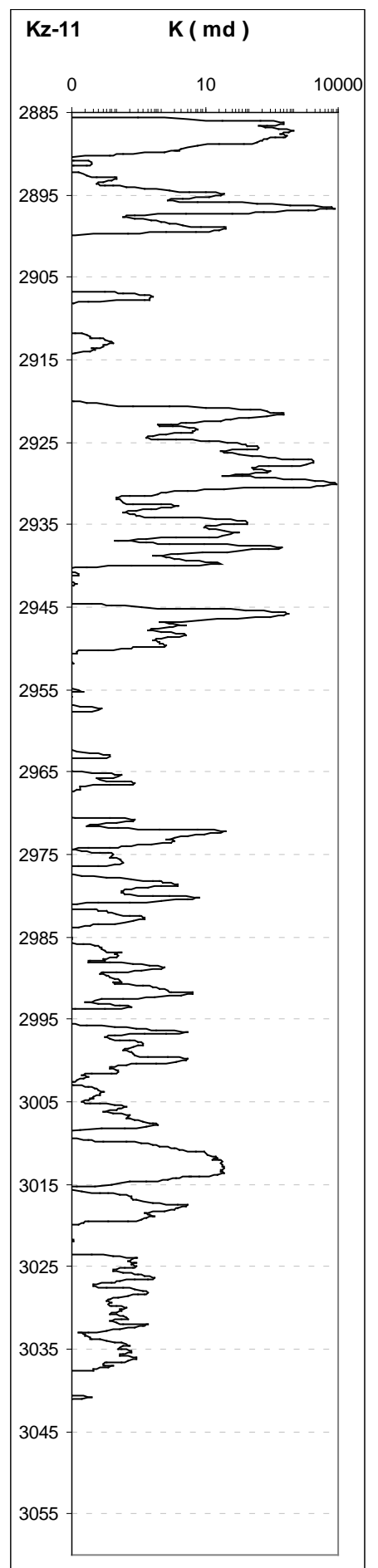
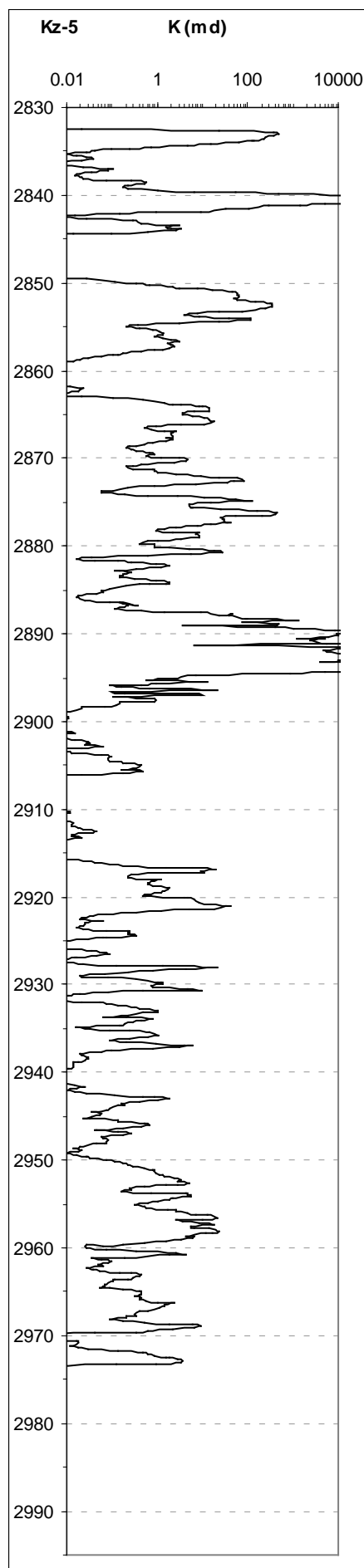
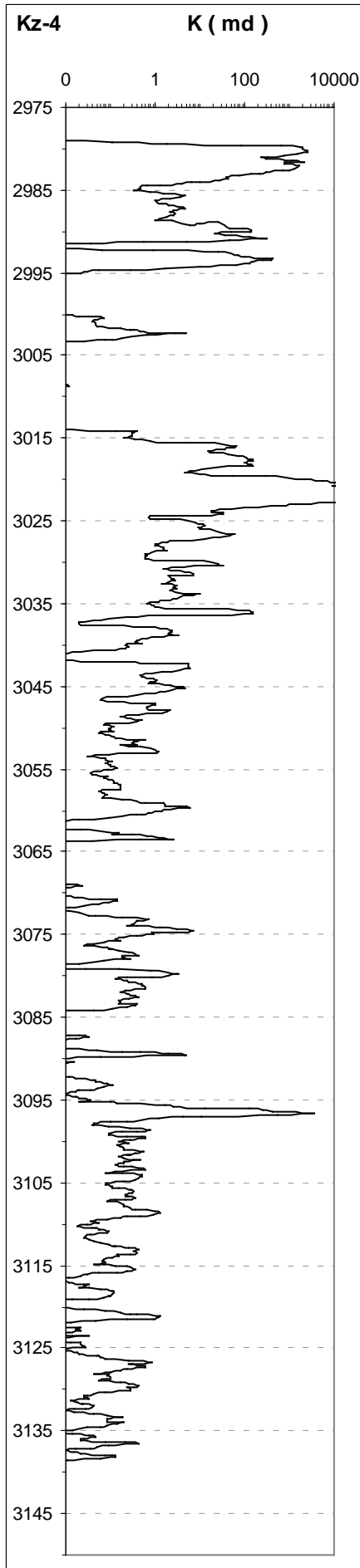
Estimated permeability (K) from the log data (GR, Neutron, Density, and Sonic) by the equation:

$$\text{Log (K)} = (-2.7 - 0.12 \cdot \text{GR} + 7.0 \cdot \Phi_D + 7.0 \cdot \Phi_N + 0.051 \cdot \Delta t)$$

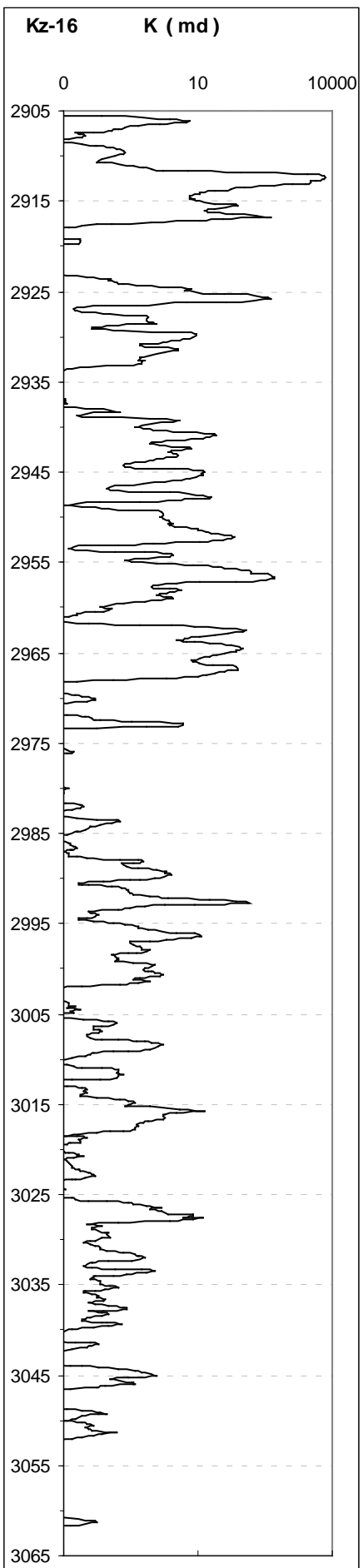
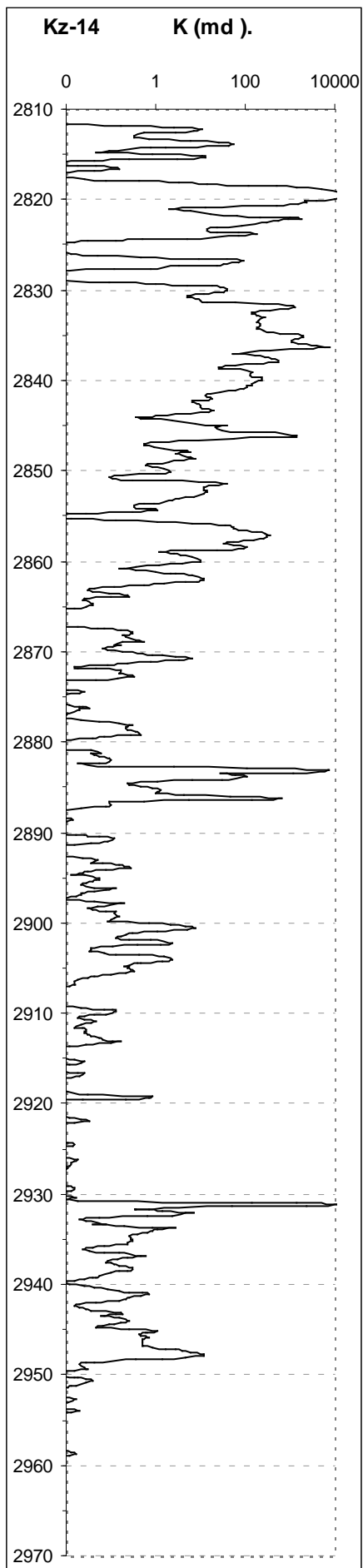
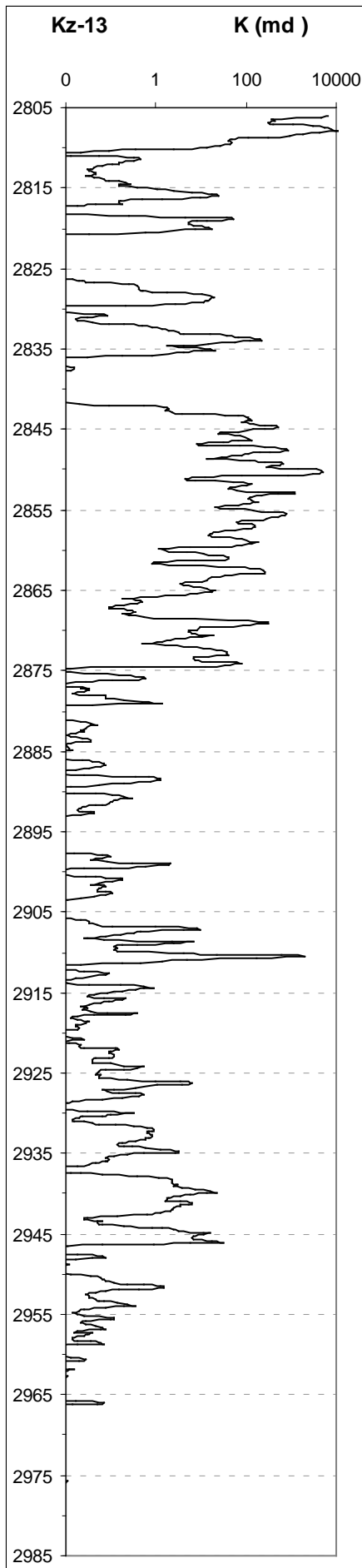
$$\text{Permeability (K)} = 10^{(-2.7 - 0.12 \cdot \text{GR} + 7.0 \cdot \Phi_D + 7.0 \cdot \Phi_N + 0.051 \cdot \Delta t)}$$

The results are illustrated by graphs for nine wells as following:





Appendix (C3): Permeability (md), Kz-13, Kz-14, and Kz-16



Appendix (D):

Porosity (Φ) and formation resistivity factor (F) measurements.
The data belong to the three wells: Kz-2, Kz-11, and Kz-16.

Well	Log Φ	Log F	Well	Log Φ	Log F
Kz-2	1.104	1.554	Kz-16	1.283	1.379
=	1.111	1.668	=	1.041	1.518
=	0.863	1.672	=	1.502	0.904
=	0.477	2.803	=	0.991	1.759
=	1.438	0.748	=	0.986	1.753
=	1.000	1.634	=	0.397	1.857
=	0.114	2.833	=	0.146	1.993
=	0.568	1.719	=	0.973	1.471
=	1.004	1.450	=	0.982	1.634
=	0.556	2.900	=	1.220	1.349
=	0.799	2.803	=	1.017	1.623
=	0.863	2.381	=	1.120	1.461
=	1.176	1.292	=	1.045	1.609
=	0.079	2.189	=	0.963	1.750
=	1.158	1.170	=	0.447	1.853
=	0.505	1.903	=	0.204	2.199
Kz-11	1.215	1.448	=	0.301	2.111
=	1.072	1.434	=	1.315	1.294
=	1.248	1.314	=	1.195	1.483
=	0.881	1.691	=	1.198	1.314
=	1.436	1.284	=	1.408	1.401
=	1.314	1.227	=	1.178	1.522
=	1.290	1.319	=	1.214	1.506
=	1.215	1.448	=	1.075	1.464
=	0.708	2.137	=	1.342	1.997
=	0.279	2.421	=	0.771	1.836
=	0.799	1.721	=	1.298	1.260
=	0.978	1.872	=	1.322	1.191
=	0.380	2.371	=	1.008	1.707
=	0.415	2.336	=	1.262	1.352
=	1.104	1.559	=	1.287	1.240
=	1.083	1.624	=	1.313	1.338
=	1.146	1.667	=	0.518	2.234
=	1.199	1.391	=	1.301	1.213
=	1.248	1.390	=	0.681	2.028
=	0.973	1.831	=	0.724	1.997
=	0.857	1.834	=	0.301	2.392
=	0.544	2.238	=	1.037	1.756
=	0.146	2.287	=	1.146	1.972
=	0.903	1.681			
=	0.279	2.080			
=	-0.097	2.654			
=	-0.222	2.497			
=	-0.046	2.497			